



Review

Recent Progress in Modeling the Macro- and Micro-Physics of Radio Jet Feedback in Galaxy Clusters

Martin A. Bourne^{1,2,*}  and Hsiang-Yi Karen Yang^{3,4,5,*} ¹ Institute of Astronomy, University of Cambridge, Madingley Road, Cambridge CB3 0HA, UK² Kavli Institute for Cosmology, University of Cambridge, Madingley Road, Cambridge CB3 0HA, UK³ Institute of Astronomy and Department of Physics, National Tsing Hua University, Hsinchu 30013, Taiwan⁴ Center for Informatics and Computation in Astronomy, National Tsing Hua University, Hsinchu 30013, Taiwan⁵ Physics Division, National Center for Theoretical Sciences, Taipei 10617, Taiwan

* Correspondence: mabourne@ast.cam.ac.uk (M.A.B.); hyang@phys.nthu.edu.tw (H.-Y.K.Y.)

† These authors contributed equally to this work.

Abstract: Radio jets and the lobes they inflate are common in cool-core clusters and are known to play a critical role in regulating the heating and cooling of the intracluster medium (ICM). This is an inherently multi-scale problem, and much effort has been made to understand the processes governing the inflation of lobes and their impact on the cluster, as well as the impact of the environment on the jet–ICM interaction, on both macro- and microphysical scales. The developments of new numerical techniques and improving computational resources have seen simulations of jet feedback in galaxy clusters become ever more sophisticated. This ranges from modeling ICM plasma physics processes such as the effects of magnetic fields, cosmic rays, and viscosity to including jet feedback in cosmologically evolved cluster environments in which the ICM thermal and dynamic properties are shaped by large-scale structure formation. In this review, we discuss the progress made over the last ~decade in capturing both the macro- and microphysical processes in numerical simulations, highlighting both the current state of the field, as well as the open questions and potential ways in which these questions can be addressed in the future.

Keywords: radio jets; active galactic nuclei; galaxy clusters; numerical modeling; simulation techniques; plasma physics; magnetohydrodynamics; cosmic rays; viscosity; thermal conduction



Citation: Bourne, M.A.; Yang, H.-Y.K. Recent Progress in Modeling the Macro- and Micro-Physics of Radio Jet Feedback in Galaxy Clusters. *Galaxies* **2023**, *11*, 73. <https://doi.org/10.3390/galaxies11030073>

Academic Editors: Thomas W. Jones, Stanislav S. Shabala

Received: 28 April 2023

Revised: 26 May 2023

Accepted: 1 June 2023

Published: 13 June 2023



Copyright: © 2023 by the authors. Licensee MDPI, Basel, Switzerland. This article is an open access article distributed under the terms and conditions of the Creative Commons Attribution (CC BY) license (<https://creativecommons.org/licenses/by/4.0/>).

1. Overview

1.1. Jet Feedback in Galaxy Clusters: Observations and Theoretical Motivation

Clusters of galaxies are the largest gravitationally collapsed objects in the Universe. Because of their deep gravitational potentials, the virial temperature of gas falling into clusters during hierarchical structure formation is heated to 10^{7-8} K, producing Bremsstrahlung emission in X-rays. Because the Bremsstrahlung emissivity of the intracluster medium (ICM) is proportional to the gas density squared, near the center of many massive clusters where the central density is high, the gas can cool significantly due to the strong radiation—the so-called “radiative cooling”. For clusters with central cooling times that are much smaller than the Hubble time, i.e., the cool-core (CC) clusters, it is predicted by the cooling-flow model [1] that there should be a significant inflow of gas toward the cluster center, triggering intensive star formation within the central brightest cluster galaxies (BCGs). However, there is a lack of observational evidence for such cooling flows, and the star formation rates (SFRs) of the BCGs are typically 10–100 times lower than those predicted by the cooling-flow model. This is well-known as the “cooling-flow problem” of galaxy clusters (see the articles of [2,3] for reviews).

The absence of cooling flows calls for certain heating mechanisms to balance the radiative cooling in CC clusters, among which the energetic feedback provided by relativistic

jets emerging from central supermassive black holes (SMBHs) is believed to be the most promising mechanism. This is motivated by the prevalence of X-ray cavities or bubbles, which are low-density, X-ray dim regions filled with radio-emitting plasma injected by the SMBH jets in CC clusters (e.g., [4–6]), as well as in many galaxy groups (e.g., [7–10]), which themselves represent a significant fraction of local radio galaxy hosts (e.g., [11–13]). Another compelling piece of evidence for active galactic nucleus (AGN) feedback is the observed correlation between the cavity power, which is a proxy for the jet power, and the X-ray luminosity within the cluster cores [14–17], thus suggesting that there is a global thermal balance between the heating and cooling in CC clusters. These observations have therefore motivated a picture of a self-regulated AGN feedback loop: when a cluster has increased X-ray luminosity, the ICM cooling rates and thus SMBH accretion rates are enhanced, which triggers powerful ejections of relativistic jets, heating the ICM and shutting off subsequent cooling and AGN activity [18]. While the idea of an AGN feedback cycle is an attractive solution to the cooling-flow problem, there is a huge dynamical range between the scales of SMBH accretion discs ($\sim 1\text{--}10^4$ AU) and the cores of galaxy clusters (~ 100 kpc) (see Figure 1 in Gaspari et al. [19] for an illustration of the multi-scale SMBH accretion and feedback processes involved). The vast dynamical range involved has prohibited an all-in-one simulation of AGN feedback; hence, the detailed processes of SMBH feeding and feedback mechanisms remain one of the greatest unsolved problems in astrophysics.

Because galaxy clusters are at the crossroads of cosmology and astrophysics, the advantages of understanding AGN feedback in clusters are two-fold. On the one hand, galaxy clusters are excellent laboratories for studying various astrophysical phenomena, including radiative cooling, AGN feedback, magnetic fields, shocks, turbulence, the acceleration of cosmic rays (CRs), plasma physics, etc. On the other hand, constraining these astrophysical mechanisms would enable robust predictions of cluster observables and evolution histories that are critical for the inferences of cosmological parameters, as well as the formation and evolution of galaxies (see the articles of [20,21] for relevant reviews). In turn, the large-scale environments of clusters and their evolution histories would also influence the operation of the above astrophysical processes. AGN jet feedback in clusters is one great example of this iterative process, where the theoretical understanding from both the astrophysical and cosmological perspectives has emerged in the past two decades. It is therefore our aim to review this exciting progress in this article. AGN feedback is not limited to jets in clusters. It can additionally manifest itself via radiation and accretion disc driven winds [3,22,23], and is expected to impact galaxy formation over a wide range of redshifts by shaping galaxy properties, regulating SMBH growth, and driving SMBH–host galaxy scaling relations [24–28], which themselves may aid our understanding of AGN physics. AGN feedback may even be important at the low-mass end, with recent studies of its affect on dwarf galaxies representing an area of growing interest (e.g., [29–33]). We refer interested readers to additional reviews that provide comprehensive coverage of these topics (e.g., [2,3,17,18,22,23,26,31,34–37]).

1.2. Simulating Jets in Idealized Hydrodynamic Simulations

As early as the late 1970s, and throughout the 1980s, groups were performing simulations of jets to study their propagation and structural evolution (see the article of Burns et al. [38] for an example of a review at that time). The pioneering works of Rayburn [39] and Norman et al. [40] paved the way by performing the first simulations of non-relativistic jets. Numerous works followed with a particular emphasis on understanding the radio observations of jets [41–45], as well as numerical studies on the impact of resolution [46], simulations that included magnetic fields [41,47,48], and some that were performed in 3D [49,50]. The history of simulating jets is itself an interesting topic; however, in this work, we restrict ourselves to more recent advances in modeling jet feedback in galaxy cluster environments, and instead direct the reader to reviews focusing on simulating jets in general [51,52].

While much of the early work was motivated by radio observations of jets (e.g., [53,54]), X-ray observations of galaxy clusters using ROSAT (e.g., [55–57]) and later Chandra (e.g., [58,59]) showed cavities in the ICM (as highlighted by Fabian [3], cavities had been observed earlier with the Einstein telescope [60,61], although their true nature had not yet been realized), and thus provided further motivation to understand the interaction of radio jets and the lobes they inflate with the surrounding hot ICM. Broadly speaking, two approaches were used to study this scenario: one in which the jets were simulated and the self-consistent inflation of the lobes studied [62–66], or—for simplicity—one in which this process was pre-assumed and hot bubbles were added or inflated “by hand” [67–70]. While the former approach gives insights into how the jet itself interacts with the ICM and how lobes are inflated, the latter is less computationally expensive. More complex simulations have followed and contributed to an ever-growing body of literature, which we will discuss further throughout this review.

Apart from a few examples [71–73], simulations that attempt to model the jets themselves are performed using grid-based codes that allow for high resolution in low-density regions, which are typical of jets. Traditionally such codes are Eulerian, although novel refinement techniques have meant that moving-mesh (e.g., AREPO [74]), and meshless-finite-mass (e.g., GIZMO, [75]) codes have also been used to simulate jets (e.g., [76–78]). When it comes to launching a jet, certain works place finer control on how exactly the jet is injected into the simulation domain by defining the exact thermodynamic and kinetic state within the launch region, i.e., the jet density, temperature, and velocity (e.g., [77,79–81]). Other works simply add mass, momentum, and/or energy to the injection region and allow the jets’ thermodynamic properties to arise naturally from this (e.g., [66,76,82–86]). However, the ultimate result is a pair of fast low-density jets that drive bow shocks into the ICM (and potentially internal shocks along the jets), thermalize, and then inflate high-temperature lobes that come into pressure balance with the ICM. These methods have been used to perform a wide range of simulations, from high-resolution studies of lobe inflation and energetics (e.g., [76,77,81,87–91]) to those that include SMBH accretion models from which the jet power is calculated (e.g., [84,86,92–98]); the latter are performed on Gyr time-scales to understand how jets can regulate the thermodynamic state of the ICM. On top of this, additional physics relevant to jet feedback and galaxy clusters has been included in dedicated jet simulations, such as magnetic fields [77,87,88,98–108], relativistic effects [91,109–113], viscosity [114–117], thermal conduction [95,118–125], and CR physics [76,77,88,90,126–132].

There are now many works that have coupled jet power to SMBH accretion rates (e.g., [82–86,92,94,96,98,133–136]). The physical connection between accretion and jet power, expected to depend on the properties of the SMBH and its accretion flow (see e.g., Section 4 of [17] for a discussion), is still to be fully understood. For simplicity, the simulations discussed here often assume a fixed scaling between accretion rate, \dot{M} , and jet power, \dot{E}_{jet} , of the form

$$\dot{E}_{\text{jet}} = \epsilon \dot{M} c^2, \quad (1)$$

where c is the speed of light and ϵ is a constant feedback efficiency (although variable spin-dependent efficiencies have also been included in recently developed models [73,97,137,138]). Cattaneo and Teyssier [82] presented some of the earliest simulations that coupled a jet feedback scheme [66] to a Bondi accretion model; therefore, they capture self-regulated jet feedback in a galaxy cluster. The jets were injected using a combination of momentum and thermal energy. While the feedback was able to prevent over-cooling of the ICM, it was overly effective and unable to preserve a CC. Numerous works followed, and they similarly investigated injecting a combination of thermal energy and momentum [85,135], as well as works that considered purely kinetic jets [86,92,94,95,134] that were able to inhibit cooling and match a range of observed cluster properties. Specifically, it has been found that combining momentum-driven jets with cold-accretion models [85,86,93,94,96,98,134,136,139], whereby the SMBH grows due to accretion of cold gas, can regulate ICM cooling while maintaining the properties of CC clusters (albeit only in idealized cluster environments). However, as

discussed in the next section, reproducing thermodynamic profiles and the CC/non-CC dichotomy is difficult to achieve in full cosmological simulations.

1.3. AGN Feedback in Cosmological Simulations

The simulations discussed above, typically performed in hydrostatic atmospheres, place emphasis on understanding the detailed processes governing lobe inflation and interaction with the ICM, which requires high spatial (often achieved with dedicated lobe refinement techniques) and time resolutions. However, the study of cluster formation and evolution requires simulations that capture structure formation processes over cosmic time, i.e., cosmological simulations. Such simulations span a wide range of galaxy masses and include various models to capture a wide array of physical processes important to galaxy formation, and we direct the reader to relevant reviews for more detailed discussions (e.g., [140,141]). The inclusion of AGN feedback in cosmological simulations has been shown to be an important ingredient for creating realistic galaxy populations, particularly at the high mass end (e.g., [142–147]). There are a growing number of cosmological simulations that capture the formation and evolution of galaxy clusters to understand the processes that shape their properties (e.g., [143,148–157]). Such simulations have performed remarkably well at matching a range of observed cluster properties; however, achieving realistic thermodynamic profiles in cluster cores and explaining the CC/non-CC dichotomy is challenging, with several works concluding a need for modified AGN feedback models (e.g., [151,155,158]).

Cosmological simulations, by the necessity of space and time resolution constraints, implement simplified and/or low-resolution models of AGN feedback that do not necessarily capture the processes of lobe inflation and their interaction with the ICM in detail. In the most straightforward implementation, feedback energy is injected thermally in resolution elements local to the SMBH (e.g., [142,144,156,159–161]). Modifications are often made to such models in order to circumvent the over-cooling problem (see e.g., [143,144,160,162] for a discussion); for example, by temporarily switching off radiative cooling [156,163], or by storing energy until gas can be heated to a minimum temperature [143,144,160,161] or when a fixed duty cycle has passed [155]. Alternatively, the energy can be injected as a kinetic outflow [83,133,146,147,164,165]. While some works assume a single feedback mode that is the same irrelevant of the SMBH mass or accretion rate (e.g., [144,156,161]), others implement separate “quasar” and “radio” modes (e.g., [133,145–147,164–166]), with the latter typically being used for low accretion rates. One of the earliest such examples of dual AGN modes was introduced by Sijacki et al. [166], who took inspiration from early bubble models of jet feedback [67,69,167] by including the jet mode as thermal bubbles displaced from the central SMBH. This model has subsequently been used in the Illustris [145] and Fable [155] simulation suites. On the other hand, Dubois et al. [83] built on the work of Omma et al. [66] and Cattaneo and Teyssier [82] to implement mass-loaded bipolar outflows, which aimed to capture a sub-relativistic accretion disc wind as jet-like outflows and can self-consistently produce cavity-like structures in the ICM. This model has since been used in the HorizonAGN [146] and NewHorizon [168] simulations, as well as in other studies of feedback in galaxy clusters (e.g., [97,125]). In a somewhat similar vein, Davé et al. [165] implement a jet feedback model for the low accretion rate regime in the form of a slow, highly collimated bipolar outflow in the SIMBA suite of simulations; however, the jet was hydrodynamically decoupled during its initial phase, meaning that it does not interact with the inner parts of galaxies and clusters, and instead couples its energy on larger scales. Alternatively, certain simulation suites, such as IllustrisTNG [147], take a different approach; instead of attempting to model jet feedback, they implement an efficient kinetic wind model for high mass SMBHs in the low accretion rate regime that injects kinetic energy into the local gas in a random direction [164], which acts to effectively quench high-mass galaxies.

1.4. The Importance of Macrophysics and Microphysics

Thanks to the advancement in computing power and numerical algorithms over the past decade, numerical simulations of jet feedback in clusters have become increasingly sophisticated with more realistic initial conditions from cosmological contexts, as well as with complex physical processes including magnetic fields, CRs, plasma effects, etc. The latter is often dubbed as “microphysics” in clusters because the gyro-radii of charged particles and CRs in the magnetized ICM (on the order of \sim AU for GeV CRs in μ G magnetic fields) are many orders of magnitude smaller than the size of clusters (\sim Mpc). Consequently, transport processes in the ICM, including thermal conduction, viscosity, and CR propagation, are determined by plasma physics that happen on the microscopic scales of the particle gyro-radii (Section 3). As will be discussed in detail in later sections, recent simulations have demonstrated that both the macrophysics from the large-scale environments of clusters and the microphysics have crucial impacts on the AGN feeding and feedback processes, as well as on the evolution of clusters—thus, they will be the focus of this review. We also advise, however, that despite the vast computational capabilities now available to the community, there is still a need for robust, physically motivated analytic components and sub-grid models to link between the scales above and below the resolution limit of simulations.

The structure of this article is as follows. In Section 2, we review the important progress regarding the modeling of the macrophysical processes of AGN feedback. We will first start by introducing the fundamental processes of AGN lobe formation and lobe-ICM interaction (Section 2.1). This is followed by discussions about the role of the cluster environment (Section 2.2), as well as open questions and future opportunities (Section 2.3). In Section 3, important findings regarding the microphysical processes are summarized. Specifically, in Section 3.1 we discuss the roles of CRs in AGN feedback and their observational signatures. We then discuss the roles of plasma physics, such as transport processes, e.g., conduction and viscosity in the ICM, in Section 3.2. Open questions and future opportunities regarding microphysics are discussed in Section 3.3. Finally, Section 4 contains our concluding remarks.

2. Modeling the Macrophysics

There is now significant literature on the hydrodynamic and magnetohydrodynamic (MHD) modeling of the large-scale processes driving the inflation of jet lobes and their macroscopic evolution. Figure 1 provides a general diagrammatic overview of the phases of lobe inflation and subsequent evolution, which we discuss throughout this section. Specifically, in Section 2.1, we first consider the processes that are intrinsic to the jets and lobes, including their energetics and processes through which they interact with the ICM. Meanwhile, in Section 2.2, we additionally discuss the role of the cluster environment, including cluster weather, and the role this has on shaping lobe properties and cluster heating.

2.1. Bubbles, Shocks, and Waves

2.1.1. Morphology, Direction, and Energetics

Observed jets have long been classified based on their radio morphology, as was set out by Fanaroff and Riley (FR) [169]. They are broadly characterized as either center-brightened FR-I sources, e.g., 3C 449 [170], that are expected to form due to decelerating and becoming turbulent on small (\sim kpc) scales (e.g., [171–175]), although frustrated and bent jets, such as wide/narrow angle tailed radio galaxies, can also provide morphological analogues to FR-I sources, e.g., [176–179]), or edge-brightened FR-II sources (e.g., Cygnus A, [180]), which are highly collimated and expected to be relativistic along their entire length. Although the differences are expected to result from the dynamics of the jets and depend on both their power and how they interact with their environment, some debate remains over the exact role of the central engine (see the review of [36] for a fuller discussion), with a number of works, both theoretical and observational, considering the relationships between AGN

properties, such as radio loudness, morphology, and/or excitation, and the properties of the accretion flow and/or SMBH [181–189]. Several parameter studies that vary the jet (e.g., power, opening angle, velocity) and environmental properties have been performed that can recover both FR-I and FR-II sources (e.g., [80,88,175,190–195]), with Massaglia et al. [190] suggesting that simulating FR-I sources is challenging and requires high-resolution 3D simulations to fully capture their turbulent properties.

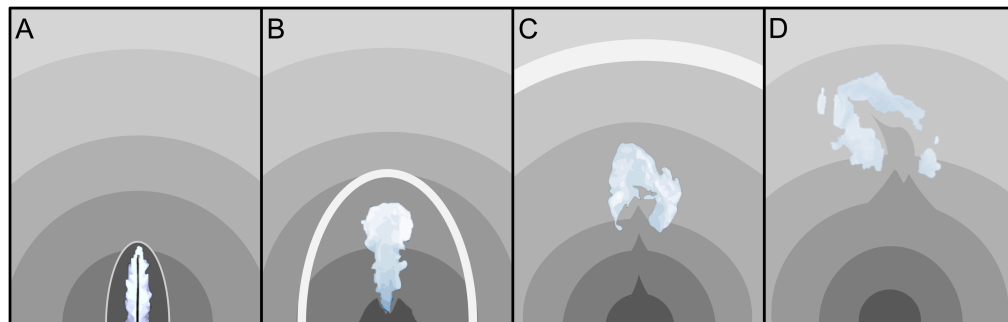


Figure 1. Diagram illustrating the general processes that occur during and after lobe inflation. (A): A fast jet drives into the ambient medium, forms a bow shock, and inflates a hot lobe that expands into the ICM. The lobe morphology can depend sensitively on the injected jet properties (e.g., content, velocity, geometry). The expanding shock wave results in a layer of shocked ICM material surrounding the jet lobe. (B): As the lobe expansion slows, which may or may not be accompanied by the jet switching off, the shock driven into the ICM broadens into a sound wave that can detach from the lobes. (C): Once the jet has ceased and as the lobe buoyantly rises through the ICM, dense, low entropy material can be entrained and pulled up in the wake. Moreover, instabilities can lead to mixing of the lobe and ICM material. Sound waves generated by the lobe expansion can continue to propagate to large distances depending on the ICM viscosity. (D): This process continues at late times, with mixing continuing to dilute the lobe material, although the rate at which this occurs can sensitively depend on the ICM physical processes including magnetic fields, viscosity, and cluster weather (i.e., the ICM and sub-structure motions, see Section 2.2).

As discussed in Section 1.2, several methods have been developed to launch jets and to capture the lobe inflation process within the framework of galaxy cluster evolution. It was found early on that to create a cocoon structure the jet needs to have a lower density than the surrounding medium (see discussion in e.g., [77,79,196] and the references therein). As outlined in Section 1.2, many studies now make use of fast collimated outflows that efficiently thermalize through shocks to inflate lobes of hot gas; however, a range of morphologies are still seen in simulations depending on both the numerical and physical choices for how the jet is injected, as was recently illustrated by Huško and Lacey [71] and is shown in Figure 2. The choice of using a cylindrical (0° opening angle) versus conical injection, as well as the jet opening angle itself, can impact jet properties (e.g., [71,80,195,197]). Moreover, the jet opening angle is a possible determinant of whether the jet has FR-I or FR-II morphology [80,195]. In regard to the jet power, it is possible to achieve the same value by either having fast/light jets or slow/heavy jets. Jets with a high momentum density, which occurs in slow/heavy jets, are typically elongated along the jet direction with narrow lobes, whereas light/fast jets are found to be shorter and to inflate wide lobes, which have a notable expansion perpendicular to the jet direction (e.g., [71,77–79,103,116,195,198–200]). Huško and Lacey [71] additionally found that these trends can break down for very slow outflows that are unable to inflate hot lobes or generate significant backflows (see third row of Figure 2). In terms of regulating cluster cooling and heating, the recent study of Weinberger et al. [200] highlighted that the behavior of very light jets inflating wider lobes makes them more effective than heavy jets at removing low entropy material from cluster cores and inhibiting cooling flows (see also [78]).

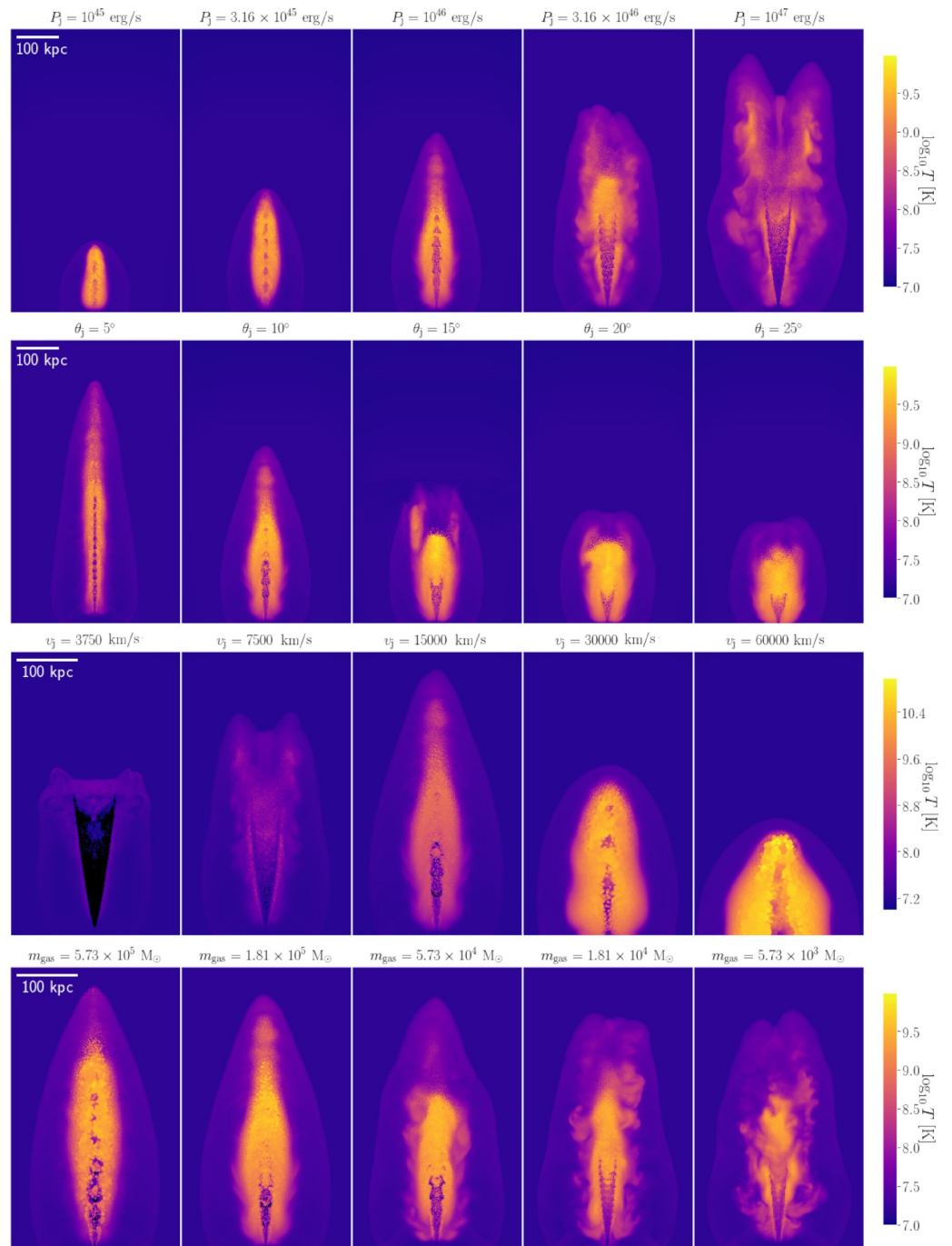


Figure 2. Thin temperature projections illustrate how jet injection parameters impact jet and lobe morphologies. All jets are 100 Myr old, with each row illustrating the effect of changing one parameter: from top to bottom, these are jet power, half opening angle, velocity, and resolution, respectively. These quantities take fiducial values of 10^{46} erg s^{-1} , 10° , 15,000 km s^{-1} , and $1.81 \times 10^5 M_\odot$, unless being varied. Color bars shown to the right of each row extend down to 10^7 K, and the gas below this is shown in black. (Figure 6 from Huško and Lacey [71], CC BY 4.0.)

Some works have also considered if and how injecting magnetic fields with jets can influence lobe morphology and dynamics (e.g., [77,87,88,103,110,191]). Gaibler et al. [103] found that injected fields, amplified in the jet head, can stabilize against Kelvin–Helmholtz instabilities and can generate a cleaner lobe structure. Works that consider magnetic fields with moderate-to-high values of plasma β (defined as the ratio between thermal and magnetic pressure, $\beta \equiv P_{\text{th}}/P_B$) find, as expected, that they have limited impact on

the overall lobe dynamics [77,87,88,110], although they can affect the long-term stability of lobes by suppressing instabilities that would otherwise mix the jet and ICM material (e.g., [77,88]). On the other hand, Massaglia et al. [191] show that strong fields ($\beta = 3$) can impact morphology, leading to the jet becoming distorted due to non-axisymmetric modes. In terms of observational constraints, lobe magnetic fields have been measured using inverse-Compton observations of FR-II sources (e.g., [201–204]), with Ineson et al. [203] finding observed field strengths to be below equipartition in all of their sources with a median ratio of 0.4 and hence very low values of β would seem unlikely, although Croston et al. [202] do find some magnetically dominated sources. Another important factor that many simulations of jet feedback on galaxy cluster scales neglect is the effect of relativity, both in terms of the jet dynamics and in correctly accounting for high-temperature gas. For jet speeds approaching the speed of light, the effects of relativity are expected to play an important role in shaping lobe properties and to increase the efficiency and volume over which jets can heat the ICM [91,109,111]. Additionally, the behavior where fast-light jets inflate wider lobes that interact more isotropically with the ICM is found to extend into the relativistic regime [110,195], while simulations that consider CR-dominated jets also produce “fat” lobes (see Section 3.1).

The mechanisms that launch a jet and determine its direction occur on scales of the accretion disc or smaller (e.g., [183,205–209]), which is far below the resolution limit of galaxy cluster simulations (a binary companion can also result in jet precession [210,211], although the mechanisms governing this are also not resolved in large-scale cluster simulations). As such, ab-initio modeling of the jet direction evolution is not possible. Traditionally, simulations of jets in galaxy clusters assume a fixed jet direction, potentially with some small angle precession (e.g., [76,85,86,134,212,213]), although some works instead randomly re-orientate the jet direction by hand (e.g., [214]) to improve the coupling between the jet and ICM. Several subgrid models have been developed recently that, while differing in the exact assumptions made regarding the subgrid accretion disc properties, can track SMBH spin evolution (e.g., [73,125,215–217]). Dubois et al. [215] additionally used the SMBH spin to determine the radiative efficiencies and jet direction, while Beckmann et al. [97] further developed this model to use the spin-dependent jet efficiencies derived from GRMHD simulations [218]. In a similar vein, Talbot et al. [137] coupled a jet feedback model [76] to the accretion disc model of Fiacconi et al. [216], in which they have assumed spin-dependent Blandford-Znajek jet efficiencies derived from GRMHD simulations [183] as well as the back reaction of the jet on the SMBH evolution. While the models of Dubois et al. [215] and Fiacconi et al. [216] both assume a thin α -disc, Huško et al. [73] assumed a thick disc, which typically leads to slower spin alignment timescales. While such methods are not necessary for modeling single feedback events, simulations that capture self-regulated feedback on Gyr timescales and include spin evolution find that the jets can re-orient and inject energy more isotropically within the cluster [73,97].

The energetics governing lobe inflation has been an important area of study; in particular, due to its influence on how the feedback heats the ICM. Observational measurements of the lobe pressure and volume are often used to constrain the lobe and jet energetics, which show a correlation between the estimated lobe power and ICM cooling rate [3,16,17]. These lobe powers have also been compared to estimated Bondi [219] accretion rates in order to constrain the efficiency, i.e., ϵ in Equation (1), of the central engine [220–224], with some studies requiring $\epsilon > 1$. Setting aside the uncertainties in estimating lobe powers and Bondi accretion rates from observations (e.g., [223]), high efficiencies could indicate that modes other than Bondi are needed to feed the SMBH, such as cold accretion (see e.g., [18] for further discussion, including on the limitations of the Bondi model). Alternatively, these results could be evidence that jets can extract spin energy from the SMBH via the Blandford–Znajek mechanism [225], which allows efficiencies over 100% [184,205,218]. In any case, considering the lobe inflation process in more detail—as highlighted by McNamara and Nulsen [2]—under the assumption that the jet kinetic energy is efficiently thermalized

and that the lobe inflation proceeds in pressure equilibrium with the ICM, the total energy needed to inflate the lobe is given by the lobe enthalpy:

$$H = E_{\text{lobe}} + PV = \frac{\gamma}{\gamma - 1} PV, \quad (2)$$

where γ is the adiabatic index of the lobe gas, E_{lobe} is the internal energy of the lobe, and PV is the product of the lobe pressure and volume. The resulting ratio of injected jet energy to lobe energy to work done is $E_{\text{jet}}:E_{\text{lobe}}:PV = 1:1/\gamma:(\gamma - 1)/\gamma$, which for a non-relativistic gas ($\gamma = 5/3$, commonly assumed in simulations) suggests that the lobes should retain 60% of the injected energy, with the remaining 40% going into the ICM via the work done. However, whether such behavior is seen in reality depends on what dominates the lobes (e.g., relativistic or non-relativistic particles, magnetic fields, etc.) and hence determines the effective value of γ and on the suitability of assuming that lobes are inflated in pressure equilibrium with their environment, i.e., how explosive the feedback is. With respect to the latter point, Tang and Churazov [226] performed idealized simulations of spherically symmetric AGN feedback events with varied energies and duration, finding that shorter, more explosive, injection events result in larger fractions of energy (up to $\sim 88\%$) going into shocks. Meanwhile, for longer, gentler, injection events, the fraction of injected energy ending up in shocks is negligible. As such, the lobe enthalpy varies from ~ 0 for instantaneous injection, up to roughly the injected energy for infinitely long injection episodes. Hydrodynamic simulations of jets in a cluster environment performed by Hardcastle and Krause [81] found that while the lobe energy is dominated by the thermal component, there are non-negligible kinetic and potential energy contributions. They additionally find that the ratio of lobe energy to energy gain by the ICM achieves a roughly constant value of ~ 1 after an initial lobe inflation phase where the ratio can be larger, thereby highlighting the non-negligible kinetic energy content of the lobe and the fact that they can be over-pressured compared to the ICM. The follow-up work of English et al. [110] presented relativistic jet simulations both with and without MHD for a range of jet velocities and powers. All the jets studied had inflated lobes that experienced an initial phase of being over-pressured (up to a factor of ~ 5) before lobe pressures rapidly declined, and while low-power jets tend to come into rough pressure equilibrium with the ICM, the lobe pressure ratios for their highest power jets never dropped below ~ 2 ; furthermore, they began to increase again as the lobes moved to larger radii. They additionally find that the shock-to-lobe energy ratios attain a roughly constant value of ~ 1.5 , which is consistent with the results of earlier MHD simulations by Hardcastle and Krause [87] and slightly higher than values found in the pure hydrodynamic simulations of Hardcastle and Krause [81]. Other jet simulations have additionally found ratios of $\gtrsim 1$, with varying levels of lobe kinetic energy, for both purely hydrodynamical simulations [71,76,89,227,228] and those including magnetic fields [77,87,88]. Bourne and Sijacki [228] found that due to the lobes initially being over-pressured, the instantaneous PV and lobe enthalpy (calculated from Equation (2)) underestimated the integrated PdV work done during lobe inflation and total jet energy, respectively. Perucho et al. [111] additionally highlighted the importance of modeling relativistic jets, which can result in larger lobe pressures by at least a factor of two.

2.1.2. The Lobe–ICM Interaction

While it is clear that shocks play a critical role in lobe inflation, they can also make an important contribution to heating the ICM. While the jet itself drives a bow shock into the ICM, the initial rapid expansion of the jet lobes can also drive lateral shocks. As the lobe expansion slows, the shocks become weaker and potentially broaden into sound waves, providing a mechanism through which energy can be communicated isotropically to the ICM (e.g., [64,73,76,77,86,94,96,213,227,229]). It is also worth noting that, similar to typical observations of jet feedback in galaxy clusters [230–233], many modern simulations find that shocks are often not very strong (e.g., [71,85,88,96,228,229,234]). Li et al. [96]

explicitly tracked the numerical dissipation within shock cells and found that heating due to shocks exceeded that which was due to turbulence by \sim an order of magnitude and, as shown in Figure 3 (which is taken from Li et al. [96]), that the vast majority of shocks were weak. Other works such as Yang and Reynolds [86] and Martizzi et al. [213] estimate the dissipation rates from the expected entropy jump for weak shocks:

$$ds \simeq \frac{2\gamma k_B}{3(\gamma + 1)^2 \mu m_H} (\mathcal{M}^2 - 1)^3. \quad (3)$$

They found that strong shocks can play an important role within the jet cone, while weak shocks can dominate heating outside the cones; however, Yang and Reynolds [86] find that weak shocks alone are unable to completely offset cooling. Bourne and Sijacki [228], who perform simulations in a cosmologically evolved cluster, make use of more conservative criteria to define shocks in order to avoid misclassification due to galaxy formation processes (see [235,236] for details). They also find that weak shocks are an important component of the energy budget, albeit with somewhat lower levels of direct dissipation; thus, they instead highlight the importance of compressive heating at shock fronts.

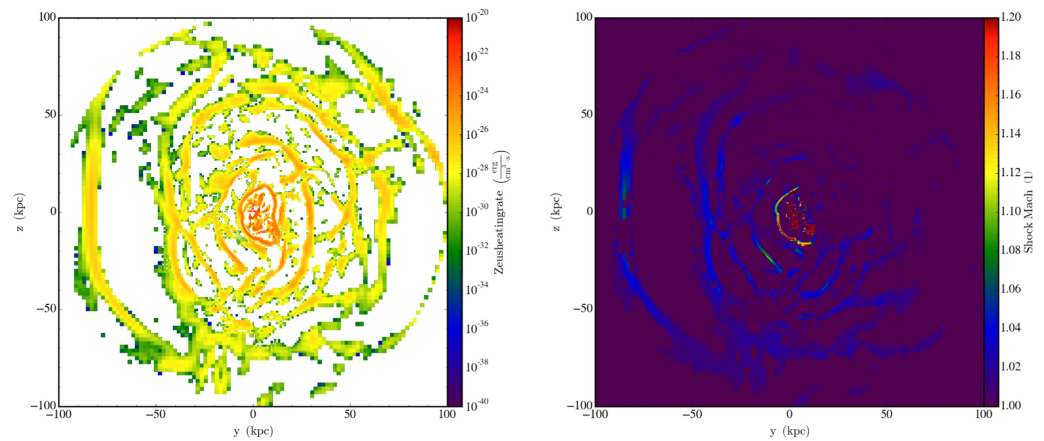


Figure 3. An illustration of the jet-driven shocks within the central 100 kpc of a simulated cluster. The simulation includes self-regulated AGN feedback that assumes the jet power is coupled to the SMBH accretion of cold gas with an efficiency parameter of $\epsilon = 1\%$ (as defined in Equation (1)). The jets are assumed to have a small angle precession ($\theta = 0.15$), with a 10 Myr period around the z -axis in the simulation. The left panel shows the energy dissipation rate, while the right-hand panel shows shock Mach numbers, illustrating that stronger shocks and hence higher dissipation rates are seen closer to the jet; however, overall the shocks are typically quite weak. (Figure 1 from Li et al. [96], ©AAS, reproduced with permission).

As well as shocks, simulations exhibit sound/compression waves, which are driven by lobe expansion. These sound waves “detach” from the lobes once the expansion speed drops below the ICM sound speed and have the potential to travel isotropically to large distances [73,76,83,227,228,234,237,238]. Bambic and Reynolds [239] recently presented a detailed study of sound wave production by momentum-driven jets in an ICM atmosphere (see Section 3.2.3 for further discussion), finding that constructive interference can lead to $\gtrsim 25\%$ of the jet energy being converted to sound waves, exceeding the level expected from spherical blast waves ($\sim 10\%$) [226]. However, the rate of heating and volume over which sound waves are energetically important depend on the microphysics of the ICM (see Section 3.2.3), which dictate the cluster viscosity [237,238,240,241].

Several early simulations assumed that lobes can be simply modeled as low-density bubbles of hot gas that rise buoyantly through the cluster atmosphere [67–70,167]. However, in omitting the inflation phase, these simulations miss the potential impact that the jet momentum has on bow shock production and the dynamics of the lobes, which may, at least initially, propagate on timescales shorter than the buoyant rise time [66,76,88,112]. Observa-

tions of clusters can exhibit multiple old cavities that go out to large radii [9,10,231,242,243]. Early simulations of bubbles were found to be disrupted by Rayleigh–Taylor and Kelvin–Helmholtz instabilities on relatively short timescales unless additional physics such as physical viscosity [114,240] or magnetic fields [244–248] were included. However, Sternberg and Soker [249] showed that the formation of a dense layer of gas around jet-inflated lobes can inhibit the development of such instabilities, thus allowing bubbles to travel further and live longer. That being said, simulations of wide jets (large opening angle) have found that vortices can develop that effectively mix lobe material with the ICM [250–252], with Hillel and Soker [251] finding that it is more effective than both turbulence and shock heating (see also, [86,96]). On the other hand, simulations that make use of narrow jets (0° opening angle) find that mixing of jet material into the ICM via Kelvin–Helmholtz instabilities is sub-dominant [76,77,213] and that the level of mixing reduces with increasing jet power [88,228]. Bourne and Sijacki [76] highlight the impact of resolution on mixing, finding that lower resolutions result in increased levels of mixing, citing the existence of larger Kelvin–Helmholtz vortices in this regime, as well as additionally highlighting that appropriate refinement of the jet lobes is required to avoid excessive numerical mixing (see also [77]). Martizzi et al. [213] highlight that the level of mixing can depend upon the hydro-solver implemented, which can impact how well mixing instabilities are resolved (see also [253]). Further, the inclusion of magnetic fields has the potential to inhibit mixing (e.g., [77,88,244–248,254]). In addition, the ability to effectively mix lobe and ICM material depends on the constitution of the lobe material [90] and the plasma properties of the ICM (see Section 3.2.2).

Observations of galaxy clusters can show multiple cavities at a range of radii representing different generations of jet lobes that have risen buoyantly through the ICM [9,231,242,243,255]. Such rising bubbles can displace significant amounts of ICM material and increase its gravitational potential energy [72,77,81,87,90,228]. It was argued early on that displaced material would fall back behind a rising cavity, thus driving turbulence and ultimately converting its potential energy into heat—a process known as cavity heating [7,67,256]. Yang and Reynolds [86] pointed out that the exact heating rate is dependent on the ICM viscosity, and they found that in any case, kinetic energy within the wake, which would be the source of cavity heating, accounts for only a small fraction of the injected energy. Instead, Yang and Reynolds [86] found that clusters can exhibit large circulation patterns whereby gas is lifted out of the cluster core and effectively heated by shocks and mixing within the jet cone before flowing back to the cluster core. The role of jet-driven gas circulation in galaxy clusters has been highlighted by several works (e.g., [227,251,257,258]), with Chen et al. [258] suggesting that if low-entropy material can effectively mix with higher entropy material at large radii before returning to the cluster core, then this process can act somewhat akin to a heat pump. Other simulations have found that rising bubbles can lift low entropy material to larger radii, which can result in the formation of cold filaments and clumps, either through direct uplift or by stimulating condensation (e.g., [72,73,85,97,107,134,227,259–262]). Such material can display properties similar to the cold gas observed in galaxy clusters (e.g., [263–268]). Recent MHD simulations show that efficient coupling, facilitated by magnetic fields, can promote angular momentum transfer between the hot gas stirred by jets and cold material, which along with the effects of magnetic braking can have a critical impact on cold gas angular momentum [98,107,108]. Ehlert et al. [98] show that this, in turn, has an impact on cold gas morphology as it promotes the formation of transient cold discs and radial filaments as opposed to the long-lived discs seen when magnetic fields are not included. This cold gas can play an important role in the jet life-cycle as a source of future fuel, with many simulations that implement cold accretion models to power momentum-driven jets (e.g., [85,86,94,96,134,136,139]) finding good agreement between the simulated and observed CC cluster properties.

Assuming the lobe lifetimes are sufficiently long, they can excite g-modes within the cluster atmosphere [66,256,269]. It has been argued that such modes can decay into volume-filling turbulence, which then dissipates to heat the ICM [270,271]. However, the

idealized hydrodynamic simulations performed by Reynolds et al. [272] found that only a small fraction ($\lesssim 10\%$) of the injected energy ends up as turbulence; similar results were also found when including magnetic draping [254]. Other simulations that specifically include jets have found that the level of turbulence produced is subdominant compared to the total injected jet energy, and it is often located in the jet vicinity itself (e.g., [76,77,86,96,273,274]). On the other hand, Martizzi et al. [213] found that jet-driven turbulence can dominate the heating budget in the central regions of the cluster, although this is only when the jet is active; in addition, its contribution becomes negligible at large radii. The inclusion of additional physical processes may also affect the turbulent contribution to the heating budget. The simulations of Beckmann et al. [97], which include spin-driven jets, found that a continuous evolution of the jet direction can drive turbulence over a larger volume, while recent results from Wang et al. [108] found that the inclusion of magnetic fields can promote jet-driven ICM turbulence due to a tighter coupling between the jets and the ICM. Certain simulations that include “cluster weather” [76,275,276] find that large-scale turbulence and bulk motions, such as that driven by orbiting substructures or cosmic accretion, are required in combination with AGN feedback to match both the line of sight velocities and velocity dispersions measured from the Hitomi observations of the Perseus cluster [277,278]. Specifically, while simulated AGN feedback could produce the required levels of velocity dispersion, it was unable to produce other features such as the large velocity shear. Although turbulence may be energetically unimportant, it can play other roles. While the motions of rising lobes can move metals and create elongated distributions (e.g., [84,92,279,280]), jet-induced turbulence has been found to additionally effectively redistribute the metals [84,92]. Moreover, Gaspari et al. [139] showed that subsonic turbulence can promote thermal instability and provide a supply of low angular momentum cold gas to feed the central black hole through “chaotic cold accretion” (see also [93,107,261,281,282]).

2.2. The Role of Environment and Cluster Weather

As we have focused on the general macroscopic evolution of jet lobes in a galaxy cluster, we will now consider the role that the environment can play in shaping lobe properties and how they interact with the ICM in this section. At the simplest level, the ICM can be modeled as a smooth, hydrostatic atmosphere with certain radially dependent density and temperature profiles, with both the absolute density (e.g., [91,283]) and profile slope (e.g., [81,87,112,192,194]) being capable of impacting the jet morphology, propagation, and radio emission properties. Yates-Jones et al. [113] further showed that offsetting the jet launch location from the cluster center and varying the jet direction can impact the jet properties, with the jets encountering a higher density medium typically being shorter and having hot spots with higher surface brightness. Building on this, the ICM is not a simple single-phase gas but rather contains both a hot X-ray emitting plasma, as well as cold filaments and disc structures (e.g., [263–268]). Small-scale simulations ($\lesssim 1$ kpc) of jets show that their interaction with the cold dense clouds or discs can impact jet morphology and dynamics, as well as how effectively the jet couples to the surrounding medium (e.g., [137,138,179,284–286]). While in cluster-scale simulations, the interaction of jets with cold gas can help thermalize the jets [94,136], inhibit their propagation [89], and—in the case of light jets—deflect them, thus making their interaction with the ICM more isotropic [98].

Observations suggest that the ICM is turbulent (e.g., [277,278,287–292]), and while certain simulations suggest that jets can drive local turbulence [86,90,98,108,134,139,213,274], other processes such as those arising from structure formation and sloshing are expected to drive widespread turbulence and bulk motions within the ICM (e.g., [76,89,228,275,293–298]). Meanwhile, tangled magnetic fields may also drive MHD turbulence [88,276,299]. Such “cluster weather” could play an important role in lobe dynamics, with a number of studies attempting to mimic its effects by applying small perturbations to spherically symmetric environments. For example, Krause [198] included small density perturbations to a King atmosphere, finding that this results in differences in back-flow locations and small asymmetries in jet lengths.

O'Neill and Jones [104] performed MHD simulations of jets in a cluster environment containing a tangled magnetic field and an ambient medium in which fluctuations ($\pm 10\%$) in density were superimposed to match observed ICM pressure variations. However, while these fluctuations could perturb the jets, they were insufficient for significantly altering the jet dynamics, with energy only primarily coupling to the ICM within the jet cone. On the other hand, certain works have instead induced ICM gas motions; for example, Bourne and Sijacki [76] used hydrodynamic simulations to consider the long-term evolution of jets and their lobes in a cluster stirred by orbiting substructures. They found that the resulting turbulent and bulk motions could deflect the lobes and increase the mixing of lobe and ICM material when compared to a hydrostatic atmosphere. Ehlert et al. [88] studied the dynamics of jets in an ICM atmosphere including a turbulent magnetic field, and found that while magnetic draping can suppress instabilities, the presence of turbulence can reduce the effects of this draping and, in the buoyant rise phase, disrupt the jet lobes. Meanwhile, Ehlert et al. [98] found that the turbulence can deflect bubbles when assuming the jet is sufficiently light and can provide a more isotropic distribution of lobe positions, which is akin to the observations of multiple generations of lobes in certain galaxy clusters (e.g., [231,242,243,300,301]). However, as we discuss later in this section, only a handful of studies include high-resolution jets in cosmologically evolved cluster environments [89,105,195,228,302,303], and, to the best of our knowledge, only one study includes self-consistently evolved magnetic fields [105].

Observed radio jets can exhibit bent morphologies (e.g., [176,177,304]). Ram pressure due to crosswinds, which arise from the relative motion between the jets and the ICM, is expected to lead to such bending and to result in the formation of narrow-angle-tailed (NAT) and wide-angle-tailed (WAT) radio galaxies [305–309]. Further to this, cluster-merger-driven shocks can also impact jet morphology. Gan et al. [306] compared hydrodynamic and magnetically dominated jets, when subjected to crosswinds and shocks, to mimic cluster weather, finding that while the hydrodynamic jets were unable to survive, the magnetic jets can be significantly bent in the presence of a cross-wind but not solely by a shock front. O'Neill et al. [310] simulated a shock front passing a NAT radio galaxy, finding that the shock action compresses the jets and that the turbulence increases in the jet tails—which, in turn, amplifies the magnetic fields and promotes mixing. Nolting et al. [311,312] extended this work to consider the interaction of merger-like shock fronts impacting generic jet pairs. Shocks moving parallel to the jet axis can significantly affect the jet dynamics, with the post-shock flow potentially impeding or reversing the jet and destroying the cocoon [311]. Similarly, when the jet axis is in the plane of the shock front, the jet lobes are disrupted, and—in the case of active jets—the action of the shock bends them to form a NAT radio galaxy [312].

To self-consistently capture the large-scale turbulence driven by structure formation, full cosmological simulations are necessary (e.g., [144,146,155,158,161,313]). Models have been developed to capture the low accretion state associated with jet feedback; for example, by adding bubbles of hot gas to mimic radio lobes (e.g., [145,166,314]) or by driving bipolar kinetic outflows (e.g., [83,133,165]) that can regulate cooling and star formation within galaxy clusters. However, as discussed in Section 1.3, to capture representative volumes of the Universe over cosmic timescales, these models, by necessity, have to make simplifying assumptions (e.g., low velocities, high mass loading, and/or hydrodynamic decoupling) and must sacrifice resolution in the injection region and/or jet lobes. While the focus of such simulations is on capturing the global effects of the feedback on resolvable scales as opposed to studying lobe inflation and subsequent interaction with the ICM in intricate detail, they are still able to reproduce observational features, such as X-ray rims and cavities [83,166,314], and the effects of cluster weather displacing lobes and promoting mixing [315] that are seen in the high-resolution simulations discussed below. Additionally, cosmological simulations of galaxy clusters have been used, for example by Vazza et al. [316], to study how cluster dynamics can impact the evolution of relativistic electron populations and the magnetic fields produced by radio galaxies (see also [317,318]),

finding that cluster motions interact with radio lobes, affecting their dynamics, constituent magnetic fields, and radio properties.

Brüggen et al. [319] presented some of the earliest simulations that considered radio mode feedback in a cosmologically evolved cluster; this was achieved by injecting thermal energy off-center from the cluster core in order to mimic the inflation of jet lobes in a dynamic environment. However, Heinz et al. [302] presented the first example of high-resolution bipolar jets in a dynamic cluster environment, using non-radiative, hydrodynamic simulations that included 10^{46} erg s^{-1} jets in the center of a cosmologically evolved, $7 \times 10^{14} M_{\odot}$, cluster (while these simulations were non-radiative, those used to produce the initial conditions included radiative cooling and star formation [320]). ICM motions were able to effectively move the lobes and redistribute material, helping to make the energy injection into the ICM more isotropic and helping to replenish the higher-density material at small radii for later jets to couple to. Mock radio and X-ray images exhibit lobe and jet morphologies and features that are seen in real observations. A further parameter study using the same cluster but varying jet power and lifetimes was performed by Morsony et al. [303]. As in Heinz et al. [302], the ICM motions effectively displace, disrupt, and mix the jet lobes, with more powerful jets being able to affect the ICM at larger radii. Interestingly, Morsony et al. [303] found that single AGN outbursts can potentially be realized as multiple independent lobe structures that could otherwise be interpreted as multiple jet outbursts. MHD simulations performed by Mendygral et al. [105] studied 6×10^{44} erg s^{-1} jets in a non-radiative cosmologically evolved cluster that had not undergone any recent mergers. They found that the magnetic field lines were swept up by and draped over the inflated lobes, and that, despite the dynamically relaxed nature of the system, ICM motions can still impact the lobe morphologies and dynamics, with mock radio images exhibiting morphologies akin to WAT radio galaxies with bent jets.

Later work by Bourne et al. [89] presented radiative hydrodynamic moving-mesh simulations of a 4×10^{44} erg s^{-1} jet pair in a low-redshift cosmologically evolved cluster that exhibited a massive cold central disc structure. Mock X-ray images showed classic cavities and bright rim structures, with both the cold gas and cluster weather affecting the lobe structure and location, whereby the latter acted to displace the lobes from their initial trajectory. Shocks were initially driven into the ICM during lobe inflation and, similar to the results in hydrostatic atmospheres (e.g., [76,77,81,110]), $\sim 40\%$ of the jet energy goes into PdV work. However, at later times, the cluster weather can effectively mix the jet and ICM material, with the aid of an in-falling substructure that directly impacts one of the lobes. Bourne and Sijacki [228] extended this work to study different jet powers and perform a more detailed analysis of ICM heating. Figure 4 (taken from Bourne and Sijacki [228]) illustrates the evolution of different power jets and the lobes that they inflate when subjected to cluster weather. Overall, they found that weak shocks and weather-aided mixing dominate the heating budget, and that while high-power jets drove stronger shocks that were more efficient at thermalizing energy, the lower-power jets and the lobes they inflated simply moved material around and were more susceptible to weather-aided mixing (see also [88]). As well as recovering cavities and rims in mock X-ray observations, mock radio images show morphologies ranging from FR-I at low power to FR-II at high power (see also [88,190]).

Both FR-I and FR-II jet morphologies were also realized in the simulations of Yates-Jones et al. [195], who presented the initial results of the CosmoDRAGoN project, which were the first simulations to study relativistic jets in cosmologically evolved clusters. The project performed a parameter study by simulating fixed power jets in a cosmologically evolved cluster (taken from the 300 Project [321]), where both velocity (from non-relativistic to relativistic) and the jet opening angle were varied. They produced mock radio surface brightness maps that illustrate both core-brightened FR-I and edge-brightened FR-II sources. As in previous works that were performed in idealized cluster environments [80], they recovered the result that FR-I sources can arise from wider jets. They further found that slower jets transition from being FR-II to FR-I sources sooner, and they additionally

highlighted that even their most powerful jets eventually transition to FR-I, provided it has a wide enough opening angle. Although to a lesser extent than found in some of the simulations discussed above, Yates-Jones et al. [195] also found that cluster weather can affect lobe morphology, particularly in low power (FR-I) sources once the jet has been switched off and the lobe enters the buoyant rise phase (see also [228]).

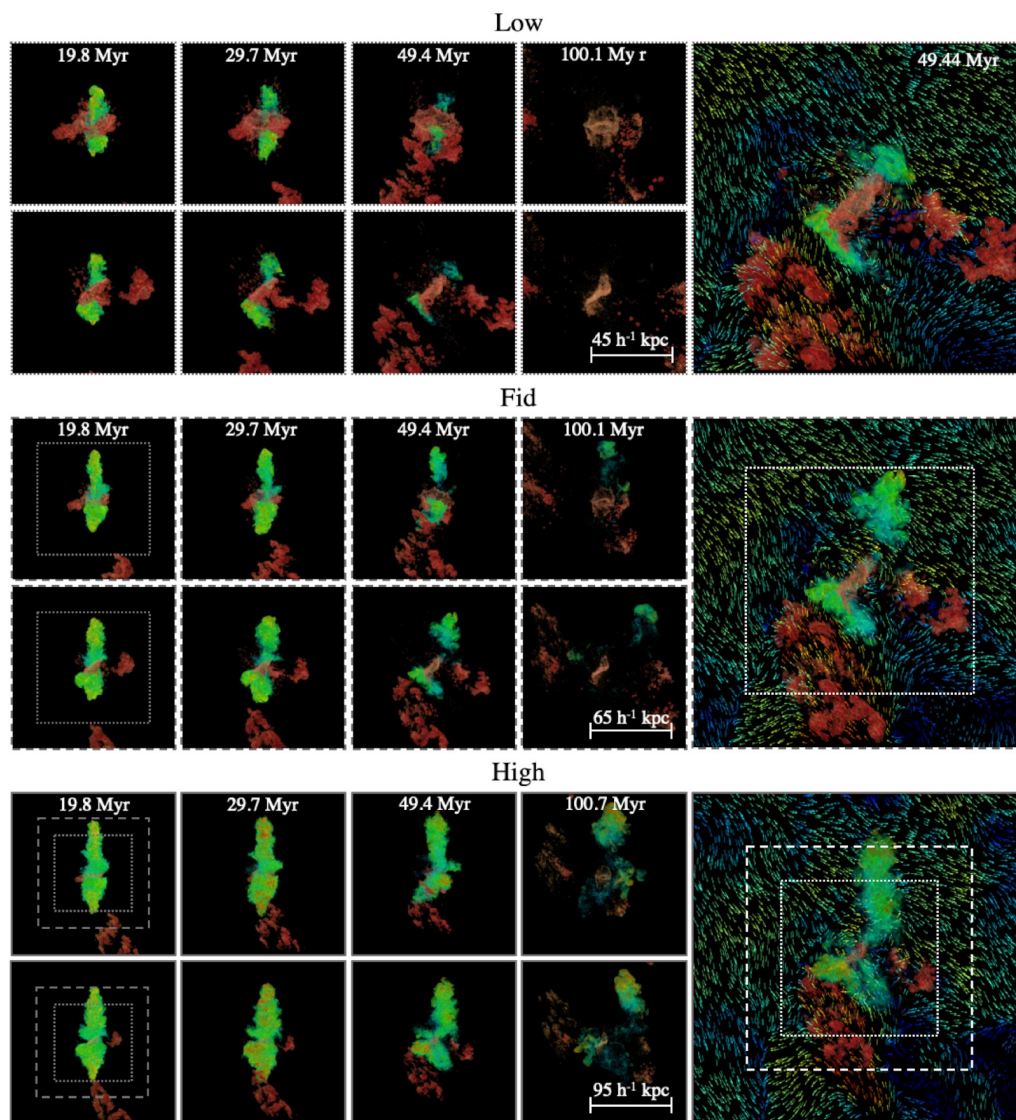


Figure 4. Volume rendering of jet lobes (green) and cold material (red) within a cosmologically evolved galaxy cluster. The top, middle, and bottom rows show low, medium (labeled “Fid”), and high-power jets, respectively. The small panels show the evolution of the jet lobes for two different viewing angles (rotated by 90° about the z-axis with respect to each other), while the large panels also overlay the gas velocity field. Overall, the jet lobes can be displaced, disrupted, and mixed by cluster weather and cold structures, with lower-power jets being more susceptible. (Figure 2 from Bourne and Sijacki [228], CC BY 4.0.)

Vernaleo and Reynolds [322] raised the problem that if jet direction remains unchanged, the low-density path cleared by an early jet episode remains, and later feedback events can escape largely uninhibited, resulting in inefficient coupling between the jet and the ICM. As discussed in Section 2.1.1, various approaches have been taken to improve the coupling between the jets and ICM, as well as to distribute energy more isotropically (e.g., jet precession/reorientation, large opening angles, light jets). Processes driving both precession and jet re-orientation are still somewhat uncertain and whether or not

accretion discs can do this on short timescales is debated [323], with SMBH binaries being an alternative method to drive precession [210,211]. In any case, the simulations discussed in this section, which include dynamic cluster environments, provide an alternative natural relief to the problem by removing the low-density channels, redistributing the lobes, and promoting both mixing and distributing the energy isotropically. In displacing lobes, cluster weather may also provide a mechanism through which to explain the observations of multiple lobe generations having quite different trajectories [231,242,243,255,324].

As already mentioned in Section 2.1, magnetic fields can play a potentially important role in lobe dynamics and interactions. Observations of galaxy clusters show they have an extended magnetic field, with a strength of a few to tens of μG and plasma $\beta \sim 100$ [325,326]. Simulations have shown that bubbles that move above the Alfvén speed can “sweep up” field lines and form a draping layer, in which the magnetic field is amplified. This can suppress instabilities along the direction of the field lines, and can reduce mixing and cause a slowing of the bubble due to magnetic tension (e.g., [88,244–248,254]). Provided the Alfvén speed in the draping layer is sufficiently large compared to the buoyancy or shear velocities, Rayleigh–Taylor and Kelvin–Helmholtz instabilities with wavelengths up to an order of magnitude larger than the layer thickness can be suppressed [245]. While the formation of the draping layer is found to require that the coherence scale of the magnetic field is larger than the bubble [246,248,327], O’Neill et al. [248] also highlighted that the dynamical effect of the draping layer can be reduced by tangled magnetic fields, and that effective amplification requires that the scale on which the fields are tangled is greater than the bubble. Further, the existence of turbulence in the ambient medium can perturb the lobe surface, inhibit magnetic draping, and potentially reduce its effectiveness at suppressing mixing [88]. 3D simulations of jets in tangled magnetic fields have also shown that field lines carried with the jet lobes can align as they are stretched and amplified within the wake of rising bubbles [88,104,105,246]. As mentioned in Section 2.1.2, the ICM magnetic fields can promote coupling between the jet and ambient medium, thus leading to the generation of ICM turbulence [108]. Meanwhile, cold gas angular momentum can also be affected due to magnetic braking and increased coupling between the hot and cold gas phases [98,107,108], which directly impacts cold gas morphology and has implications for SMBH feeding. On the other hand, Bambic et al. [254] found that magnetic tension can inhibit g-modes from decaying into volume-filling turbulence. Finally, it is becoming ever more important to include realistic magnetic fields in cluster simulations to explore microphysical processes such as anisotropic thermal conduction (Section 3.2.1), anisotropic viscosity (Section 3.2.2), and CR transport mechanisms (Section 3.1).

2.3. Open Questions and Future Opportunities

As is clear from the examples given in previous subsections, there is a burgeoning collection of jet models implemented in a range of codes that are currently used in the literature. While many of these models, which include self-regulated feedback, are now able to successfully prevent over-cooling within galaxy clusters, the mechanisms through which this is achieved are not necessarily agreed upon. Certain processes such as the generation of weak shocks are common between simulations, albeit with different relative importance to the heating budget. On the other hand, processes such as mixing and the generation of turbulence appear to be dependent on the jet injection model, resolution, and/or refinement techniques and physics included (e.g., MHD, viscosity, cluster weather, etc.); as such, they are not firmly settled upon. That being said, several works are now finding that the process is expected to be a gentle continuous one [86,98,136,228]. Martizzi et al. [213] showed that the type of Riemann solver used can affect the jet and lobe evolution depending on how diffusive the solver is and on how well the small-scale physical processes, such as mixing, are captured. Additionally, the recent study of Weinberger et al. [200] argued that differences between codes, as well as the differences between the model parameters within a code, create bigger differences in the results than by having high resolution or numerical convergence. As such, while we can accept that jet feedback regulates the

thermodynamics of the ICM, the exact mechanisms are not agreed upon and further constraints need to be placed on jet feedback models that are based on observations. This could be achieved by making more use of mock X-ray and radio images and comparing them to observations of lobe morphologies, distributions, and lifetimes (e.g., [328]). Future X-ray missions with a larger effective area and hence higher signal-to-noise ratio, such as AXIS [329] (<https://axis.astro.umd.edu/> (accessed on 5 June 2023)), could potentially reveal faint cavities at larger radii and could increase the sample size of cavities for a more comprehensive statistical study.

The role of environment is still an open question, only a few works include high-resolution jet feedback in clusters with self-consistently driven weather [89,105,228,302,303], and even fewer include cluster weather and magnetic fields [105]. A parameter space study of different cluster environments, with a range of dynamical states and over cosmologically interesting timescales needs to be considered to fully understand the role that cluster weather can play in displacing lobes and mixing lobe material, and the role that magnetic fields can play in these processes, i.e., to what levels of ICM turbulence are the fields still able to inhibit mixing? In relation to the dynamical state of the system, recent works suggested cluster mergers play an important role in driving the CC/NCC distribution [153,154,330,331], although another recent work found little difference in the dynamical state of CC versus NCC clusters [152]. As highlighted by Bourne and Sijacki [228], if CC clusters are more dynamically quiet, one could expect that lobes are more likely to survive; conversely, if NCCs are dynamically active, it could be that the lobes are more likely to be disrupted, and such behaviour could additionally explain why lobes and bubbles are prevalent in CC clusters [3,332]. However, there is also an observational bias toward being able to detect cavities in CC vs. NCC clusters due to higher X-ray photon counts in the former (e.g., [17,333]). The upcoming XRISM mission [334] (<https://xrism.isas.jaxa.jp/en/> (accessed on 5 June 2023)), a replacement for the ill-fated Hitomi mission (<https://www.isas.jaxa.jp/en/missions/spacecraft/past/hitomi> (accessed on 5 June 2023)), as well as more distant missions such as Athena [335] (<https://www.the-athena-x-ray-observatory.eu/en> (accessed on 5 June 2023)), will provide unprecedented measurements of the ICM velocity structure and turbulence. Such measurements combined with observations of jet lobes should allow us to begin to address the interplay between cluster weather and AGN feedback. It is also possible that such observations, in combination with future simulations that include both ICM motions and models that track the evolution of SMBH/accretion disc angular momentum and jet direction, could play a role in untangling the apparent degeneracy between intrinsic jet direction and cluster weather when determining lobe spatial distributions.

The focus of this review is on the role of AGN feedback in the form of jets, often dubbed the “radio mode” [3], which is expected to be the dominant mechanism for regulating heating and cooling in the ICM. That being said, accreting SMBHs can also release energy in the form of radiation and wide-angled winds that have the potential to impact their environment. Several models employed in cosmological simulations have been developed that invoke separate modes of feedback—“quasar” vs. “radio”—during periods of high and low accretion (in terms of the Eddington rate), respectively, to differentiate between radiatively efficient vs. radiatively inefficient accretion (e.g., [133,145,147,165,166]). However, as highlighted by Qiu et al. [336], studies on the effects of radiative feedback in CCs are lacking. To begin to remedy this, Qiu et al. [336] performed simulations invoking both kinetic outflows and radiative feedback in an idealized Perseus-like cluster. Further, while they invoked a transition accretion rate between radiatively efficient and inefficient modes, they allowed kinetic feedback to occur simultaneously with radiative feedback at high accretion rates and found that to prevent over-cooling of the ICM, kinetic outflows must be active across all accretion rates. Such works suggest there is ample opportunity to further study the role and impact of different feedback channels in shaping CC clusters. In addition, it has been argued by Hardcastle and Croston [36] that the “traditional” paradigm of clearly separated quasar and radio modes being distinguished by whether accretion is radiatively efficient or

inefficient, as well as their role in galaxy formation, is not so clear cut in reality. They cite, for example, populations of high-power radio jets occurring via radiatively efficient accretion at high Eddington ratios (e.g., [36,187,337,338]). Additionally, simulations of radio-mode feedback typically do not explicitly implement different models for low-power/FR-I jets and high-power/FR-II jets. However, their environmental dependence [339] and potential evolutionary sequence [340] could be used to constrain future models of accretion and/or feedback. As such, not only is there scope to consider distinct feedback regimes and how their efficiency couples to the accretion mode, but also, as in Qiu et al. [336], one can further develop and explore models for determining how feedback should be channeled, potentially simultaneously, through different mechanisms (i.e., via radiation, winds, and/or jets). Additionally, self-consistent lobe inflation, its influence on SMBH accretion, as well as the interaction of jets with the interstellar medium of the host galaxies require high-resolution simulations on galaxy scales (e.g., [137,138,179,284–286,341]). These simulations could provide valuable insights and inform future SMBH accretion and jet feedback models on cluster and cosmological scales.

Finally, as highlighted in the introduction, clusters sit at the crossroads of cosmology and astrophysics. In representing the high-mass end of the halo mass function and the culmination of hierarchical structure formation, galaxy clusters have the potential to be used as probes of cosmology [20,21]. Moreover, there are a number of current/future/proposed survey missions (e.g., DES [342] (<https://www.darkenergysurvey.org/> (accessed on 5 June 2023)), SPT-3G [343] (<https://www.anl.gov/hep/spt3g> (accessed on 5 June 2023)), eRosita [344] (<https://www.mpe.mpg.de/eROSITA> (accessed on 5 June 2023)), Advanced ACTPol [345] (<https://act.princeton.edu/> (accessed on 5 June 2023)), Euclid [346] (<https://sci.esa.int/web/euclid> (accessed on 5 June 2023)), Vera C. Rubin Observatory's LSST [347] (<https://rubinobservatory.org/> (accessed on 5 June 2023)), Athena [335] (<https://www.the-athena-x-ray-observatory.eu/en> (accessed on 5 June 2023)), SKAO [348] (<https://www.skao.int/en> (accessed on 5 June 2023)), Simons Observatory [349] (<https://simonsobservatory.org/> (accessed on 5 June 2023)), AXIS [329] (<https://axis.astro.umd.edu/> (accessed on 5 June 2023)), CMB-S4 [350] (<https://cmb-s4.org/> (accessed on 5 June 2023)), CMB-HD [351] (<https://cmb-hd.org/> (accessed on 5 June 2023)), ngVLA [352] (<https://ngvla.nrao.edu/> (accessed on 5 June 2023))) aiming to leverage this opportunity. In order to do this, one typically needs to be able to accurately measure galaxy cluster masses; however, as their mass is dominated by dark matter, this cannot be done directly. One solution is to use cluster observables (e.g., X-ray properties, Sunyaev-Zel'dovich (SZ; [353]) flux, radio emission, weak lensing) to estimate cluster masses, which requires a thorough understanding of the appropriate cluster mass scaling relations. Given that AGN feedback plays such a pivotal role in shaping the ICM properties that give rise to these observables, it is imperative to continue developing cosmological simulations of structure formation that include the robust modeling of jet feedback and additional baryonic physics—such as magnetic fields, CRs, conduction and viscosity—in order to fully understand the cluster observable scaling relations, how they evolve with redshift, and to understand any biases in the derived masses (see e.g., [150,354] for recent examples). Furthermore, in redistributing the material within galaxy groups and clusters, AGN feedback can directly impact the matter power spectrum, knowledge of which is necessary to derive cosmological parameters from weak lensing observations (see discussions in [355–357], and associated references). While existing cosmological simulations typically agree that feedback causes suppression in the matter power spectrum, the relevant levels and scales at which this occurs are model dependent (e.g., [313,355,356,358,359]), with ample scope remaining to constrain the relative importance of jet feedback in groups and clusters.

3. Modeling the Microphysics

Much of our understanding of AGN feedback in galaxy clusters has come from the extensive literature based on the ideal hydrodynamic/MHD simulations that were reviewed in the previous section. However, some of the important physical processes,

such as thermal conduction, viscosity, and CRs, have been largely neglected, and their effects on cluster feedback are relatively poorly understood. As mentioned in Section 1.4, these physical processes, including conduction and viscosity coefficients as well as the propagation of CRs, are determined by the plasma physics that occurs on microscopic scales compared to the sizes of galaxies and clusters, i.e., “microphysics”. In this section, we will review the impact of these microphysical mechanisms on AGN feedback in clusters. We will discuss the roles of CRs in Section 3.1, and the roles of ICM plasma physics in Section 3.2.

3.1. Roles of Cosmic Rays

3.1.1. Motivations for Considering Cosmic Rays

Effects of CRs on the formation and evolution of galaxies and galaxy clusters in the cosmological context have received growing recognition in recent years. In particular, state-of-the-art cosmological simulations have shown that baryonic feedback processes from stars and SMBHs play a vital role in reproducing the observed luminosity functions of galaxies (e.g., [142–147,360–362]). For lower-mass galaxies, starburst-driven galactic outflows are key sources of feedback for suppressing SFRs; however, the physical mechanisms for launching galactic outflows remain elusive. Only recently have simulations shown that outflows with mass loading factors comparable to the observed levels can be driven when the effects of CRs are included [363–365]. These studies further showed that the properties of the galactic outflows, SFRs within the galaxies, as well as the circumgalactic medium (CGM), all sensitively depend on the detailed CR transport processes on microscopic scales [366–368]. These results indicate the importance of CRs in the processes of structure formation, and underscore the necessity for understanding how CRs propagate and interact with the magnetized medium.

On the scales of galaxy clusters, CRs produced via structure formation shocks suffer strong collisional losses in the ICM [369]. Therefore, in general, CRs are not dynamically dominant in galaxy clusters. This is in contrast to the condition on galaxy scales, where CRs are in a rough energy equipartition with thermal gas, magnetic fields, and turbulence. In particular, the amount of CRs within galaxy clusters is severely constrained by the non-detection of gamma-ray radiation of clusters to be less than 10–20 per cent [370–372]. Although CRs are not energetically dominant for clusters as a whole, locally they could still play an important role, e.g., within AGN jets for which the energy composition is largely unknown.

The primary motivation for considering the effects of CRs in the context of AGN feedback can be traced back to the early observations of cluster radio bubbles. When assuming that the AGN jet-inflated bubbles are, approximately, in pressure equilibrium with the ambient ICM, it was found that for some of the cluster radio bubbles, the total bubble pressure that was inferred from the ICM ($\equiv P_{\text{ext}}$) was much greater than the internal pressure from the radiating CR electrons (CRe) (as estimated from the radio observations ($\equiv P_{\text{int}}$) of [14,373–376]). Generally speaking, the AGN bubbles could be supported by magnetic fields, thermal gas, CR protons (CRp), and CRe. Magnetic pressure typically is found in rough equipartition with the radiating CRe and hence is likely subdominant. The low X-ray surface brightness within the AGN bubbles places stringent constraints on the amount of thermal gas with a temperature of several keV [377]. Therefore, these observations suggest that the radio bubbles with high $P_{\text{ext}}/P_{\text{int}}$ ratios are likely supported by either ultra-hot thermal gas or non-radiating CRp. While feedback from thermally dominated bubbles inflated by kinetic-energy-dominated jets is more extensively studied (Section 2), the effects of CR-dominated bubbles are less well understood.

3.1.2. Impact of Cosmic Rays on AGN Feedback Processes

In terms of AGN feedback, jet-inflated bubbles filled with thermal gas versus CRs are expected to exhibit distinct properties that could potentially affect the long-term evolution of CC clusters. First, as CRs are relativistic charged particles, they have a softer equation

of state (EoS) than thermal gas, i.e., with an adiabatic index of $\gamma_{\text{cr}} = 4/3$ (when at the ultra-relativistic limit, see [378] for a more general formalism) rather than $\gamma_{\text{gas}} = 5/3$ —as is typically assumed for ideal, monatomic gas. This means that the enthalpy (given by Equation (2)) of CR-dominated lobes would be $4PV$ compared to $2.5PV$ for a non-relativistic fluid [2], suggesting that CR-dominated lobes do less work on their environment. The different adiabatic index would alter the compressibility of the fluid when CRs are mixed with the thermal gas. Second, because of the additional pressure support from CRs, AGN bubbles filled with CRs are generally less dense and more buoyant, which may uplift the ICM more efficiently than thermal bubbles. Last but not least, the CRs are expected to provide heat to the ICM via both collisional heating (including Coulomb and hadronic processes) as well as collisionless heating (through the CR streaming instability, more details below). All of the above have motivated the investigation of the effects of CRs in the context of AGN feedback.

Regarding modeling the effects of CRs in fluid simulations, there have also been substantial developments over the past decade. In particular, the CR hydrodynamic/MHD framework has matured and become one of the primary numerical tools for studying the roles of CRs in galaxies and clusters (see review by Zweibel [379,380]). In this framework, the CRs are treated as a second fluid, and an additional equation for evolving the CR energy density is solved together with the standard fluid equations, with an extra term ∇P_{cr} in the momentum equation describing the pressure force from CRs. The underlying assumption behind this fluid treatment is that the CRs are well scattered by self-excited waves in the magnetized plasma via the streaming instability [381,382], i.e., the “self-confinement picture” of CR transport, or by waves as part of the cascade of MHD turbulence, i.e., the “extrinsic turbulence picture”. In the self-confinement picture, the CRs can stream relative to the gas down their pressure gradients along the magnetic fields with the Alfvén velocity, $\mathbf{u}_s = -\text{sgn}(\hat{\mathbf{b}} \cdot \nabla P_{\text{cr}}) \mathbf{u}_A$, where \mathbf{u}_A is the Alfvén velocity and $\hat{\mathbf{b}}$ is the unit vector of the magnetic field. Therefore, the transport of CRs can be generally described as advection with the gas plus the flux terms associated with the streaming and diffusion of CRs. When CRs stream, there is also net energy transfer from the CRs to the thermal gas via Alfvén waves, which corresponds to the collisionless CR streaming heating term $-\mathbf{u}_A \cdot \nabla P_{\text{cr}}$. In the extrinsic turbulence picture, on the other hand, the CRs are scattered by forward-propagating and backward-propagating waves. Under the assumption of balanced turbulence, the transport of CRs from these waves cancels out. Thus, CRs essentially advect with the gas, and streaming heating vanishes. CR diffusion in the simulations represents not only diffusion due to gyroresonant scattering, but also CR transport due to unresolved fluctuations in the magnetic field. Regardless of the CR transport model considered, CRs could heat the ICM via collisional processes such as hadronic and Coulomb interactions. In terms of the numerical implementations of the CR hydrodynamic equations, it was recognized in earlier simulations that the CR streaming fluxes would cause spurious oscillations near the extrema of CR pressure distributions unless very stringent simulation timesteps are used [383]. More recently, this numerical difficulty has been overcome by introducing a two-moment method for solving an additional equation for CR fluxes [384,385]. With the above advancement in treating CR physics in large-scale simulations, significant progress has been made in terms of understanding the impacts of CRs on AGN feedback in clusters.

CR heating of the ICM has long been considered a possible source for the suppression of radiative cooling in CC clusters as the CRs injected by the AGN jets could diffuse or stream outside the bubbles and interact with the ICM via collisional and collisionless processes. While early simulations were not able to demonstrate the stabilization of the CCs—partially due to relatively simple setups, as well as the omission of streaming heating [369,386–390]—it was then realized that CR streaming heating via Alfvén waves could be a viable mechanism for heating the ICM, and the amount of CR heating could be sufficient for counteracting radiative cooling and stabilizing the CCs [126,391–393]. In addition to providing heat to the ICM, the CRs also affect the gas dynamics differently from thermal gas. Comparing AGN bubbles inflated by kinetic-energy-dominated jets versus

CR-energy-dominated jets, the former tends to be more elongated, while CR-dominated bubbles tend to be more oblate due to their lower momenta [90,126,315,394] (as shown in Figure 5). While AGN bubbles that are inflated by kinetic-energy-dominated jets are easily deformed by fluid instabilities due to the large shear velocity relative to the ambient medium, CR-jet-inflated bubbles are generally more stable [90,315]. The morphology of the CR-filled bubbles can thus more easily explain the “fat” bubbles with smooth surfaces that are seen in the observations of X-ray cavities, such as the young bubbles near the center of the Perseus cluster. The larger cross-sections of CR bubbles, in addition to the buoyancy of the CRs, result in a more efficient uplift of the ICM. The outward mass transfer driven by CR bubbles alone could bring the fast-cooling gas away from the core and help to reduce cooling near the cluster center [77,90,127,315]. It is worth noting that the dynamical effects arising from having CR-energy-dominated jets are, in many aspects, similar to the light jets discussed in Section 2.1.1 because of their lower momenta compared to kinetic-energy-dominated heavy jets. However, because of the differences in the EoS and heating mechanisms between CRs and thermal gas, the detailed heating processes driven by CR jets and light jets may still be different.

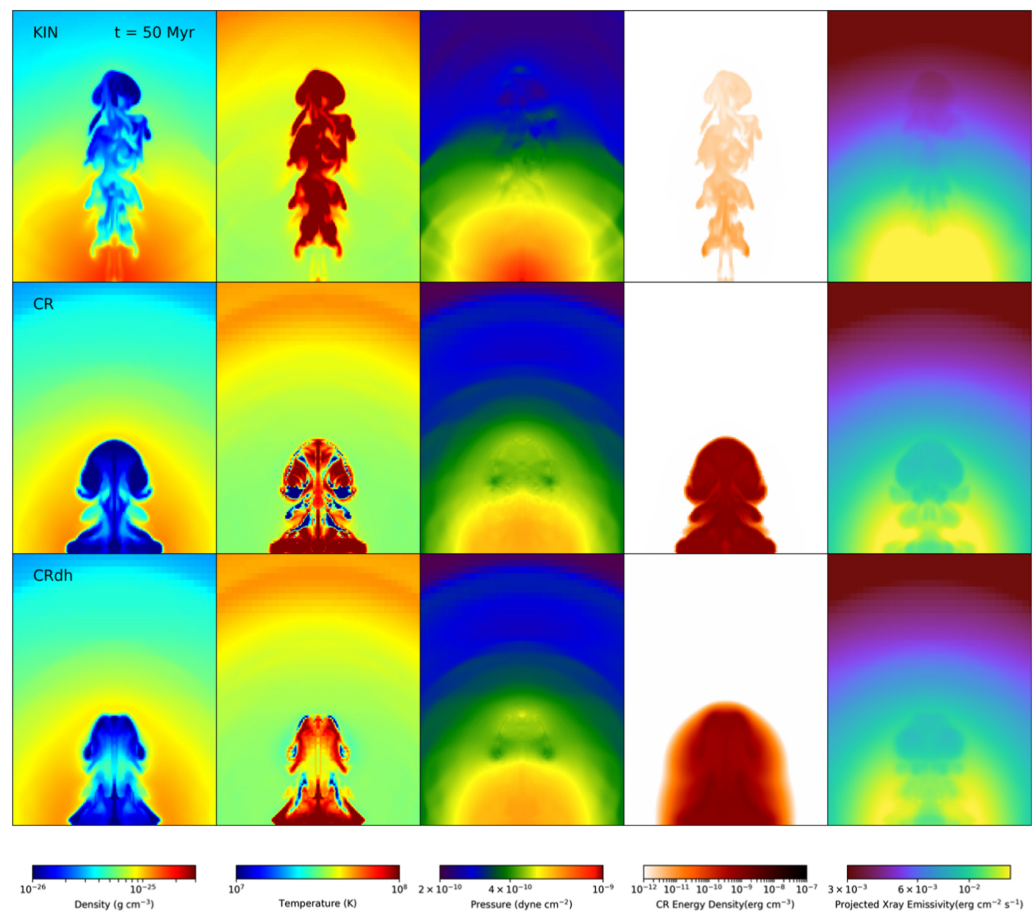


Figure 5. Comparisons of the simulation results with varied jet composition and assumptions for modeling CR transport. The simulations model a single outburst of jet activity (jet power of $5 \times 10^{45} \text{ erg s}^{-1}$ and jet duration of 10 Myr) in a Perseus-like hydrostatic atmosphere. Rows from top to bottom show the results from kinetic-energy-dominated jets (KIN), CR-dominated jets (CR), and CR-dominated jets with diffusion and heating (CRdh). The morphology of jet-inflated lobes tend to be elongated for the KIN case, whereas bubbles inflated by CR-dominated jets are wider. Comparisons between the bottom two panels show that CR heating is more efficient and the amount of cold gas is less for the CRdh case as the CRs can diffuse outside the bubbles and heat the ICM due to hadronic and Coulomb interactions. (Figure 3 from Yang et al. [90], ©AAS, reproduced with permission).

While steady-state models have shown that CR heating could be a viable mechanism for stabilizing the CCs [129,130,393], recent 3D CR hydrodynamic/MHD simulations have brought forward rich information on the interplay between the CRs and the ICM. Ehlert et al. [88] performed 3D MHD simulations of a single AGN outburst with varied jet parameters, and demonstrated that CRs could reproduce the observed diverse morphologies of radio lobes, as well as provide sufficient heating to the ICM. They identified jet energy as the critical parameter for determining the bubble morphology and CR distribution, while jet luminosity was responsible for setting the Mach numbers of shocks. Through using the 3D MHD simulations of self-regulated AGN jets dominated by CRp, Ruszkowski et al. [128] showed that the key to successful CR feedback is the CR transport mechanisms, such as CR diffusion and streaming. With these CR transport processes, CRs could then diffuse or stream outside the low-density bubbles and be in contact with the denser ambient ICM, thus allowing CR heating to operate (shown in the middle and bottom rows of Figure 5). Without CR transport (i.e., if only CR advection is considered), the amount of CR heating would be insufficient, and cooling catastrophes would still occur [107,128]. It was also found that, due to the significant outward mass transfer driven by CR bubbles, it would take longer for the cluster to contract again and trigger another cycle of AGN activity. As a result, the feeding of the central SMBH, and hence the AGN activity, tends to be more episodic when the cluster is regulated by CR feedback [128], whereas the AGN activity tends to be more quasi-continuous for a similar setup with kinetic jet feedback [86]. This implies that the composition of AGN jets is a major source of uncertainties in simulation predictions for cluster evolution, as well as for SMBH growth.

Most of the simulations of CR feedback have focused on CRp-dominated jets; however, observational constraints on the composition of cluster radio bubbles suggest that the distribution is bimodal [14,375,395]. For some bubbles, the internal pressure from radiating CRe is much lower than the external pressure of the ICM ($P_{\text{ext}}/P_{\text{int}} \gg 1$), implying significant pressure support from thermal gas or non-radiating particles. For other bubbles with $P_{\text{ext}}/P_{\text{int}} \sim 1$, the CRe pressure is enough to keep the bubbles in pressure equilibrium with the surrounding ICM. The latter case has been recently investigated by Lin et al. [132]. By comparing the feedback effects of CRp- and CRe-dominated jets, they found that, although CRe cool much faster than CRp due to IC and synchrotron radiation, the CRe-dominated bubbles quickly become thermally dominated ~ 20 Myr after injection. Consequently, the CRe bubbles would not deflate, but they behave similarly to thermal bubbles both in terms of dynamics and ICM heating. This also implies that, for bubbles inflated by CRe jets, there should be a transition of its composition from $P_{\text{ext}}/P_{\text{int}} \sim 1$ to $P_{\text{ext}}/P_{\text{int}} \gg 1$. Future measurements of this pressure contrast as a function of radius for cluster radio bubbles may be a viable way through which to probe the intrinsic composition of AGN jets/bubbles.

While the above simulations have focused on the properties of the hot ICM, more recent studies have looked into how CR-jet feedback could help suppress SFRs and quench central galaxies. Using the FIRE (feedback in realistic environments) simulations of idealized clusters of 10^{12} – $10^{14} M_{\odot}$ with toy models for AGN feedback, Su et al. [396] showed that both turbulent stirring and CR heating are efficient mechanisms for maintaining a stable, low-SFR halo over billion-year timescales, in which the core density and cooling rates are suppressed due to the non-thermal pressure support from turbulence or CRs. Later simulations of bi-polar jet feedback by Su et al. [78] further performed a thorough parameter study on the relevant jet parameters, including the jet energy composition (kinetic, thermal, CR, or magnetic), jet widths, jet precession, injected mass fluxes, and duty cycles. They showed that CR-dominated jets can most efficiently quench the central galaxy, whereas kinetic jets are less efficient unless they have wide opening angles or precession angles. They attributed the efficient CR feedback to three key factors. First, the injected CRs form wider cocoons that suppress inflows and provide pressure support to the gas, resulting in longer cooling times. Second, as shown in recent simulations of thermal instabilities [367,397], the cooling gas would remain diffuse due to the pressure support from CRs, slowing down the “precipitation” of cold gas that would be otherwise accreted onto

the central black hole. Lastly, because CRs can diffuse and stream through the gas, they tend to generate more gentle outflows rather than the more explosive ones expected for a pressure-driven blastwave. As a result, CR feedback is less likely to overheat the cluster cores compared to injections in other energy forms.

3.1.3. Observational Signatures and Constraints

Any successful CR feedback model must satisfy the observational constraints of galaxy clusters. The CRs injected from the AGN jets are expected to produce non-thermal emission that may be detected using multi-wavelength observations. For CRE, they could radiate via synchrotron emission when they interact with magnetic fields as well as via the inverse-Compton (IC) scattering of ambient photons (e.g., the cosmic microwave background (CMB))—this is often called “leptonic emission”. For CRp, their inelastic collisions with ambient nuclei could produce neutral pions, which decay into gamma rays—the so-called “hadronic interaction”. The hadronic process could also produce charged pions, which decay into charged muons then to secondary electrons and positrons together with the production of neutrinos. The secondary particles could again emit due to the synchrotron and IC radiation.

Radio observations near the cluster cores could potentially provide constraints on the amount and distributions of CRs injected by AGN. Indeed, some clusters are known to host radio mini-halos (e.g., [398–400]), which are faint, diffuse radio structures extending ~ 50 – 300 kpc, and which are characterized by steep radio spectra with typical spectral indices of $\alpha > 1$ (as defined in $S_\nu \propto \nu^{-\alpha}$, where S_ν is the flux density and ν is the frequency). The physical origin of the radio mini-halos is not yet fully understood. Generally speaking, because the cooling times of CRE are typically shorter than the time it takes to transport them to the extent of the observed mini-halos, these CRE would need to be produced in situ or be re-accelerated from an old seed population. In terms of the emission mechanisms, the mini-halos could originate from CRE that are produced either via hadronic interactions between CRp and the ambient ICM (e.g., [401–403]), via turbulence reacceleration (e.g., by sloshing motions [296,404]) or via AGN activity [405]). For the latter scenario, Jacob and Pfrommer [130] investigated, in detail, the predicted radio emission from a steady-state model of CR plus conductive heating. From comparisons with an observed sample of mini-halos, they showed that CC clusters hosting mini-halos cannot be heated by CRs, but CCs without mini-halos can. To this end, they proposed a scenario where CC clusters with recent AGN injections should host radio “micro-halos”; furthermore, after the CRs diffuse or stream out of the cores, CR heating becomes insufficient and mini-halos light up due to the secondary particles produced via hadronic interactions. More simulations on this front are needed in order to verify this picture, as well as to understand the source of the seed CRE and the interplay between AGN feedback and sloshing motions in clusters (e.g., [406,407]). Recent radio observations at low frequencies by LOFAR (<https://lofar-surveys.org> (accessed on 5 June 2023)) have also enabled constraints on the interaction between the CRs and the ICM. For example, Brienza et al. [408] found signatures of old AGN-jet-inflated bubbles that retain “mushroom-like” structures over hundreds of Myr timescales. The bubbles are not thoroughly mixed with the ambient ICM, suggesting a suppression of fluid instabilities and CR diffusion at the bubble surface, most likely under the influence of magnetic fields.

As mentioned in Section 3.1.1, the non-detection of gamma-ray emission from galaxy clusters has strongly limited the amount of hadronic CRs in clusters, which must be within a few per cent compared to the thermal pressure for clusters as a whole [370,371]. Cosmological simulations by Vazza et al. [409] investigated quasar-, jet-, and radio-mode feedback, and they found successful models that could reproduce X-ray observations of the cluster gas and yield gamma-ray emission below the upper limits set by Fermi. Other simulations including CR-dominated jets [90,128] showed that, for CR heating to balance radiative cooling, only a small amount of CR pressure support is required. In their successful self-regulated models, CR streaming is a critical ingredient as it would act to

remove energy from the CRs and to heat the gas, thus reducing the amount of CR pressure support to levels that are consistent with the gamma-ray constraints. Recent simulations by Beckmann et al. [410] have also investigated the roles of CR-dominated jets in terms of ICM heating and observable signatures. Consistent with previous works, Ji et al. and Butsky et al. [367,397] found that CRs can modify the development of thermal instabilities and can help to maintain gas in the hot and warm phases. However, they found that the simulations that included CR-dominated jets would produce gamma-ray emission in excess of the current observational limits due to the formation of an extended, CR-pressure supported warm nebula; meanwhile, AGN jets with lower CR fractions ($\sim 10\%$) were allowed and could successfully halt the strong cooling flows. The discrepancies in the results are not yet fully understood, but we list here two possible reasons that might play a role: First, the simulations in Ruszkowski et al. [128] used the mass dropout technique for the cold gas, while Beckmann et al. [410] retained cold gas in their simulations. Since the gamma-ray emission produced by hadronic interactions is proportional to the product of the CRp number density and the gas density, it is conceivable that the latter simulation would produce greater gamma-ray emission if the contribution from the cold gas is significant. Another difference between these simulations is that, in contrast to typical AGN feedback prescriptions that connect the jet properties with the black hole accretion rates, Beckmann et al. [410] additionally modeled the influence of the black hole spin on the jet directions (as is discussed in Section 2.1.1). To this end, their jets are more randomly oriented and could not penetrate and deposit the heat to larger radii compared to previous self-regulated simulations with jet precession along a fixed direction. This might have caused less effective feedback and the CR-pressure-supported warm nebula that produces the excess gamma-ray emission. More detailed studies are needed in order to pin down this issue. Regardless, the observational gamma-ray limits will provide crucial constraints on the amount of CRs allowed in the cluster cores.

3.2. Roles of Plasma Physics of the Intracluster Medium

While a lot of our understanding of AGN feedback has been gained via fluid simulations, the ICM is in fact a weakly collisional, magnetized plasma. The Coulomb mean free path of the ionized gas in the ICM is [411]

$$\lambda_{\text{mfp}} \equiv \frac{3^{3/2}(k_{\text{B}}T)^2}{4\pi^{1/2}n_e e^4 \ln \Lambda} \approx 23 \text{ kpc} \left(\frac{T}{10^8 \text{ K}} \right)^2 \left(\frac{n_e}{10^{-3} \text{ cm}^{-3}} \right)^{-1}, \quad (4)$$

where n_e is the electron number density and T is the temperature of the ICM. Typical values for λ_{mfp} range from ~ 0.1 kpc near the cluster cores to ~ 10 kpc in the cluster outskirts. The ratio between the collisional mean free path and the size of the system is thus $\lambda_{\text{mfp}}/L \sim 0.1\text{--}10^{-3}$. For regions in clusters with $\lambda_{\text{mfp}} \ll L$, the ICM could be safely approximated as a collisional fluid; for other regions where $\lambda_{\text{mfp}} \lesssim L$, the ICM is instead weakly collisional. In addition, as discussed in Section 2.2, the ICM is magnetized with typical magnetic field strengths to the order of 1–10 μG [325]. Even though the magnetic field is not dynamically dominant (plasma beta $\beta \equiv P_{\text{th}}/P_{\text{B}} \sim 100$), it significantly constrains the motions of the charged particles within the ICM as the Larmor radius of their gyro motions (r_{g}) is typically more than ten orders of magnitude smaller than the collisional mean free path, i.e., $r_{\text{g}} \ll \lambda_{\text{mfp}} \lesssim L$. As a result, transport processes such as viscosity and thermal conduction in this weakly collisional, magnetized ICM are expected to be anisotropic along magnetic field lines, whereas the perpendicular transport is significantly suppressed. In addition, the parallel transport coefficients along the field lines are mediated by plasma physics that occur on the microscopic scales of the particles' gyroradii, i.e., the microphysics. Over the past decade, there has been substantial progress in terms of our understanding of the microphysical plasma processes. These developments and the plasma properties of the ICM have been summarized in a recent review article [412]. Here, we will focus on the discussion about how these plasma effects could alter the standard hydrodynamic picture of AGN feedback that is described in the previous sections.

3.2.1. Influence of Thermal Conduction on AGN Feedback

Thermal conduction has long been proposed as one of the heating mechanisms in CC clusters as it could potentially channel the heat from the reservoir of thermal energy in the cluster outskirts toward the cluster cores (e.g., [119,120]). While balancing radiative cooling by conductive heating alone would require fine-tuning (e.g., [119,413]), it may provide partial heating to the CCs and could relieve the burden on the AGN. Indeed, certain theoretical models have considered conductive heating together with AGN jet heating (e.g., [129,414]). However, the fact that thermal conduction occurs anisotropically in the magnetized ICM has introduced further complications. In particular, it was found that the anisotropic conduction in the conditions of CCs would trigger the heat-flux-driven buoyancy instability (HBI; [415]), which would act to reorient the magnetic field lines in the direction that is perpendicular to the temperature gradients. In CCs, where the temperature gradients are primarily radial, the HBI would then wrap the field lines in the azimuthal direction, which would shut off the conductive heat fluxes from the cluster outskirts and potentially worsen the cooling-flow problem [121].

Fortunately, later simulations have found that the HBI could likely be circumvented by turbulent motions in the ICM [416], which could originate from a variety of sources, including *g*-modes excited by galaxy motions [293] and AGN jet-driven turbulence [95]. These works found that the turbulent motions can efficiently randomize the field lines and resume the heat fluxes to an effective Spitzer fraction (the suppression factor compared to the full Spitzer value) of $\sim 1/3$, which is consistent with that of the fully tangled magnetic fields. In this case, both conductive heating and AGN heating contribute to counteracting the radiative cooling in the CCs. The amount of conductive heating, though, is likely to be subdominant compared to direct AGN heating, which is shown by both the idealized cluster simulations [95] and the cosmological simulations [124]. Recently, simulations by Beckmann et al. [125], which include black-hole-spin-driven AGN jets, instead found that AGN jet-driven turbulence is only able to randomize the field lines close to the cluster cores, but the HBI could still operate outside ~ 50 kpc and isolate the CCs from conductive heating. To this end, they concluded that conductive heating plays a negligible role in regulating the radiative cooling in CCs. Again, the difference in the above results could be due to the different implementations of the AGN feedback prescriptions (see discussion in Section 3.1.3). In addition, the field-line wrapping effect of the HBI would likely be washed out if other sources of ICM turbulence from cosmic accretion or galaxy motions are included in the simulations. All of these simulations, including anisotropic conduction, have assumed full Spitzer conductivity along the field lines. If the conductive coefficient in the ICM is significantly suppressed due to microphysical plasma processes, as is suggested by recent particle-in-cell (PIC) simulations (e.g., [417–419]), then the contribution from conductive heating would be even more inhibited.

3.2.2. Influence of Viscosity on AGN Feedback

While AGN-jet-inflated bubbles in purely hydrodynamic simulations are easily deformed and disrupted by Rayleigh–Taylor and Kelvin–Helmholtz instabilities (see discussion in Section 2.1.2), the observed AGN bubbles are generally more regular and do not exhibit clear signs of instabilities. For instance, the young X-ray cavities near the center of the Perseus cluster have smooth surfaces, and the more evolved ghost cavity in the northwest direction does not break up but shows a flattened morphology [420]. These observed properties of the AGN bubbles have posed challenges to purely hydrodynamic modeling of jet-inflated bubbles and call for the consideration of additional mechanisms to suppress hydrodynamic instabilities such as magnetic fields (e.g., [244–248]) or viscosity [114,240]. In addition, the morphology of the H_{α} filaments behind the northwest ghost bubble in the Perseus cluster suggests that they may be dragged up by the buoyantly rising bubble [421]. These observations have motivated the consideration that the ICM may have a non-negligible level of viscosity.

Indeed, viscous simulations by Reynolds et al. [114] have demonstrated that isotropic viscosity could act to suppress the fluid instabilities and prevent bubbles from incurring disruption. Additionally, the streamlines behind the simulated bubbles are consistent with the coherent structure of the observed H_α filaments. Subsequent work by Sijacki and Springel [240] also showed that the properties of AGN-jet-inflated bubbles, including their morphology, maximum distance from the cluster center, and survival time, depend sensitively on the level of ICM viscosity. However, this is not the full story because viscosity is expected to be anisotropic in the magnetized ICM, and the parallel viscosity coefficient mediated by microphysical plasma processes should be considered when modeling the evolution of AGN bubbles. To this end, the simulations conducted by Dong and Stone [115] studied the buoyant evolution of initially static bubbles and included anisotropic viscosity along magnetic fields of different initial geometries. They found that anisotropic viscosity can efficiently suppress fluid instabilities in the direction parallel to the magnetic field while having little effect on the instabilities that develop perpendicular to the field. As a result, the fate of the bubbles is sensitive to the assumed geometry of the magnetic field. While the bubbles can be stabilized by viscosity along the initially horizontal fields or toroidal fields that are confined to the bubble interior, the bubbles are deformed in the case of vertical field geometry.

Kingsland et al. [117] further investigated the effects of anisotropic viscosity on AGN-jet-inflated bubbles in a more realistic, tangled magnetic field geometry and additionally considered the microphysical plasma effects that were discovered from recent PIC simulations. Specifically, for a weakly collisional, magnetized plasma such as the ICM, the viscosity originates from the pressure anisotropy that arises from the conservation of the adiabatic invariants on timescales much greater than the inverse of the ion gyrofrequency [422,423]. Recent plasma simulations have found that when the pressure anisotropy becomes greater than thresholds that are on the order of $1/\beta$ (where β is the plasma beta value), microinstabilities—including the firehose and mirror instabilities—would be triggered and the pressure anisotropy would be pinned at the marginal-stability thresholds, effectively suppressing the parallel viscosity coefficients (see [412] and the references therein). Incorporating these latest findings into Braginskii-MHD simulations, Kingsland et al. [117] found that, for anisotropic viscosity with full Braginskii values [424], the integrity of the bubbles can be preserved because the viscosity along the tangled field lines can suppress the instabilities in multiple orientations on the bubble surface (see Case C in Figure 6). However, when suppression of the parallel viscosity coefficients by the microinstabilities is considered, the suppression is so strong that the bubbles are deformed the same as in the inviscid case (Case D in Figure 6). This is because the plasma beta value in the bubble interior could be as high as 10^4 , which dramatically limits the amount of pressure anisotropy and viscosity in the vicinity of the bubbles. Therefore, they concluded that Braginskii/anisotropic viscosity is unlikely to be the primary mechanism for preserving the coherence of AGN bubbles, but other mechanisms (e.g., magnetic fields) are still required to reproduce the morphology of the observed bubbles. This further emphasized the importance of modeling the ICM plasma properties as the bubble evolution has a direct influence on their ability to uplift the ICM, as well as where the bubbles deposit the heat provided by the AGN.

Finally, since the pressure anisotropy in the ICM provides an anomalous “effective” viscosity [412], there could be heating associated with the parallel viscous dissipation of gas motions (the so-called gyroviscous heating). By assuming the pressure anisotropy is pinned at the marginal stability thresholds in the turbulent ICM, Kunz et al. [425] showed that this mechanism could provide heating rates comparable to the radiative cooling rates. Recent PIC simulations have further studied the detailed process of how particles can be gyroviscously heated by large-scale turbulent fluctuations via magnetic pumping [426]. More studies would be required in order to integrate these microphysical phenomena into the large-scale turbulence models of the ICM for a full assessment of the gyroviscous heating of the ICM.

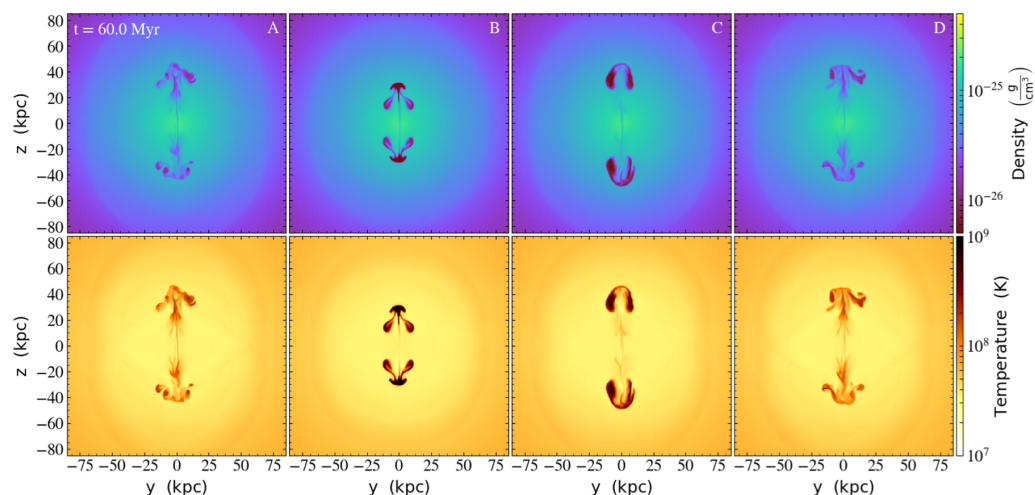


Figure 6. Impact of assumptions about ICM viscosity on the evolution of AGN-jet-inflated bubbles. Cases (A–D) show the simulations with no viscosity, isotropic viscosity with full Spitzer values, anisotropic viscosity with full Braginskii values, and anisotropic viscosity limited by microinstabilities, respectively. While the hydrodynamic instabilities are suppressed by viscosity in cases (B,C), when the parallel viscosity along the magnetic field lines is suppressed by microinstabilities (case (D)), the viscosity is strongly limited and the bubbles are deformed as in the inviscid case (A). This illustrates the importance of modeling the ICM microphysics in AGN simulations. (Figure 1 from Kingsland et al. [117], ©AAS, reproduced with permission).

3.2.3. Heating by Sound-Wave Dissipation

In the X-ray images of the Perseus cluster, there are ripple-like structures that were interpreted as sound waves driven by central episodic AGN outbursts [421,427]. Motivated by this observational finding, early simulations have shown that the viscous dissipation of sound waves could be a viable mechanism for heating the ICM [237,238], although certain studies found that their energy content may be small due to viscous damping [240]. Sound-wave heating is an attractive solution for the cooling-flow problem because it could heat the ICM isotropically as the waves propagate from the cluster center outward. The question of whether sound-wave dissipation could be a significant contributor to ICM heating could be broken down into two parts: how much of the injected energy by the AGN can be stored in the form of sound waves, and how do the waves propagate and dissipate in the ICM? We will summarize the progress along these lines below.

Several recent simulations have been conducted in order to quantify how much of the injected AGN energy can be converted into sound waves. Using simulations of spherical injections into a uniform medium with varied injected energy and duration, Tang and Churazov [226] found that the fraction of AGN energy that goes into sound waves is dependent on the duration of the injection. When the duration is long, i.e., when the solution approaches the “slow piston” limit, the energy of the sound waves is close to zero. For instantaneous outbursts (duration approaches zero), the energy fraction of the sound waves is $\lesssim 12\%$. Bambic and Reynolds [239] further performed a parameter study using axisymmetric simulations of an AGN outburst with bipolar jet geometries. Figure 7 is taken from their paper and illustrates the generation of sound waves by a jet. They found that up to $\sim 25\%$ of the injected energy could be stored in the form of sound waves for optimal parameter combinations. Using the jet parameters informed by previous self-regulated AGN feedback simulations, Wang and Yang [428] found that the production efficiency of compressional waves (including weak shocks and sound waves) is $\sim 9\%$ for a single AGN energy injection. However, this production efficiency drops to less than $\sim 3\%$ in self-regulated feedback simulations. This is because, with repeated AGN outbursts, shocks are almost continuously generated and their energy dominates that of the weak shocks. To this end, shock dissipation together with the destructive interference of sound waves would act to reduce the amount of energy in compressional waves. Considering the above

effects, they concluded that sound-wave heating may be a subdominant source of heating in CC clusters. However, Wang and Yang [428] have assumed powerful AGN injections via bipolar jets. Using the viscous simulations of a single spherical, gentle (longer-duration) AGN outburst, Choudhury and Reynolds [429] found that the $\sim 20\%$ of the injected power can be carried away by sound waves. Overall, the above results suggest that the production efficiency of sound waves is $\sim 3\text{--}25\%$, depending on how the feedback energy is injected (e.g., geometry, duration) and how the waves generated by repeated events interfere with each other. Finally, the above estimates are derived based on the hydrodynamic treatments of the ICM, and there may be additional plasma effects that need to be taken into account in terms of sound-wave generation. For instance, Kempster et al. [430] have performed Braginskii-MHD simulations including CRs, and showed that the phase shifts between CR pressure and density fluctuations would generate instabilities when the CR fraction is greater than a threshold proportional to the plasma beta. Therefore in an ICM with high plasma beta values, this mechanism could potentially be important for exciting sound waves.

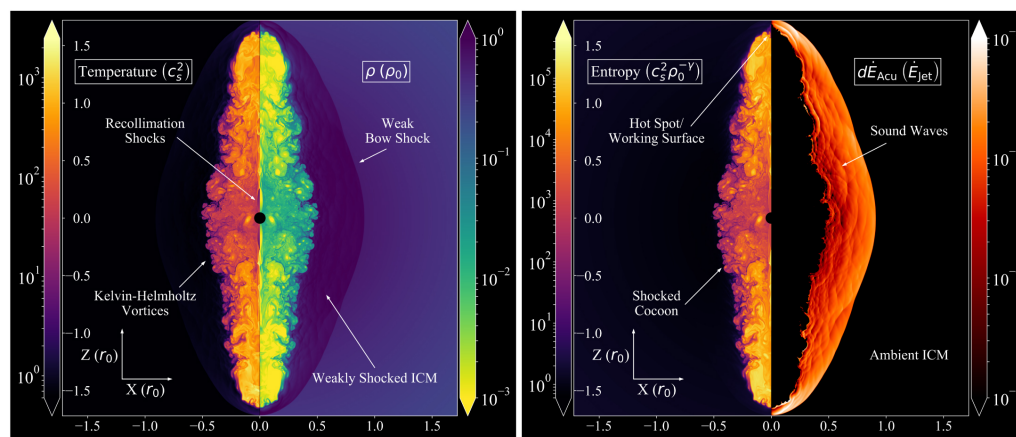


Figure 7. Illustration of the sound waves generated by jets. The left-hand panel shows the jet and cocoon temperature and density structure, with key features labeled. The right-hand panel shows jet entropy and the acoustic flux density, with the structure in the latter illustrating the production of sound waves within the shocked ICM material. (Figure 1 from Bambi and Reynolds [239], ©AAS, reproduced with permission).

Another question to address is the propagation and dissipation of sound waves in the ICM. Pioneering work by Fabian et al. [420] showed that nearly adiabatic acoustic waves will damp within one wavelength of their source and will overheat the cluster core if thermal conductivity and viscosity are at their full Braginskii values. If this is true, it would pose challenges to the interpretation of observed ripples propagating sound waves. Assuming thermal conduction is completely suppressed and viscosity is reduced to 10% of the Braginskii value, heating due to sound-wave dissipation could then balance radiative cooling for a power-law spectrum of waves. More recently, Zweibel et al. [241] revisited this topic by additionally taking into account the self-limiting nature of electron thermal conduction, differences between electron and ion temperatures, and the plasma effects from kinetic theories. Though the kinetic effects somewhat suppress damping and mitigate the problem of wave propagation, the conclusions reinforced that, in order for acoustic waves to propagate to large radii and to heat the CC, drastic suppression of the transport coefficients is needed. Such reduced transport could come from increased effective collisionality of the ICM due to magnetic field fluctuations on small scales driven by plasma instabilities (e.g., [417,431]). However, future works are still required to fully assess the generation and damping of acoustic waves under the influence of plasma instabilities, as well as for the realistic sources and geometries.

3.3. Open Questions and Future Opportunities

Following the discussion in Section 3.1, it is clear that constraining the composition of AGN jets and bubbles is one of the key questions to address since different jet compositions have different dynamical and thermal impacts on the ICM, which would then affect the long term evolution of clusters, as well as the SMBH accretion histories. One of the proposed ways to distinguish the AGN bubbles dominated by ultrahot thermal gas and CRs is by using the SZ effect [353], which arises due to the IC scattering of the CMB photons by electrons in the ICM. It was shown by Pfrommer et al. [432] that, because the SZ increment/decrement at observed frequencies below ~ 400 GHz is greater for thermal gas than for a power-law distribution of relativistic CRs, the CR-dominated bubbles would show a clear deficit in the SZ signal—thus creating “SZ cavities” that are similar to the X-ray cavities. In contrast, there should be no evident SZ cavities associated with the thermally dominated bubbles. The level of the SZ deficits is estimated to be ~ 6 – 9% for sightlines passing through the CR bubbles [90]. Recent simulations by Ehlert et al. [299] have also examined the potential systematic effects when modeling the SZ signal of AGN bubbles. They found that the cut-out method for identifying bubbles would fail to account for the shock-enhanced pressure cocoon outside the bubbles, especially when the jets are nearly aligned with the line of sight. Additionally, in this case, the kinetic SZ effects become relevant and need to be modeled. Observationally, the detection of SZ cavities in the cluster MS 0735.6 + 7421 was first reported by Abdulla et al. [433] and later confirmed by Orłowski-Scherer et al. [434], which suggests that the AGN bubbles in MS 0735.6 + 7421 are supported by the non-thermal pressure provided by CRs, though thermal gas with a temperature greater than ~ 150 keV has not yet been ruled out. High-resolution, high-sensitivity SZ observations such as ALMA [435] (<http://almaobservatory.org/en/home/> (accessed on 5 June 2023)), MUSTANG-2 [436] (<https://greenbankobservatory.org/science/gbt-observers/mustang-2/> (accessed on 5 June 2023)), and NIKA2 [437] (<https://ipag.osug.fr/~ponthien/NIKA2/Welcome.html> (accessed on 5 June 2023)) will be able to obtain important constraints on the composition of a larger sample of AGN bubbles in the near future.

Much of the detail of the AGN feedback processes relies on our understanding of the plasma properties of the ICM. While recent PIC simulations have allowed tremendous progress on the theoretical front, observational constraints are demanded in order to pin down what is the best description for the weakly collisional, magnetized ICM. In particular, constraints on the transport coefficients would be key to understanding the ICM properties. For instance, previous X-ray observations of the sharpness of cold fronts have ruled out ICM conductivity at the full Braginskii value (e.g., [438]). Comparisons between simulation predictions and observations also suggest that either full Braginskii viscosity or isotropic Spitzer viscosity (with a suppression factor $f_{sp} \sim 10\%$) is consistent with the observed cold fronts [439]. Observations of the ram-pressure stripping tails of galaxies infalling into the ICM could also be used to probe the viscosity of the ICM. Previous studies [440,441] have placed constraints on the ICM viscosity, at a level of $f_{sp} \sim 5$ – 20% compared to the full Spitzer value (assuming isotropic viscosity). Observations of the ICM turbulence spectrum down to the scale where transport processes become relevant could also yield constraints on ICM viscosity. Through using the Chandra observations of the Coma cluster and inferring the turbulence spectrum from X-ray surface brightness fluctuations, Zhuravleva et al. [442] found that the ICM viscosity must be strongly suppressed, with an effective isotropic viscosity of $f_{sp} \sim 0.1$ – 10% . Improved measurements from upcoming and future X-ray missions including XRISM [334] (<https://xrism.isas.jaxa.jp/en/> (accessed on 5 June 2023)), AXIS [329] (<https://axis.astro.umd.edu/> (accessed on 5 June 2023)), LEM [443] (<https://www.lem-observatory.org> (accessed on 5 June 2023)), Athena [335] (<https://www.the-athena-x-ray-observatory.eu/en> (accessed on 5 June 2023)), and Lynx [444] (<https://www.lynxobservatory.com> (accessed on 5 June 2023)) will provide crucial constraints on the transport processes in the ICM and hence provide further understanding about the AGN feedback mechanisms.

4. Concluding Remarks

Thanks to cutting-edge numerical simulations with increasing resolutions and complexities in terms of input physics, tremendous progress has been made over the past decade regarding the understanding of the macro- and microphysics of radio jet feedback in galaxy clusters. As reviewed in this article, while extensive studies have reinforced the importance of jet feedback in suppressing cooling flows in massive clusters, many details are not yet fully understood. In particular, the relative importance among the various heating mechanisms, including mixing, shocks, sound waves, turbulence, and CRs, as well as their subsequent impact on SMBH feeding and cluster evolution, critically depend on the properties of the jet injections (e.g., composition, duration, direction) and how the lobes are inflated and evolve with time (e.g., whether the hydrodynamic instabilities can be suppressed, and whether the bubbles could be preserved to large radii by magnetic fields or viscosity). Some of the open questions and future opportunities have been discussed in Sections 2.3 and 3.3. Here we conclude by highlighting some of the key unresolved questions:

- What are the next steps for improving sub-grid AGN models in numerical simulations? Do we require other feedback channels in addition to radio jets to regulate galaxy clusters?;
- How exactly is the SMBH feeding and feedback cycle established across such a huge dynamical range? What is the best way to model the evolution of black hole spins and couple them to jet feedback?;
- How does environment (e.g., cluster weather, magnetic fields) impact the effectiveness and mechanisms through which jet feedback couples to the ICM, and how does it impact lobes distributions, lifetimes, and morphologies?;
- What is the composition of AGN jets and bubbles? Are the jets light or heavy? Are they energetically dominated by ultra-hot thermal gas, CRp, CRe, or magnetic fields? How does the composition vary (e.g., with morphological types, environment, launching mechanisms)? How does the jet composition impact the AGN feeding and feedback processes?;
- How important are CRs in the process of AGN feedback and how can they be constrained by using observations of the non-thermal emission they produce? What is the best way to model CR transport in the turbulent, magnetized ICM?;
- What is the valid prescription for modeling the weakly collisional, magnetized ICM plasma? What are the levels of thermal conductivity and viscosity in the ICM?;
- Can we extrapolate our knowledge about cluster feedback down to scales of galaxy groups and elliptical galaxies? Does AGN feedback operate in the same way across different mass scales?

Author Contributions: Both authors contributed to Sections 1 and 4. M.A.B. was the main contributor to Section 2 and H.-Y.K.Y. was the main contributor to Section 3. All authors have read and agreed to the published version of the manuscript.

Funding: M.A.B. was supported by the Science and Technology Facilities Council (STFC). H.-Y.K.Y. was supported by the National Science and Technology Council (NSTC) of Taiwan (109-2112-M-007-037-MY3) and the Yushan Scholar Program of the Ministry of Education (MoE) of Taiwan.

Acknowledgments: We are grateful to the anonymous reviewers for their constructive reports that helped to improve the clarity and breadth of this work. We also thank Filip Huško, Yuan Li, and Chris Bambic for allowing use of their figures, as well as Chris Reynolds, Debora Sijacki, Franco Vazza, and Sophie Koudmani for their useful advice, comments, and feedback on the article.

Conflicts of Interest: The authors declare no conflict of interest.

References

1. Fabian, A.C. Cooling Flows in Clusters of Galaxies. *Annu. Rev. Astron. Astrophys.* **1994**, *32*, 277–318. [[CrossRef](#)]
2. McNamara, B.R.; Nulsen, P.E.J. Heating Hot Atmospheres with Active Galactic Nuclei. *Annu. Rev. Astron. Astrophys.* **2007**, *45*, 117–175. [[CrossRef](#)]
3. Fabian, A.C. Observational Evidence of Active Galactic Nuclei Feedback. *Annu. Rev. Astron. Astrophys.* **2012**, *50*, 455–489. [[CrossRef](#)]
4. Best, P.N.; von der Linden, A.; Kauffmann, G.; Heckman, T.M.; Kaiser, C.R. On the prevalence of radio-loud active galactic nuclei in brightest cluster galaxies: Implications for AGN heating of cooling flows. *Mon. Not. R. Astron. Soc.* **2007**, *379*, 894–908. [[CrossRef](#)]
5. Mittal, R.; Hudson, D.S.; Reiprich, T.H.; Clarke, T. AGN heating and ICM cooling in the HIFLUGCS sample of galaxy clusters. *Astron. Astrophys.* **2009**, *501*, 835–850. [[CrossRef](#)]
6. Birzan, L.; Rafferty, D.A.; Nulsen, P.E.J.; McNamara, B.R.; Röttgering, H.J.A.; Wise, M.W.; Mittal, R. The duty cycle of radio-mode feedback in complete samples of clusters. *Mon. Not. R. Astron. Soc.* **2012**, *427*, 3468–3488. [[CrossRef](#)]
7. Birzan, L.; Rafferty, D.A.; McNamara, B.R.; Wise, M.W.; Nulsen, P.E.J. A Systematic Study of Radio-induced X-ray Cavities in Clusters, Groups, and Galaxies. *Astrophys. J.* **2004**, *607*, 800–809. [[CrossRef](#)]
8. David, L.P.; O’Sullivan, E.; Jones, C.; Giacintucci, S.; Vrtilik, J.; Raychaudhury, S.; Nulsen, P.E.J.; Forman, W.; Sun, M.; Donahue, M. Active-galactic-nucleus-driven Weather and Multiphase Gas in the Core of the NGC 5044 Galaxy Group. *Astrophys. J.* **2011**, *728*, 162. [[CrossRef](#)]
9. Randall, S.W.; Forman, W.R.; Giacintucci, S.; Nulsen, P.E.J.; Sun, M.; Jones, C.; Churazov, E.; David, L.P.; Kraft, R.; Donahue, M.; et al. Shocks and Cavities from Multiple Outbursts in the Galaxy Group NGC 5813: A Window to Active Galactic Nucleus Feedback. *Astrophys. J.* **2011**, *726*, 86. [[CrossRef](#)]
10. Randall, S.W.; Nulsen, P.E.J.; Jones, C.; Forman, W.R.; Bulbul, E.; Clarke, T.E.; Kraft, R.; Blanton, E.L.; David, L.; Werner, N.; et al. A Very Deep Chandra Observation of the Galaxy Group NGC 5813: AGN Shocks, Feedback, and Outburst History. *Astrophys. J.* **2015**, *805*, 112. [[CrossRef](#)]
11. Best, P.N. The environmental dependence of radio-loud AGN activity and star formation in the 2dFGRS. *Mon. Not. R. Astron. Soc.* **2004**, *351*, 70–82. [[CrossRef](#)]
12. Croston, J.H.; Hardcastle, M.J.; Birkinshaw, M.; Worrall, D.M.; Laing, R.A. An XMM-Newton study of the environments, particle content and impact of low-power radio galaxies. *Mon. Not. R. Astron. Soc.* **2008**, *386*, 1709–1728. [[CrossRef](#)]
13. Ching, J.H.Y.; Croom, S.M.; Sadler, E.M.; Robotham, A.S.G.; Brough, S.; Baldry, I.K.; Bland-Hawthorn, J.; Colless, M.; Driver, S.P.; Holwerda, B.W.; et al. Galaxy And Mass Assembly (GAMA): The environments of high- and low-excitation radio galaxies. *Mon. Not. R. Astron. Soc.* **2017**, *469*, 4584–4599. [[CrossRef](#)]
14. Rafferty, D.A.; McNamara, B.R.; Nulsen, P.E.J.; Wise, M.W. The Feedback-regulated Growth of Black Holes and Bulges through Gas Accretion and Starbursts in Cluster Central Dominant Galaxies. *Astrophys. J.* **2006**, *652*, 216–231. [[CrossRef](#)]
15. Dunn, R.J.H.; Fabian, A.C. Investigating heating and cooling in the BCS and B55 cluster samples. *Mon. Not. R. Astron. Soc.* **2008**, *385*, 757–768. [[CrossRef](#)]
16. Hlavacek-Larrondo, J.; Fabian, A.C.; Edge, A.C.; Ebeling, H.; Sanders, J.S.; Hogan, M.T.; Taylor, G.B. Extreme AGN feedback in the MAssive Cluster Survey: A detailed study of X-ray cavities at $z > 0.3$. *Mon. Not. R. Astron. Soc.* **2012**, *421*, 1360–1384. [[CrossRef](#)]
17. Hlavacek-Larrondo, J.; Li, Y.; Churazov, E. AGN Feedback in Groups and Clusters of Galaxies. In *Handbook of X-ray and Gamma-ray Astrophysics*. Edited by Cosimo Bambi and Andrea Santangelo; Springer: Singapore, 2022; p. 5. [[CrossRef](#)]
18. McNamara, B.R.; Nulsen, P.E.J. Mechanical feedback from active galactic nuclei in galaxies, groups and clusters. *New J. Phys.* **2012**, *14*, 055023. [[CrossRef](#)]
19. Gaspari, M.; Tombesi, F.; Cappi, M. Linking macro-, meso- and microscales in multiphase AGN feeding and feedback. *Nat. Astron.* **2020**, *4*, 10–13. [[CrossRef](#)]
20. Kravtsov, A.V.; Borgani, S. Formation of Galaxy Clusters. *Annu. Rev. Astron. Astrophys.* **2012**, *50*, 353–409. [[CrossRef](#)]
21. Allen, S.W.; Evrard, A.E.; Mantz, A.B. Cosmological Parameters from Observations of Galaxy Clusters. *Annu. Rev. Astron. Astrophys.* **2011**, *49*, 409–470. [[CrossRef](#)]
22. King, A.; Pounds, K. Powerful Outflows and Feedback from Active Galactic Nuclei. *Annu. Rev. Astron. Astrophys.* **2015**, *53*, 115–154. [[CrossRef](#)]
23. Morganti, R. The many routes to AGN feedback. *Front. Astron. Space Sci.* **2017**, *4*, 42. [[CrossRef](#)]
24. Magorrian, J.; Tremaine, S.; Richstone, D.; Bender, R.; Bower, G.; Dressler, A.; Faber, S.M.; Gebhardt, K.; Green, R.; Grillmair, C.; et al. The Demography of Massive Dark Objects in Galaxy Centers. *Astron. J.* **1998**, *115*, 2285. [[CrossRef](#)]
25. Ferrarese, L.; Merritt, D. A Fundamental Relation between Supermassive Black Holes and Their Host Galaxies. *Astrophys. J. Lett.* **2000**, *539*, L9–L12. [[CrossRef](#)]
26. Kormendy, J.; Ho, L.C. Coevolution (Or Not) of Supermassive Black Holes and Host Galaxies. *Annu. Rev. Astron. Astrophys.* **2013**, *51*, 511–653. [[CrossRef](#)]
27. McConnell, N.J.; Ma, C.P. Revisiting the Scaling Relations of Black Hole Masses and Host Galaxy Properties. *Astrophys. J.* **2013**, *764*, 184. [[CrossRef](#)]

28. Sahu, N.; Graham, A.W.; Davis, B.L. Black Hole Mass Scaling Relations for Early-type Galaxies. I. $M_{BH-M_{*,sph}}$ and $M_{BH-M_{*,gal}}$. *Astrophys. J.* **2019**, *876*, 155. [[CrossRef](#)]
29. Reines, A.E.; Greene, J.E.; Geha, M. Dwarf Galaxies with Optical Signatures of Active Massive Black Holes. *Astrophys. J.* **2013**, *775*, 116. [[CrossRef](#)]
30. Manzano-King, C.M.; Canalizo, G.; Sales, L.V. AGN-Driven Outflows in Dwarf Galaxies. *Astrophys. J.* **2019**, *884*, 54. [[CrossRef](#)]
31. Mezcua, M. Feeding and feedback from little monsters: AGN in dwarf galaxies. In *Galaxy Evolution and Feedback across Different Environments*; Storchi Bergmann, T., Forman, W., Overzier, R., Riffel, R., Eds.; Cambridge University Press: Cambridge, UK, 2021; Volume 359, pp. 238–242. [[CrossRef](#)]
32. Koudmani, S.; Sijacki, D.; Smith, M.C. Two can play at that game: Constraining the role of supernova and AGN feedback in dwarf galaxies with cosmological zoom-in simulations. *Mon. Not. R. Astron. Soc.* **2022**, *516*, 2112–2141. [[CrossRef](#)]
33. Sharma, R.S.; Brooks, A.M.; Tremmel, M.; Bellovary, J.; Ricarte, A.; Quinn, T.R. A Hidden Population of Massive Black Holes in Simulated Dwarf Galaxies. *Astrophys. J.* **2022**, *936*, 82. [[CrossRef](#)]
34. Harrison, C.M. Impact of supermassive black hole growth on star formation. *Nat. Astron.* **2017**, *1*, 0165. [[CrossRef](#)]
35. Harrison, C.M.; Costa, T.; Tadhunter, C.N.; Flütsch, A.; Kakkad, D.; Perna, M.; Vietri, G. AGN outflows and feedback twenty years on. *Nat. Astron.* **2018**, *2*, 198–205. [[CrossRef](#)]
36. Hardcastle, M.J.; Croston, J.H. Radio galaxies and feedback from AGN jets. *New Astron. Rev.* **2020**, *88*, 101539. [[CrossRef](#)]
37. Veilleux, S.; Maiolino, R.; Bolatto, A.D.; Aalto, S. Cool outflows in galaxies and their implications. *A&A Rev.* **2020**, *28*, 2. [[CrossRef](#)]
38. Burns, J.O.; Norman, M.L.; Clarke, D.A. Numerical Models of Extragalactic Radio Sources. *Science* **1991**, *253*, 522–530. [[CrossRef](#)]
39. Rayburn, D.R. A numerical study of the continuous beam model of extragalactic radio sources. *Mon. Not. R. Astron. Soc.* **1977**, *179*, 603–617. [[CrossRef](#)]
40. Norman, M.L.; Winkler, K.H.A.; Smarr, L.; Smith, M.D. Structure and dynamics of supersonic jets. *Astron. Astrophys.* **1982**, *113*, 285–302.
41. Clarke, D.A.; Norman, M.L.; Burns, J.O. Numerical Observations of a Simulated Jet with a Passive Helical Magnetic Field. *Astrophys. J.* **1989**, *342*, 700. [[CrossRef](#)]
42. Clarke, D.A.; Bridle, A.H.; Burns, J.O.; Perley, R.A.; Norman, M.L. Origin of the Structures and Polarization in the Classical Double 3C 219. *Astrophys. J.* **1992**, *385*, 173. [[CrossRef](#)]
43. Falle, S.A.E.G.; Wilson, M.J. A theoretical model of the M 87 jet. *Mon. Not. R. Astron. Soc.* **1985**, *216*, 79–84. [[CrossRef](#)]
44. Smith, M.D.; Norman, M.L.; Winkler, K.H.A.; Smarr, L. Hotspots in radio galaxies: A comparison with hydrodynamic simulations. *Mon. Not. R. Astron. Soc.* **1985**, *214*, 67–85. [[CrossRef](#)]
45. Wilson, M.J.; Scheuer, P.A.G. The anisotropy of emission from hotspots in extragalactic radio sources. *Mon. Not. R. Astron. Soc.* **1983**, *205*, 449–463. [[CrossRef](#)]
46. Koessl, D.; Mueller, E. Numerical simulations of astrophysical jets: The influence of boundary conditions and grid resolution. *Astron. Astrophys.* **1988**, *206*, 204–218.
47. Clarke, D.A.; Norman, M.L.; Burns, J.O. Numerical Simulations of a Magnetically Confined Jet. *Astrophys. J. Lett.* **1986**, *311*, L63. [[CrossRef](#)]
48. Lind, K.R.; Payne, D.G.; Meier, D.L.; Blandford, R.D. Numerical Simulations of Magnetized Jets. *Astrophys. J.* **1989**, *344*, 89. [[CrossRef](#)]
49. Arnold, C.N.; Arnett, W.D. Three-dimensional Structure and Dynamics of a Supersonic Jet. *Astrophys. J. Lett.* **1986**, *305*, L57. [[CrossRef](#)]
50. Clarke, D.A.; Stone, J.M.; Norman, M.L. MHD Jet Simulations in Three Dimensions. *Proc. Bull. Am. Astron. Soc.* **1990**, *22*, 801.
51. Komissarov, S.; Porth, O. Numerical simulations of jets. *New Astron. Rev.* **2021**, *92*, 101610. [[CrossRef](#)]
52. Martí, J.M. Numerical Simulations of Jets from Active Galactic Nuclei. *Galaxies* **2019**, *7*, 24. [[CrossRef](#)]
53. Miley, G. The structure of extended extragalactic radio sources. *Annu. Rev. Astron. Astrophys.* **1980**, *18*, 165–218. [[CrossRef](#)]
54. Biretta, J.A.; Owen, F.N.; Hardee, P.E. Observations of the M 87 jet at 15 GHz with 0".12 resolution. *Astrophys. J. Lett.* **1983**, *274*, L27–L30. [[CrossRef](#)]
55. Boehringer, H.; Voges, W.; Fabian, A.C.; Edge, A.C.; Neumann, D.M. A ROSAT HRI study of the interaction of the X-ray emitting gas and radio lobes of NGC 1275. *Mon. Not. R. Astron. Soc.* **1993**, *264*, L25–L28. [[CrossRef](#)]
56. Carilli, C.L.; Perley, R.A.; Harris, D.E. Observations of interaction between cluster gas and the radio lobes of Cygnus A. *Mon. Not. R. Astron. Soc.* **1994**, *270*, 173–177. [[CrossRef](#)]
57. Huang, Z.; Sarazin, C.L. A High-Resolution ROSAT X-ray Study of Abell 4059. *Astrophys. J.* **1998**, *496*, 728–736. [[CrossRef](#)]
58. Fabian, A.C.; Sanders, J.S.; Ettori, S.; Taylor, G.B.; Allen, S.W.; Crawford, C.S.; Iwasawa, K.; Johnstone, R.M.; Ogle, P.M. Chandra imaging of the complex X-ray core of the Perseus cluster. *Mon. Not. R. Astron. Soc.* **2000**, *318*, L65–L68. [[CrossRef](#)]
59. McNamara, B.R.; Wise, M.; Nulsen, P.E.J.; David, L.P.; Sarazin, C.L.; Bautz, M.; Markevitch, M.; Vikhlinin, A.; Forman, W.R.; Jones, C.; et al. Chandra X-Ray Observations of the Hydra A Cluster: An Interaction between the Radio Source and the X-ray-emitting Gas. *Astrophys. J. Lett.* **2000**, *534*, L135–L138. [[CrossRef](#)]
60. Branduardi-Raymont, G.; Fabricant, D.; Feigelson, E.; Gorenstein, P.; Grindlay, J.; Soltan, A.; Zamorani, G. Soft X-ray images of the central region of the Perseus cluster. *Astrophys. J.* **1981**, *248*, 55–60. [[CrossRef](#)]
61. Fabian, A.C.; Hu, E.M.; Cowie, L.L.; Grindlay, J. The distribution and morphology of X-ray emitting gas in the core of the Perseus cluster. *Astrophys. J.* **1981**, *248*, 47–54. [[CrossRef](#)]

62. Clarke, D.A.; Harris, D.E.; Carilli, C.L. Formation of cavities in the X-ray emitting cluster gas of Cygnus A. *Mon. Not. R. Astron. Soc.* **1997**, *284*, 981–993. [[CrossRef](#)]
63. Rizza, E.; Loken, C.; Bliton, M.; Roettiger, K.; Burns, J.O.; Owen, F.N. X-ray and Radio Interactions in the Cores of Cooling Flow Clusters. *Astron. J.* **2000**, *119*, 21–31. [[CrossRef](#)]
64. Reynolds, C.S.; Heinz, S.; Begelman, M.C. Shocks and Sonic Booms in the Intracluster Medium: X-ray Shells and Radio Galaxy Activity. *Astrophys. J. Let.* **2001**, *549*, L179–L182. [[CrossRef](#)]
65. Reynolds, C.S.; Heinz, S.; Begelman, M.C. The hydrodynamics of dead radio galaxies. *Mon. Not. R. Astron. Soc.* **2002**, *332*, 271–282. [[CrossRef](#)]
66. Omma, H.; Binney, J.; Bryan, G.; Slyz, A. Heating cooling flows with jets. *Mon. Not. R. Astron. Soc.* **2004**, *348*, 1105–1119. [[CrossRef](#)]
67. Churazov, E.; Brügggen, M.; Kaiser, C.R.; Böhringer, H.; Forman, W. Evolution of Buoyant Bubbles in M87. *Astrophys. J.* **2001**, *554*, 261–273. [[CrossRef](#)]
68. Brügggen, M.; Kaiser, C.R. Buoyant radio plasma in clusters of galaxies. *Mon. Not. R. Astron. Soc.* **2001**, *325*, 676–684. [[CrossRef](#)]
69. Quilis, V.; Bower, R.G.; Balogh, M.L. Bubbles, feedback and the intracluster medium: Three-dimensional hydrodynamic simulations. *Mon. Not. R. Astron. Soc.* **2001**, *328*, 1091–1097. [[CrossRef](#)]
70. Brügggen, M.; Kaiser, C.R.; Churazov, E.; Enßlin, T.A. Simulation of radio plasma in clusters of galaxies. *Mon. Not. R. Astron. Soc.* **2002**, *331*, 545–555. [[CrossRef](#)]
71. Huško, F.; Lacey, C.G. Active galactic nuclei jets simulated with smoothed particle hydrodynamics. *Mon. Not. R. Astron. Soc.* **2023**, *520*, 5090–5109. [[CrossRef](#)]
72. Huško, F.; Lacey, C.G. The complex interplay of AGN jet-inflated bubbles and the intracluster medium. *Mon. Not. R. Astron. Soc.* **2023**, *521*, 4375–4394. [[CrossRef](#)]
73. Huško, F.; Lacey, C.G.; Schaye, J.; Schaller, M.; Nobels, F.S.J. Spin-driven jet feedback in idealized simulations of galaxy groups and clusters. *Mon. Not. R. Astron. Soc.* **2022**, *516*, 3750–3772. [[CrossRef](#)]
74. Springel, V. E pur si muove: Galilean-invariant cosmological hydrodynamical simulations on a moving mesh. *Mon. Not. R. Astron. Soc.* **2010**, *401*, 791–851. [[CrossRef](#)]
75. Hopkins, P.F. A new class of accurate, mesh-free hydrodynamic simulation methods. *Mon. Not. R. Astron. Soc.* **2015**, *450*, 53–110. [[CrossRef](#)]
76. Bourne, M.A.; Sijacki, D. AGN jet feedback on a moving mesh: Cocoon inflation, gas flows and turbulence. *Mon. Not. R. Astron. Soc.* **2017**, *472*, 4707–4735. [[CrossRef](#)]
77. Weinberger, R.; Ehlert, K.; Pfrommer, C.; Pakmor, R.; Springel, V. Simulating the interaction of jets with the intracluster medium. *Mon. Not. R. Astron. Soc.* **2017**, *470*, 4530–4546. [[CrossRef](#)]
78. Su, K.Y.; Hopkins, P.F.; Bryan, G.L.; Somerville, R.S.; Hayward, C.C.; Anglés-Alcázar, D.; Faucher-Giguère, C.A.; Wellons, S.; Stern, J.; Terrazas, B.A.; et al. Which AGN jets quench star formation in massive galaxies? *Mon. Not. R. Astron. Soc.* **2021**, *507*, 175–204. [[CrossRef](#)]
79. Krause, M. Very light jets. I. Axisymmetric parameter study and analytic approximation. *Astron. Astrophys.* **2003**, *398*, 113–125. [[CrossRef](#)]
80. Krause, M.; Alexander, P.; Riley, J.; Hopton, D. A new connection between the jet opening angle and the large-scale morphology of extragalactic radio sources. *Mon. Not. R. Astron. Soc.* **2012**, *427*, 3196–3208. [[CrossRef](#)]
81. Hardcastle, M.J.; Krause, M.G.H. Numerical modelling of the lobes of radio galaxies in cluster environments. *Mon. Not. R. Astron. Soc.* **2013**, *430*, 174–196. [[CrossRef](#)]
82. Cattaneo, A.; Teyssier, R. AGN self-regulation in cooling flow clusters. *Mon. Not. R. Astron. Soc.* **2007**, *376*, 1547–1556. [[CrossRef](#)]
83. Dubois, Y.; Devriendt, J.; Slyz, A.; Teyssier, R. Jet-regulated cooling catastrophe. *Mon. Not. R. Astron. Soc.* **2010**, *409*, 985–1001. [[CrossRef](#)]
84. Gaspari, M.; Melioli, C.; Brighenti, F.; D’Ercole, A. The dance of heating and cooling in galaxy clusters: three-dimensional simulations of self-regulated active galactic nuclei outflows. *Mon. Not. R. Astron. Soc.* **2011**, *411*, 349–372. [[CrossRef](#)]
85. Li, Y.; Bryan, G.L. Modeling Active Galactic Nucleus Feedback in Cool-core Clusters: The Balance between Heating and Cooling. *Astrophys. J.* **2014**, *789*, 54. [[CrossRef](#)]
86. Yang, H.Y.K.; Reynolds, C.S. How AGN Jets Heat the Intracluster Medium—Insights from Hydrodynamic Simulations. *Astrophys. J.* **2016**, *829*, 90. [[CrossRef](#)]
87. Hardcastle, M.J.; Krause, M.G.H. Numerical modelling of the lobes of radio galaxies in cluster environments—II. Magnetic field configuration and observability. *Mon. Not. R. Astron. Soc.* **2014**, *443*, 1482–1499. [[CrossRef](#)]
88. Ehlert, K.; Weinberger, R.; Pfrommer, C.; Pakmor, R.; Springel, V. Simulations of the dynamics of magnetized jets and cosmic rays in galaxy clusters. *Mon. Not. R. Astron. Soc.* **2018**, *481*, 2878–2900. [[CrossRef](#)]
89. Bourne, M.A.; Sijacki, D.; Puchwein, E. AGN jet feedback on a moving mesh: Lobe energetics and X-ray properties in a realistic cluster environment. *Mon. Not. R. Astron. Soc.* **2019**, *490*, 343–349. [[CrossRef](#)]
90. Yang, H.Y.K.; Gaspari, M.; Marlow, C. The Impact of Radio AGN Bubble Composition on the Dynamics and Thermal Balance of the Intracluster Medium. *Astrophys. J.* **2019**, *871*, 6. [[CrossRef](#)]
91. Perucho, M.; Martí, J.M.; Quilis, V. Long-term FR II jet evolution in dense environments. *Mon. Not. R. Astron. Soc.* **2022**, *510*, 2084–2096. [[CrossRef](#)]

92. Gaspari, M.; Brighenti, F.; D’Ercole, A.; Melioli, C. AGN feedback in galaxy groups: The delicate touch of self-regulated outflows. *Mon. Not. R. Astron. Soc.* **2011**, *415*, 1549–1568. [[CrossRef](#)]
93. Gaspari, M.; Brighenti, F.; Temi, P. Chaotic cold accretion on to black holes in rotating atmospheres. *Astron. Astrophys.* **2015**, *579*, A62. [[CrossRef](#)]
94. Prasad, D.; Sharma, P.; Babul, A. Cool Core Cycles: Cold Gas and AGN Jet Feedback in Cluster Cores. *Astrophys. J.* **2015**, *811*, 108. [[CrossRef](#)]
95. Yang, H.Y.K.; Reynolds, C.S. Interplay Among Cooling, AGN Feedback, and Anisotropic Conduction in the Cool Cores of Galaxy Clusters. *Astrophys. J.* **2016**, *818*, 181. [[CrossRef](#)]
96. Li, Y.; Ruszkowski, M.; Bryan, G.L. AGN Heating in Simulated Cool-core Clusters. *Astrophys. J.* **2017**, *847*, 106. [[CrossRef](#)]
97. Beckmann, R.S.; Dubois, Y.; Guillard, P.; Salome, P.; Olivares, V.; Polles, F.; Cadiou, C.; Combes, F.; Hamer, S.; Lehnert, M.D.; et al. Dense gas formation and destruction in a simulated Perseus-like galaxy cluster with spin-driven black hole feedback. *Astron. Astrophys.* **2019**, *631*, A60. [[CrossRef](#)]
98. Ehlert, K.; Weinberger, R.; Pfrommer, C.; Pakmor, R.; Springel, V. Self-regulated AGN feedback of light jets in cool-core galaxy clusters. *Mon. Not. R. Astron. Soc.* **2022**, *518*, 4622–4645. [[CrossRef](#)]
99. Robinson, K.; Dursi, L.J.; Ricker, P.M.; Rosner, R.; Calder, A.C.; Zingale, M.; Truran, J.W.; Linde, T.; Caceres, A.; Fryxell, B.; et al. Morphology of Rising Hydrodynamic and Magnetohydrodynamic Bubbles from Numerical Simulations. *Astrophys. J.* **2004**, *601*, 621–643. [[CrossRef](#)]
100. Li, H.; Lapenta, G.; Finn, J.M.; Li, S.; Colgate, S.A. Modeling the Large-Scale Structures of Astrophysical Jets in the Magnetically Dominated Limit. *Astrophys. J.* **2006**, *643*, 92–100. [[CrossRef](#)]
101. Ruszkowski, M.; Enßlin, T.A.; Brügggen, M.; Begelman, M.C.; Churazov, E. Cosmic ray confinement in fossil cluster bubbles. *Mon. Not. R. Astron. Soc.* **2008**, *383*, 1359–1365. [[CrossRef](#)]
102. Dubois, Y.; Devriendt, J.; Slyz, A.; Silk, J. Influence of AGN jets on the magnetized ICM. *Mon. Not. R. Astron. Soc.* **2009**, *399*, L49–L53. [[CrossRef](#)]
103. Gaibler, V.; Krause, M.; Camenzind, M. Very light magnetized jets on large scales—I. Evolution and magnetic fields. *Mon. Not. R. Astron. Soc.* **2009**, *400*, 1785–1802. [[CrossRef](#)]
104. O’Neill, S.M.; Jones, T.W. Three-Dimensional Simulations of Bi-Directed Magnetohydrodynamic Jets Interacting with Cluster Environments. *Astrophys. J.* **2010**, *710*, 180–196. [[CrossRef](#)]
105. Mendygral, P.J.; Jones, T.W.; Dolag, K. MHD Simulations of Active Galactic Nucleus Jets in a Dynamic Galaxy Cluster Medium. *Astrophys. J.* **2012**, *750*, 166. [[CrossRef](#)]
106. Sutter, P.M.; Yang, H.Y.K.; Ricker, P.M.; Foreman, G.; Pugmire, D. An examination of magnetized outflows from active galactic nuclei in galaxy clusters. *Mon. Not. R. Astron. Soc.* **2012**, *419*, 2293–2314. [[CrossRef](#)]
107. Wang, C.; Ruszkowski, M.; Yang, H.Y.K. Chaotic cold accretion in giant elliptical galaxies heated by AGN cosmic rays. *Mon. Not. R. Astron. Soc.* **2020**, *493*, 4065–4076. [[CrossRef](#)]
108. Wang, C.; Ruszkowski, M.; Pfrommer, C.; Oh, S.P.; Yang, H.Y.K. Non-Kolmogorov turbulence in multiphase intracluster medium driven by cold gas precipitation and AGN jets. *Mon. Not. R. Astron. Soc.* **2021**, *504*, 898–909. [[CrossRef](#)]
109. Perucho, M.; Martí, J.M.; Quilis, V.; Ricciardelli, E. Large-scale jets from active galactic nuclei as a source of intracluster medium heating: Cavities and shocks. *Mon. Not. R. Astron. Soc.* **2014**, *445*, 1462–1481. [[CrossRef](#)]
110. English, W.; Hardcastle, M.J.; Krause, M.G.H. Numerical modelling of the lobes of radio galaxies in cluster environments—III. Powerful relativistic and non-relativistic jets. *Mon. Not. R. Astron. Soc.* **2016**, *461*, 2025–2043. [[CrossRef](#)]
111. Perucho, M.; Martí, J.M.; Quilis, V.; Borja-Lloret, M. Radio mode feedback: Does relativity matter? *Mon. Not. R. Astron. Soc.* **2017**, *471*, L120–L124. [[CrossRef](#)]
112. English, W.; Hardcastle, M.J.; Krause, M.G.H. Numerical modelling of the lobes of radio galaxies in cluster environments—IV. Remnant radio galaxies. *Mon. Not. R. Astron. Soc.* **2019**, *490*, 5807–5819. [[CrossRef](#)]
113. Yates-Jones, P.M.; Shabala, S.S.; Krause, M.G.H. Dynamics of relativistic radio jets in asymmetric environments. *Mon. Not. R. Astron. Soc.* **2021**, *508*, 5239–5250. [[CrossRef](#)]
114. Reynolds, C.S.; McKernan, B.; Fabian, A.C.; Stone, J.M.; Vernaleo, J.C. Buoyant radio lobes in a viscous intracluster medium. *Mon. Not. R. Astron. Soc.* **2005**, *357*, 242–250. [[CrossRef](#)]
115. Dong, R.; Stone, J.M. Buoyant Bubbles in Intracluster Gas: Effects of Magnetic Fields and Anisotropic Viscosity. *Astrophys. J.* **2009**, *704*, 1309–1320. [[CrossRef](#)]
116. Guo, F. The Shape of X-Ray Cavities in Galaxy Clusters: Probing Jet Properties and Viscosity. *Astrophys. J.* **2015**, *803*, 48. [[CrossRef](#)]
117. Kingsland, M.; Yang, H.Y.K.; Reynolds, C.S.; Zuhone, J.A. Effects of Anisotropic Viscosity on the Evolution of Active Galactic Nuclei Bubbles in Galaxy Clusters. *Astrophys. J. Lett.* **2019**, *883*, L23. [[CrossRef](#)]
118. Ruszkowski, M.; Begelman, M.C. Heating, Conduction, and Minimum Temperatures in Cooling Flows. *Astrophys. J.* **2002**, *581*, 223–228. [[CrossRef](#)]
119. Zakamska, N.L.; Narayan, R. Models of Galaxy Clusters with Thermal Conduction. *Astrophys. J.* **2003**, *582*, 162–169. [[CrossRef](#)]
120. Voigt, L.M.; Fabian, A.C. Thermal conduction and reduced cooling flows in galaxy clusters. *Mon. Not. R. Astron. Soc.* **2004**, *347*, 1130–1149. [[CrossRef](#)]

121. Parrish, I.J.; Quataert, E.; Sharma, P. Anisotropic Thermal Conduction and the Cooling Flow Problem in Galaxy Clusters. *Astrophys. J.* **2009**, *703*, 96–108. [[CrossRef](#)]
122. Bogdanović, T.; Reynolds, C.S.; Balbus, S.A.; Parrish, I.J. Simulations of Magnetohydrodynamics Instabilities in Intracluster Medium Including Anisotropic Thermal Conduction. *Astrophys. J.* **2009**, *704*, 211–225. [[CrossRef](#)]
123. Avara, M.J.; Reynolds, C.S.; Bogdanović, T. Role of Magnetic Field Strength and Numerical Resolution in Simulations of the Heat-flux-driven Buoyancy Instability. *Astrophys. J.* **2013**, *773*, 171. [[CrossRef](#)]
124. Kannan, R.; Vogelsberger, M.; Pfrommer, C.; Weinberger, R.; Springel, V.; Hernquist, L.; Puchwein, E.; Pakmor, R. Increasing Black Hole Feedback-induced Quenching with Anisotropic Thermal Conduction. *Astrophys. J. Lett.* **2017**, *837*, L18. [[CrossRef](#)]
125. Beckmann, R.S.; Dubois, Y.; Pellissier, A.; Polles, F.L.; Olivares, V. AGN jets do not prevent the suppression of conduction by the heat buoyancy instability in simulated galaxy clusters. *Astron. Astrophys.* **2022**, *666*, A71. [[CrossRef](#)]
126. Guo, F.; Oh, S.P. Feedback heating by cosmic rays in clusters of galaxies. *Mon. Not. R. Astron. Soc.* **2008**, *384*, 251–266. [[CrossRef](#)]
127. Mathews, W.G.; Brighenti, F. Energetics of X-Ray Cavities and Radio Lobes in Galaxy Clusters. *Astrophys. J.* **2008**, *685*, 128–137. [[CrossRef](#)]
128. Ruszkowski, M.; Yang, H.Y.K.; Reynolds, C.S. Cosmic-Ray Feedback Heating of the Intracluster Medium. *Astrophys. J.* **2017**, *844*, 13. [[CrossRef](#)]
129. Jacob, S.; Pfrommer, C. Cosmic ray heating in cool core clusters—I. Diversity of steady state solutions. *Mon. Not. R. Astron. Soc.* **2017**, *467*, 1449–1477. [[CrossRef](#)]
130. Jacob, S.; Pfrommer, C. Cosmic ray heating in cool core clusters—II. Self-regulation cycle and non-thermal emission. *Mon. Not. R. Astron. Soc.* **2017**, *467*, 1478–1495. [[CrossRef](#)]
131. Prokhorov, D.A.; Churazov, E.M. Confinement and diffusion time-scales of CR hadrons in AGN-inflated bubbles. *Mon. Not. R. Astron. Soc.* **2017**, *470*, 3388–3394. [[CrossRef](#)]
132. Lin, Y.H.; Yang, H.Y.K.; Owen, E.R. Evolution and feedback of AGN jets of different cosmic ray composition. *Mon. Not. R. Astron. Soc.* **2023**, *520*, 963–975. [[CrossRef](#)]
133. Dubois, Y.; Devriendt, J.; Slyz, A.; Teyssier, R. Self-regulated growth of supermassive black holes by a dual jet-heating active galactic nucleus feedback mechanism: Methods, tests and implications for cosmological simulations. *Mon. Not. R. Astron. Soc.* **2012**, *420*, 2662–2683. [[CrossRef](#)]
134. Gaspari, M.; Ruszkowski, M.; Sharma, P. Cause and Effect of Feedback: Multiphase Gas in Cluster Cores Heated by AGN Jets. *Astrophys. J.* **2012**, *746*, 94. [[CrossRef](#)]
135. Yang, H.Y.K.; Ruszkowski, M.; Ricker, P.M.; Zweibel, E.; Lee, D. The Fermi Bubbles: Supersonic Active Galactic Nucleus Jets with Anisotropic Cosmic-Ray Diffusion. *Astrophys. J.* **2012**, *761*, 185. [[CrossRef](#)]
136. Meece, G.R.; Voit, G.M.; O’Shea, B.W. Triggering and Delivery Algorithms for AGN Feedback. *Astrophys. J.* **2017**, *841*, 133. [[CrossRef](#)]
137. Talbot, R.Y.; Bourne, M.A.; Sijacki, D. Blandford-Znajek jets in galaxy formation simulations: Method and implementation. *Mon. Not. R. Astron. Soc.* **2021**, *504*, 3619–3650. [[CrossRef](#)]
138. Talbot, R.Y.; Sijacki, D.; Bourne, M.A. Blandford-Znajek jets in galaxy formation simulations: Exploring the diversity of outflows produced by spin-driven AGN jets in Seyfert galaxies. *Mon. Not. R. Astron. Soc.* **2022**, *514*, 4535–4559. [[CrossRef](#)]
139. Gaspari, M.; Ruszkowski, M.; Oh, S.P. Chaotic cold accretion on to black holes. *Mon. Not. R. Astron. Soc.* **2013**, *432*, 3401–3422. [[CrossRef](#)]
140. Somerville, R.S.; Davé, R. Physical Models of Galaxy Formation in a Cosmological Framework. *Annu. Rev. Astron. Astrophys.* **2015**, *53*, 51–113. [[CrossRef](#)]
141. Vogelsberger, M.; Marinacci, F.; Torrey, P.; Puchwein, E. Cosmological simulations of galaxy formation. *Nature Reviews Physics* **2020**, *2*, 42–66. [[CrossRef](#)]
142. Di Matteo, T.; Springel, V.; Hernquist, L. Energy input from quasars regulates the growth and activity of black holes and their host galaxies. *Nature* **2005**, *433*, 604–607. [[CrossRef](#)]
143. Le Brun, A.M.C.; McCarthy, I.G.; Schaye, J.; Ponman, T.J. Towards a realistic population of simulated galaxy groups and clusters. *Mon. Not. R. Astron. Soc.* **2014**, *441*, 1270–1290. [[CrossRef](#)]
144. Schaye, J.; Crain, R.A.; Bower, R.G.; Furlong, M.; Schaller, M.; Theuns, T.; Dalla Vecchia, C.; Frenk, C.S.; McCarthy, I.G.; Helly, J.C.; et al. The EAGLE project: Simulating the evolution and assembly of galaxies and their environments. *Mon. Not. R. Astron. Soc.* **2015**, *446*, 521–554. [[CrossRef](#)]
145. Sijacki, D.; Vogelsberger, M.; Genel, S.; Springel, V.; Torrey, P.; Snyder, G.F.; Nelson, D.; Hernquist, L. The Illustris simulation: The evolving population of black holes across cosmic time. *Mon. Not. R. Astron. Soc.* **2015**, *452*, 575–596. [[CrossRef](#)]
146. Dubois, Y.; Peirani, S.; Pichon, C.; Devriendt, J.; Gavazzi, R.; Welker, C.; Volonteri, M. The HORIZON-AGN simulation: Morphological diversity of galaxies promoted by AGN feedback. *Mon. Not. R. Astron. Soc.* **2016**, *463*, 3948–3964. [[CrossRef](#)]
147. Weinberger, R.; Springel, V.; Pakmor, R.; Nelson, D.; Genel, S.; Pillepich, A.; Vogelsberger, M.; Marinacci, F.; Naiman, J.; Torrey, P.; et al. Supermassive black holes and their feedback effects in the IllustrisTNG simulation. *Mon. Not. R. Astron. Soc.* **2018**, *479*, 4056–4072. [[CrossRef](#)]
148. Dubois, Y.; Devriendt, J.; Teyssier, R.; Slyz, A. How active galactic nucleus feedback and metal cooling shape cluster entropy profiles. *Mon. Not. R. Astron. Soc.* **2011**, *417*, 1853–1870. [[CrossRef](#)]

149. Bahé, Y.M.; Barnes, D.J.; Dalla Vecchia, C.; Kay, S.T.; White, S.D.M.; McCarthy, I.G.; Schaye, J.; Bower, R.G.; Crain, R.A.; Theuns, T.; et al. The Hydrangea simulations: Galaxy formation in and around massive clusters. *Mon. Not. R. Astron. Soc.* **2017**, *470*, 4186–4208. [[CrossRef](#)]
150. Barnes, D.J.; Kay, S.T.; Henson, M.A.; McCarthy, I.G.; Schaye, J.; Jenkins, A. The redshift evolution of massive galaxy clusters in the MACSIS simulations. *Mon. Not. R. Astron. Soc.* **2017**, *465*, 213–233. [[CrossRef](#)]
151. Barnes, D.J.; Kay, S.T.; Bahé, Y.M.; Dalla Vecchia, C.; McCarthy, I.G.; Schaye, J.; Bower, R.G.; Jenkins, A.; Thomas, P.A.; Schaller, M.; et al. The Cluster-EAGLE project: Global properties of simulated clusters with resolved galaxies. *Mon. Not. R. Astron. Soc.* **2017**, *471*, 1088–1106. [[CrossRef](#)]
152. Barnes, D.J.; Vogelsberger, M.; Kannan, R.; Marinacci, F.; Weinberger, R.; Springel, V.; Torrey, P.; Pillepich, A.; Nelson, D.; Pakmor, R.; et al. A census of cool-core galaxy clusters in IllustrisTNG. *Mon. Not. R. Astron. Soc.* **2018**, *481*, 1809–1831. [[CrossRef](#)]
153. Hahn, O.; Martizzi, D.; Wu, H.Y.; Evrard, A.E.; Teyssier, R.; Wechsler, R.H. rhapsody-g simulations - I. The cool cores, hot gas and stellar content of massive galaxy clusters. *Mon. Not. R. Astron. Soc.* **2017**, *470*, 166–186. [[CrossRef](#)]
154. Rasia, E.; Borgani, S.; Murante, G.; Planelles, S.; Beck, A.M.; Biffi, V.; Ragone-Figueroa, C.; Granato, G.L.; Steinborn, L.K.; Dolag, K. Cool Core Clusters from Cosmological Simulations. *Astrophys. J. Let.* **2015**, *813*, L17. [[CrossRef](#)]
155. Henden, N.A.; Puchwein, E.; Shen, S.; Sijacki, D. The FABLE simulations: A feedback model for galaxies, groups, and clusters. *Mon. Not. R. Astron. Soc.* **2018**, *479*, 5385–5412. [[CrossRef](#)]
156. Tremmel, M.; Quinn, T.R.; Ricarte, A.; Babul, A.; Chadayammuri, U.; Natarajan, P.; Nagai, D.; Pontzen, A.; Volonteri, M. Introducing ROMULUS: A cosmological simulation of a galaxy cluster with an unprecedented resolution. *Mon. Not. R. Astron. Soc.* **2019**, *483*, 3336–3362. [[CrossRef](#)]
157. Pakmor, R.; Springel, V.; Coles, J.P.; Guillet, T.; Pfrommer, C.; Bose, S.; Barrera, M.; Delgado, A.M.; Ferlito, F.; Frenk, C.; et al. The MillenniumTNG Project: The hydrodynamical full physics simulation and a first look at its galaxy clusters. *arXiv* **2022**, arXiv:2210.10060. [[CrossRef](#)]
158. Genel, S.; Vogelsberger, M.; Springel, V.; Sijacki, D.; Nelson, D.; Snyder, G.; Rodriguez-Gomez, V.; Torrey, P.; Hernquist, L. Introducing the Illustris project: The evolution of galaxy populations across cosmic time. *Mon. Not. R. Astron. Soc.* **2014**, *445*, 175–200. [[CrossRef](#)]
159. Springel, V.; Di Matteo, T.; Hernquist, L. Modelling feedback from stars and black holes in galaxy mergers. *Mon. Not. R. Astron. Soc.* **2005**, *361*, 776–794. [[CrossRef](#)]
160. Booth, C.M.; Schaye, J. Cosmological simulations of the growth of supermassive black holes and feedback from active galactic nuclei: Method and tests. *Mon. Not. R. Astron. Soc.* **2009**, *398*, 53–74. [[CrossRef](#)]
161. McCarthy, I.G.; Schaye, J.; Bird, S.; Le Brun, A.M.C. The BAHAMAS project: Calibrated hydrodynamical simulations for large-scale structure cosmology. *Mon. Not. R. Astron. Soc.* **2017**, *465*, 2936–2965. [[CrossRef](#)]
162. Bourne, M.A.; Zubovas, K.; Nayakshin, S. The resolution bias: Low-resolution feedback simulations are better at destroying galaxies. *Mon. Not. R. Astron. Soc.* **2015**, *453*, 1829–1842. [[CrossRef](#)]
163. Tremmel, M.; Karcher, M.; Governato, F.; Volonteri, M.; Quinn, T.R.; Pontzen, A.; Anderson, L.; Bellovary, J. The Romulus cosmological simulations: A physical approach to the formation, dynamics and accretion models of SMBHs. *Mon. Not. R. Astron. Soc.* **2017**, *470*, 1121–1139. [[CrossRef](#)]
164. Weinberger, R.; Springel, V.; Hernquist, L.; Pillepich, A.; Marinacci, F.; Pakmor, R.; Nelson, D.; Genel, S.; Vogelsberger, M.; Naiman, J.; et al. Simulating galaxy formation with black hole driven thermal and kinetic feedback. *Mon. Not. R. Astron. Soc.* **2017**, *465*, 3291–3308. [[CrossRef](#)]
165. Davé, R.; Anglés-Alcázar, D.; Narayanan, D.; Li, Q.; Rafieferantsoa, M.H.; Appleby, S. SIMBA: Cosmological simulations with black hole growth and feedback. *Mon. Not. R. Astron. Soc.* **2019**, *486*, 2827–2849. [[CrossRef](#)]
166. Sijacki, D.; Springel, V.; Di Matteo, T.; Hernquist, L. A unified model for AGN feedback in cosmological simulations of structure formation. *Mon. Not. R. Astron. Soc.* **2007**, *380*, 877–900. [[CrossRef](#)]
167. Dalla Vecchia, C.; Bower, R.G.; Theuns, T.; Balogh, M.L.; Mazzotta, P.; Frenk, C.S. Quenching cluster cooling flows with recurrent hot plasma bubbles. *Mon. Not. R. Astron. Soc.* **2004**, *355*, 995–1004. [[CrossRef](#)]
168. Dubois, Y.; Beckmann, R.; Bournaud, F.; Choi, H.; Devriendt, J.; Jackson, R.; Kaviraj, S.; Kimm, T.; Kraljic, K.; Laigle, C.; et al. Introducing the NEWHORIZON simulation: Galaxy properties with resolved internal dynamics across cosmic time. *Astron. Astrophys.* **2021**, *651*, A109. [[CrossRef](#)]
169. Fanaroff, B.L.; Riley, J.M. The morphology of extragalactic radio sources of high and low luminosity. *Mon. Not. R. Astron. Soc.* **1974**, *167*, 31P–36P. [[CrossRef](#)]
170. Perley, R.A.; Willis, A.G.; Scott, J.S. The structure of the radio jets in 3C 449. *Nature* **1979**, *281*, 437–442. [[CrossRef](#)]
171. Komissarov, S.S. Mass-Loaded Relativistic Jets. *Mon. Not. R. Astron. Soc.* **1994**, *269*, 394. [[CrossRef](#)]
172. Rossi, P.; Mignone, A.; Bodo, G.; Massaglia, S.; Ferrari, A. Formation of dynamical structures in relativistic jets: The FRI case. *Astron. Astrophys.* **2008**, *488*, 795–806. [[CrossRef](#)]
173. Perucho, M.; Martí, J.M.; Cela, J.M.; Hanasz, M.; de La Cruz, R.; Rubio, F. Stability of three-dimensional relativistic jets: Implications for jet collimation. *Astron. Astrophys.* **2010**, *519*, A41. [[CrossRef](#)]
174. Laing, R.A.; Bridle, A.H. Systematic properties of decelerating relativistic jets in low-luminosity radio galaxies. *Mon. Not. R. Astron. Soc.* **2014**, *437*, 3405–3441. [[CrossRef](#)]

175. Tchekhovskoy, A.; Bromberg, O. Three-dimensional relativistic MHD simulations of active galactic nuclei jets: Magnetic kink instability and Fanaroff-Riley dichotomy. *Mon. Not. R. Astron. Soc.* **2016**, *461*, L46–L50. [[CrossRef](#)]
176. Dehghan, S.; Johnston-Hollitt, M.; Franzen, T.M.O.; Norris, R.P.; Miller, N.A. Bent-tailed Radio Sources in the Australia Telescope Large Area Survey of the Chandra Deep Field South. *Astron. J.* **2014**, *148*, 75. [[CrossRef](#)]
177. O'Brien, A.N.; Norris, R.P.; Tothill, N.F.H.; Filipović, M.D. The spatial correlation of bent-tail galaxies and galaxy clusters. *Mon. Not. R. Astron. Soc.* **2018**, *481*, 5247–5262. [[CrossRef](#)]
178. Murthy, S.; Morganti, R.; Wagner, A.Y.; Oosterloo, T.; Guillard, P.; Mukherjee, D.; Bicknell, G. Cold gas removal from the centre of a galaxy by a low-luminosity jet. *Nature Astronomy* **2022**, *6*, 488–495. [[CrossRef](#)]
179. Mukherjee, D.; Bicknell, G.V.; Wagner, A.Y.; Sutherland, R.S.; Silk, J. Relativistic jet feedback—III. Feedback on gas discs. *Mon. Not. R. Astron. Soc.* **2018**, *479*, 5544–5566. [[CrossRef](#)]
180. Carilli, C.L.; Barthel, P.D. Cygnus A. *A&A Rev.* **1996**, *7*, 1–54. [[CrossRef](#)]
181. Wilson, A.S.; Colbert, E.J.M. The Difference between Radio-loud and Radio-quiet Active Galaxies. *Astrophys. J.* **1995**, *438*, 62. [[CrossRef](#)]
182. Sikora, M.; Stawarz, Ł.; Lasota, J.P. Radio Loudness of Active Galactic Nuclei: Observational Facts and Theoretical Implications. *Astrophys. J.* **2007**, *658*, 815–828. [[CrossRef](#)]
183. Tchekhovskoy, A.; Narayan, R.; McKinney, J.C. Black Hole Spin and The Radio Loud/Quiet Dichotomy of Active Galactic Nuclei. *Astrophys. J.* **2010**, *711*, 50–63. [[CrossRef](#)]
184. Tchekhovskoy, A.; McKinney, J.C.; Narayan, R. General Relativistic Modeling of Magnetized Jets from Accreting Black Holes. *J. Phys. Conf. Ser.s* **2012**, *372*, 012040. [[CrossRef](#)]
185. Best, P.N.; Heckman, T.M. On the fundamental dichotomy in the local radio-AGN population: accretion, evolution and host galaxy properties. *Mon. Not. R. Astron. Soc.* **2012**, *421*, 1569–1582. [[CrossRef](#)]
186. Gendre, M.A.; Best, P.N.; Wall, J.V.; Ker, L.M. The relation between morphology, accretion modes and environmental factors in local radio AGN. *Mon. Not. R. Astron. Soc.* **2013**, *430*, 3086–3101. [[CrossRef](#)]
187. Mingo, B.; Hardcastle, M.J.; Croston, J.H.; Dicken, D.; Evans, D.A.; Morganti, R.; Tadhunter, C. An X-ray survey of the 2 Jy sample-I. Is there an accretion mode dichotomy in radio-loud AGN? *Mon. Not. R. Astron. Soc.* **2014**, *440*, 269–297. [[CrossRef](#)]
188. Ineson, J.; Croston, J.H.; Hardcastle, M.J.; Kraft, R.P.; Evans, D.A.; Jarvis, M. The link between accretion mode and environment in radio-loud active galaxies. *Mon. Not. R. Astron. Soc.* **2015**, *453*, 2682–2706. [[CrossRef](#)]
189. Mingo, B.; Croston, J.H.; Best, P.N.; Duncan, K.J.; Hardcastle, M.J.; Kondapally, R.; Prandoni, I.; Sabater, J.; Shimwell, T.W.; Williams, W.L.; et al. Accretion mode versus radio morphology in the LOFAR Deep Fields. *Mon. Not. R. Astron. Soc.* **2022**, *511*, 3250–3271. [[CrossRef](#)]
190. Massaglia, S.; Bodo, G.; Rossi, P.; Capetti, S.; Mignone, A. Making Fanaroff-Riley I radio sources. I. Numerical hydrodynamic 3D simulations of low-power jets. *Astron. Astrophys.* **2016**, *596*, A12. [[CrossRef](#)]
191. Massaglia, S.; Bodo, G.; Rossi, P.; Capetti, S.; Mignone, A. Making Fanaroff-Riley I radio sources. II. The effects of jet magnetization. *Astron. Astrophys.* **2019**, *621*, A132. [[CrossRef](#)]
192. Massaglia, S.; Bodo, G.; Rossi, P.; Capetti, A.; Mignone, A. Making Fanaroff-Riley I radio sources. III. The effects of the magnetic field on relativistic jets' propagation and source morphologies. *Astron. Astrophys.* **2022**, *659*, A139. [[CrossRef](#)]
193. Li, Y.; Wiita, P.J.; Schuh, T.; Elghossain, G.; Hu, S. Radio-loud Active Galactic Nucleus Variability from Three-dimensional Propagating Relativistic Jets. *Astrophys. J.* **2018**, *869*, 32. [[CrossRef](#)]
194. Mandal, S.; Duffell, P.C.; Li, Y. Numerical Investigation of Dynamical and Morphological Trends in Relativistic Jets. *Astrophys. J.* **2022**, *935*, 42. [[CrossRef](#)]
195. Yates-Jones, P.M.; Shabala, S.S.; Power, C.; Krause, M.G.H.; Hardcastle, M.J.; Mohd Noh Velastín, E.A.N.; Stewart, G.S.C. CosmoDRAGoN simulations—I. Dynamics and observable signatures of radio jets in cosmological environments. **2023**, *40*, e014. [[CrossRef](#)]
196. Ferrari, A. Modeling Extragalactic Jets. *Annu. Rev. Astron. Astrophys.* **1998**, *36*, 539–598. [[CrossRef](#)]
197. Falle, S.A.E.G. Self-similar jets. *Mon. Not. R. Astron. Soc.* **1991**, *250*, 581–596. [[CrossRef](#)]
198. Krause, M. Very light jets II: Bipolar large scale simulations in King atmospheres. *Astron. Astrophys.* **2005**, *431*, 45–64. [[CrossRef](#)]
199. Guo, F. On the Importance of Very Light Internally Subsonic AGN Jets in Radio-mode AGN Feedback. *Astrophys. J.* **2016**, *826*, 17. [[CrossRef](#)]
200. Weinberger, R.; Su, K.Y.; Ehlert, K.; Pfrommer, C.; Hernquist, L.; Bryan, G.L.; Springel, V.; Li, Y.; Burkhart, B.; Choi, E.; et al. Active galactic nucleus jet feedback in hydrostatic halos. *Mon. Not. R. Astron. Soc.* **2023**, *523*, 1104–1125. [[CrossRef](#)]
201. Kataoka, J.; Stawarz, Ł. X-Ray Emission Properties of Large-Scale Jets, Hot Spots, and Lobes in Active Galactic Nuclei. *Astrophys. J.* **2005**, *622*, 797–810. [[CrossRef](#)]
202. Croston, J.H.; Hardcastle, M.J.; Harris, D.E.; Belsole, E.; Birkinshaw, M.; Worrall, D.M. An X-Ray Study of Magnetic Field Strengths and Particle Content in the Lobes of FR II Radio Sources. *Astrophys. J.* **2005**, *626*, 733–747. [[CrossRef](#)]
203. Ineson, J.; Croston, J.H.; Hardcastle, M.J.; Mingo, B. A representative survey of the dynamics and energetics of FR II radio galaxies. *Mon. Not. R. Astron. Soc.* **2017**, *467*, 1586–1607. [[CrossRef](#)]
204. Harwood, J.J.; Croston, J.H.; Intema, H.T.; Stewart, A.J.; Ineson, J.; Hardcastle, M.J.; Godfrey, L.; Best, P.; Brienza, M.; Heesen, V.; et al. FR II radio galaxies at low frequencies—I. Morphology, magnetic field strength and energetics. *Mon. Not. R. Astron. Soc.* **2016**, *458*, 4443–4455. [[CrossRef](#)] [[PubMed](#)]

205. Tchekhovskoy, A.; Narayan, R.; McKinney, J.C. Efficient generation of jets from magnetically arrested accretion on a rapidly spinning black hole. *Mon. Not. R. Astron. Soc.* **2011**, *418*, L79–L83. [[CrossRef](#)]
206. Sądowski, A.; Narayan, R. Powerful radiative jets in supercritical accretion discs around non-spinning black holes. *Mon. Not. R. Astron. Soc.* **2015**, *453*, 3213–3221. [[CrossRef](#)]
207. Liska, M.; Hesp, C.; Tchekhovskoy, A.; Ingram, A.; van der Klis, M.; Markoff, S. Formation of precessing jets by tilted black hole discs in 3D general relativistic MHD simulations. *Mon. Not. R. Astron. Soc.* **2018**, *474*, L81–L85. [[CrossRef](#)]
208. Liska, M.; Tchekhovskoy, A.; Ingram, A.; van der Klis, M. Bardeen-Petterson alignment, jets, and magnetic truncation in GRMHD simulations of tilted thin accretion discs. *Mon. Not. R. Astron. Soc.* **2019**, *487*, 550–561. [[CrossRef](#)]
209. Lu, R.S.; Asada, K.; Krichbaum, T.P.; Park, J.; Tazaki, F.; Pu, H.Y.; Nakamura, M.; Lobanov, A.; Hada, K.; Akiyama, K.; et al. A ring-like accretion structure in M87 connecting its black hole and jet. *Nature* **2023**, *616*, 686–690. [[CrossRef](#)]
210. Begelman, M.C.; Blandford, R.D.; Rees, M.J. Massive black hole binaries in active galactic nuclei. *Nature* **1980**, *287*, 307–309. [[CrossRef](#)]
211. Krause, M.G.H.; Shabala, S.S.; Hardcastle, M.J.; Bicknell, G.V.; Böhringer, H.; Chon, G.; Nawaz, M.A.; Sarzi, M.; Wagner, A.Y. How frequent are close supermassive binary black holes in powerful jet sources? *Mon. Not. R. Astron. Soc.* **2019**, *482*, 240–261. [[CrossRef](#)]
212. Falceta-Gonçalves, D.; Caproni, A.; Abraham, Z.; Teixeira, D.M.; de Gouveia Dal Pino, E.M. Precessing Jets and X-ray Bubbles from NGC 1275 (3C 84) in the Perseus Galaxy Cluster: A View from Three-dimensional Numerical Simulations. *Astrophys. J. Let.* **2010**, *713*, L74–L78. [[CrossRef](#)]
213. Martizzi, D.; Quataert, E.; Faucher-Giguère, C.A.; Fielding, D. Simulations of jet heating in galaxy clusters: Successes and challenges. *Mon. Not. R. Astron. Soc.* **2019**, *483*, 2465–2486. [[CrossRef](#)]
214. Cielo, S.; Babul, A.; Antonuccio-Delogu, V.; Silk, J.; Volonteri, M. Feedback from reorienting AGN jets. I. Jet-ICM coupling, cavity properties and global energetics. *Astron. Astrophys.* **2018**, *617*, A58. [[CrossRef](#)]
215. Dubois, Y.; Volonteri, M.; Silk, J.; Devriendt, J.; Slyz, A. Black hole evolution—II. Spinning black holes in a supernova-driven turbulent interstellar medium. *Mon. Not. R. Astron. Soc.* **2014**, *440*, 2333–2346. [[CrossRef](#)]
216. Fiacconi, D.; Sijacki, D.; Pringle, J.E. Galactic nuclei evolution with spinning black holes: Method and implementation. *Mon. Not. R. Astron. Soc.* **2018**, *477*, 3807–3835. [[CrossRef](#)]
217. Bustamante, S.; Springel, V. Spin evolution and feedback of supermassive black holes in cosmological simulations. *Mon. Not. R. Astron. Soc.* **2019**, *490*, 4133–4153. [[CrossRef](#)]
218. McKinney, J.C.; Tchekhovskoy, A.; Blandford, R.D. General relativistic magnetohydrodynamic simulations of magnetically choked accretion flows around black holes. *Mon. Not. R. Astron. Soc.* **2012**, *423*, 3083–3117. [[CrossRef](#)]
219. Bondi, H. On spherically symmetrical accretion. *Mon. Not. R. Astron. Soc.* **1952**, *112*, 195. [[CrossRef](#)]
220. Allen, S.W.; Dunn, R.J.H.; Fabian, A.C.; Taylor, G.B.; Reynolds, C.S. The relation between accretion rate and jet power in X-ray luminous elliptical galaxies. *Mon. Not. R. Astron. Soc.* **2006**, *372*, 21–30. [[CrossRef](#)]
221. Merloni, A.; Heinz, S. Measuring the kinetic power of active galactic nuclei in the radio mode. *Mon. Not. R. Astron. Soc.* **2007**, *381*, 589–601. [[CrossRef](#)]
222. McNamara, B.R.; Rohanizadegan, M.; Nulsen, P.E.J. Are Radio Active Galactic Nuclei Powered by Accretion or Black Hole Spin? *Astrophys. J.* **2011**, *727*, 39. [[CrossRef](#)]
223. Russell, H.R.; McNamara, B.R.; Edge, A.C.; Hogan, M.T.; Main, R.A.; Vantyghem, A.N. Radiative efficiency, variability and Bondi accretion on to massive black holes: The transition from radio AGN to quasars in brightest cluster galaxies. *Mon. Not. R. Astron. Soc.* **2013**, *432*, 530–553. [[CrossRef](#)]
224. Nemmen, R.S.; Tchekhovskoy, A. On the efficiency of jet production in radio galaxies. *Mon. Not. R. Astron. Soc.* **2015**, *449*, 316–327. [[CrossRef](#)]
225. Blandford, R.D.; Znajek, R.L. Electromagnetic extraction of energy from Kerr black holes. *Mon. Not. R. Astron. Soc.* **1977**, *179*, 433–456. [[CrossRef](#)]
226. Tang, X.; Churazov, E. Sound wave generation by a spherically symmetric outburst and AGN feedback in galaxy clusters. *Mon. Not. R. Astron. Soc.* **2017**, *468*, 3516–3532. [[CrossRef](#)]
227. Guo, F.; Duan, X.; Yuan, Y.F. Reversing cooling flows with AGN jets: Shock waves, rarefaction waves and trailing outflows. *Mon. Not. R. Astron. Soc.* **2018**, *473*, 1332–1345. [[CrossRef](#)]
228. Bourne, M.A.; Sijacki, D. AGN jet feedback on a moving mesh: Gentle cluster heating by weak shocks and lobe disruption. *Mon. Not. R. Astron. Soc.* **2021**, *506*, 488–513. [[CrossRef](#)]
229. Brüggén, M.; Heinz, S.; Roediger, E.; Ruszkowski, M.; Simionescu, A. Shock heating by Fanaroff-Riley type I radio sources in galaxy clusters. *Mon. Not. R. Astron. Soc.* **2007**, *380*, L67–L70. [[CrossRef](#)]
230. Fabian, A.C.; Sanders, J.S.; Taylor, G.B.; Allen, S.W.; Crawford, C.S.; Johnstone, R.M.; Iwasawa, K. A very deep Chandra observation of the Perseus cluster: Shocks, ripples and conduction. *Mon. Not. R. Astron. Soc.* **2006**, *366*, 417–428. [[CrossRef](#)]
231. Forman, W.; Jones, C.; Churazov, E.; Markevitch, M.; Nulsen, P.; Vikhlinin, A.; Begelman, M.; Böhringer, H.; Eilek, J.; Heinz, S.; et al. Filaments, Bubbles, and Weak Shocks in the Gaseous Atmosphere of M87. *Astrophys. J.* **2007**, *665*, 1057–1066. [[CrossRef](#)]
232. Croston, J.H.; Hardcastle, M.J.; Mingo, B.; Evans, D.A.; Dicken, D.; Morganti, R.; Tadhunter, C.N. A Large-scale Shock Surrounding a Powerful Radio Galaxy? *Astrophys. J. Let.* **2011**, *734*, L28. [[CrossRef](#)]

233. Sanders, J.S.; Fabian, A.C.; Taylor, G.B.; Russell, H.R.; Blundell, K.M.; Canning, R.E.A.; Hlavacek-Larrondo, J.; Walker, S.A.; Grimes, C.K. A very deep Chandra view of metals, sloshing and feedback in the Centaurus cluster of galaxies. *Mon. Not. R. Astron. Soc.* **2016**, *457*, 82–109. [[CrossRef](#)]
234. Sternberg, A.; Soker, N. Sound waves excitation by jet-inflated bubbles in clusters of galaxies. *Mon. Not. R. Astron. Soc.* **2009**, *395*, 228–233. [[CrossRef](#)]
235. Schaal, K.; Springel, V. Shock finding on a moving mesh - I. Shock statistics in non-radiative cosmological simulations. *Mon. Not. R. Astron. Soc.* **2015**, *446*, 3992–4007. [[CrossRef](#)]
236. Schaal, K.; Springel, V.; Pakmor, R.; Pfrommer, C.; Nelson, D.; Vogelsberger, M.; Genel, S.; Pillepich, A.; Sijacki, D.; Hernquist, L. Shock finding on a moving-mesh - II. Hydrodynamic shocks in the Illustris universe. *Mon. Not. R. Astron. Soc.* **2016**, *461*, 4441–4465. [[CrossRef](#)]
237. Ruszkowski, M.; Brügggen, M.; Begelman, M.C. Cluster Heating by Viscous Dissipation of Sound Waves. *Astrophys. J.* **2004**, *611*, 158–163. [[CrossRef](#)]
238. Ruszkowski, M.; Brügggen, M.; Begelman, M.C. Three-Dimensional Simulations of Viscous Dissipation in the Intracluster Medium. *Astrophys. J.* **2004**, *615*, 675–680. [[CrossRef](#)]
239. Bambic, C.J.; Reynolds, C.S. Efficient Production of Sound Waves by AGN Jets in the Intracluster Medium. *Astrophys. J.* **2019**, *886*, 78. [[CrossRef](#)]
240. Sijacki, D.; Springel, V. Physical viscosity in smoothed particle hydrodynamics simulations of galaxy clusters. *Mon. Not. R. Astron. Soc.* **2006**, *371*, 1025–1046. [[CrossRef](#)]
241. Zweibel, E.G.; Mirnov, V.V.; Ruszkowski, M.; Reynolds, C.S.; Yang, H.Y.K.; Fabian, A.C. Acoustic Disturbances in Galaxy Clusters. *Astrophys. J.* **2018**, *858*, 5. [[CrossRef](#)]
242. Diehl, S.; Li, H.; Fryer, C.L.; Rafferty, D. Constraining the Nature of X-Ray Cavities in Clusters and Galaxies. *Astrophys. J.* **2008**, *687*, 173–192. [[CrossRef](#)]
243. Fabian, A.C.; Sanders, J.S.; Allen, S.W.; Canning, R.E.A.; Churazov, E.; Crawford, C.S.; Forman, W.; Gabany, J.; Hlavacek-Larrondo, J.; Johnstone, R.M.; et al. A wide Chandra view of the core of the Perseus cluster. *Mon. Not. R. Astron. Soc.* **2011**, *418*, 2154–2164. [[CrossRef](#)]
244. Jones, T.W.; De Young, D.S. Magnetohydrodynamic Simulations of Relic Radio Bubbles in Clusters. *Astrophys. J.* **2005**, *624*, 586–605. [[CrossRef](#)]
245. Dursi, L.J. Bubble Wrap for Bullets: The Stability Imparted by a Thin Magnetic Layer. *Astrophys. J.* **2007**, *670*, 221–230. [[CrossRef](#)]
246. Ruszkowski, M.; Enßlin, T.A.; Brügggen, M.; Heinz, S.; Pfrommer, C. Impact of tangled magnetic fields on fossil radio bubbles. *Mon. Not. R. Astron. Soc.* **2007**, *378*, 662–672. [[CrossRef](#)]
247. Dursi, L.J.; Pfrommer, C. Draping of Cluster Magnetic Fields over Bullets and Bubbles—Morphology and Dynamic Effects. *Astrophys. J.* **2008**, *677*, 993–1018. [[CrossRef](#)]
248. O'Neill, S.M.; De Young, D.S.; Jones, T.W. Three-Dimensional Magnetohydrodynamic Simulations of Buoyant Bubbles in Galaxy Clusters. *Astrophys. J.* **2009**, *694*, 1317–1330. [[CrossRef](#)]
249. Sternberg, A.; Soker, N. Rising jet-inflated bubbles in clusters of galaxies. *Mon. Not. R. Astron. Soc.* **2008**, *389*, L13–L17. [[CrossRef](#)]
250. Gilkis, A.; Soker, N. Heating the intra-cluster medium perpendicular to the jets axis. *Mon. Not. R. Astron. Soc.* **2012**, *427*, 1482–1489. [[CrossRef](#)]
251. Hillel, S.; Soker, N. Heating the intracluster medium by jet-inflated bubbles. *Mon. Not. R. Astron. Soc.* **2016**, *455*, 2139–2148. [[CrossRef](#)]
252. Hillel, S.; Soker, N. Gentle Heating by Mixing in Cooling Flow Clusters. *Astrophys. J.* **2017**, *845*, 91. [[CrossRef](#)]
253. Ogiya, G.; Biernacki, P.; Hahn, O.; Teyssier, R. Physical and numerical stability and instability of AGN bubbles in a hot intracluster medium. *arXiv* **2018**, arXiv:1802.02177. [[CrossRef](#)]
254. Bambic, C.J.; Morsony, B.J.; Reynolds, C.S. Suppression of AGN-driven Turbulence by Magnetic Fields in a Magnetohydrodynamic Model of the Intracluster Medium. *Astrophys. J.* **2018**, *857*, 84. [[CrossRef](#)]
255. Dunn, R.J.H.; Fabian, A.C.; Sanders, J.S. Precession of the super-massive black hole in NGC 1275 (3C 84)? *Mon. Not. R. Astron. Soc.* **2006**, *366*, 758–766. [[CrossRef](#)]
256. Churazov, E.; Sunyaev, R.; Forman, W.; Böhringer, H. Cooling flows as a calorimeter of active galactic nucleus mechanical power. *Mon. Not. R. Astron. Soc.* **2002**, *332*, 729–734. [[CrossRef](#)]
257. Soker, N.; Hillel, S.; Sternberg, A. Rescuing the intracluster medium of NGC 5813. *Res. Astron. Astrophys.* **2016**, *16*, 100. [[CrossRef](#)]
258. Chen, Y.H.; Heinz, S.; Enßlin, T.A. Jets, bubbles, and heat pumps in galaxy clusters. *Mon. Not. R. Astron. Soc.* **2019**, *489*, 1939–1949. [[CrossRef](#)]
259. Revaz, Y.; Combes, F.; Salomé, P. Formation of cold filaments in cooling flow clusters. *Astron. Astrophys.* **2008**, *477*, L33–L36. [[CrossRef](#)]
260. Brighenti, F.; Mathews, W.G.; Temi, P. Hot Gaseous Atmospheres in Galaxy Groups and Clusters Are Both Heated and Cooled by X-ray Cavities. *Astrophys. J.* **2015**, *802*, 118. [[CrossRef](#)]
261. Wang, C.; Li, Y.; Ruszkowski, M. AGN feedback and multiphase gas in giant elliptical galaxies. *Mon. Not. R. Astron. Soc.* **2019**, *482*, 3576–3590. [[CrossRef](#)]
262. Zhang, C.; Zhuravleva, I.; Gendron-Marsolais, M.L.; Churazov, E.; Schekochihin, A.A.; Forman, W.R. Bubble-driven gas uplift in galaxy clusters and its velocity features. *Mon. Not. R. Astron. Soc.* **2022**, *517*, 616–631. [[CrossRef](#)]

263. Salomé, P.; Combes, F.; Edge, A.C.; Crawford, C.; Erlund, M.; Fabian, A.C.; Hatch, N.A.; Johnstone, R.M.; Sanders, J.S.; Wilman, R.J. Cold molecular gas in the Perseus cluster core. Association with X-ray cavity, H α filaments and cooling flow. *Astron. Astrophys.* **2006**, *454*, 437–445. [[CrossRef](#)]
264. McDonald, M.; Veilleux, S.; Rupke, D.S.N. Optical Spectroscopy of H α Filaments in Cool Core Clusters: Kinematics, Reddening, and Sources of Ionization. *Astrophys. J.* **2012**, *746*, 153. [[CrossRef](#)]
265. Hamer, S.L.; Edge, A.C.; Swinbank, A.M.; Oonk, J.B.R.; Mittal, R.; McNamara, B.R.; Russell, H.R.; Bremer, M.N.; Combes, F.; Fabian, A.C.; et al. Cold gas dynamics in Hydra-A: Evidence for a rotating disc. *Mon. Not. R. Astron. Soc.* **2014**, *437*, 862–878. [[CrossRef](#)]
266. Hamer, S.L.; Edge, A.C.; Swinbank, A.M.; Wilman, R.J.; Combes, F.; Salomé, P.; Fabian, A.C.; Crawford, C.S.; Russell, H.R.; Hlavacek-Larrondo, J.; et al. Optical emission line nebulae in galaxy cluster cores 1: The morphological, kinematic and spectral properties of the sample. *Mon. Not. R. Astron. Soc.* **2016**, *460*, 1758–1789. [[CrossRef](#)]
267. Fabian, A.C.; Walker, S.A.; Russell, H.R.; Pinto, C.; Canning, R.E.A.; Salome, P.; Sanders, J.S.; Taylor, G.B.; Zweibel, E.G.; Conselice, C.J.; et al. HST imaging of the dusty filaments and nucleus swirl in NGC4696 at the centre of the Centaurus Cluster. *Mon. Not. R. Astron. Soc.* **2016**, *461*, 922–928. [[CrossRef](#)]
268. Russell, H.R.; McDonald, M.; McNamara, B.R.; Fabian, A.C.; Nulsen, P.E.J.; Bayliss, M.B.; Benson, B.A.; Brodwin, M.; Carlstrom, J.E.; Edge, A.C.; et al. Alma Observations of Massive Molecular Gas Filaments Encasing Radio Bubbles in the Phoenix Cluster. *Astrophys. J.* **2017**, *836*, 130. [[CrossRef](#)]
269. Zhang, C.; Churazov, E.; Schekochihin, A.A. Generation of internal waves by buoyant bubbles in galaxy clusters and heating of intracluster medium. *Mon. Not. R. Astron. Soc.* **2018**, *478*, 4785–4798. [[CrossRef](#)]
270. Zhuravleva, I.; Churazov, E.; Schekochihin, A.A.; Allen, S.W.; Arévalo, P.; Fabian, A.C.; Forman, W.R.; Sanders, J.S.; Simionescu, A.; Sunyaev, R.; et al. Turbulent heating in galaxy clusters brightest in X-rays. *Nature* **2014**, *515*, 85–87. [[CrossRef](#)]
271. Zhuravleva, I.; Churazov, E.; Arévalo, P.; Schekochihin, A.A.; Forman, W.R.; Allen, S.W.; Simionescu, A.; Sunyaev, R.; Vikhlinin, A.; Werner, N. The nature and energetics of AGN-driven perturbations in the hot gas in the Perseus Cluster. *Mon. Not. R. Astron. Soc.* **2016**, *458*, 2902–2915. [[CrossRef](#)]
272. Reynolds, C.S.; Balbus, S.A.; Schekochihin, A.A. Inefficient Driving of Bulk Turbulence By Active Galactic Nuclei in a Hydrodynamic Model of the Intracluster Medium. *Astrophys. J.* **2015**, *815*, 41. [[CrossRef](#)]
273. Hillel, S.; Soker, N. Hitomi observations of Perseus support heating by mixing. *Mon. Not. R. Astron. Soc.* **2017**, *466*, L39–L42. [[CrossRef](#)].
274. Prasad, D.; Sharma, P.; Babul, A. Cool-core Clusters: The Role of BCG, Star Formation, and AGN-driven Turbulence. *Astrophys. J.* **2018**, *863*, 62. [[CrossRef](#)]
275. Lau, E.T.; Gaspari, M.; Nagai, D.; Coppi, P. Physical Origins of Gas Motions in Galaxy Cluster Cores: Interpreting Hitomi Observations of the Perseus Cluster. *Astrophys. J.* **2017**, *849*, 54. [[CrossRef](#)]
276. Ehlert, K.; Weinberger, R.; Pfrommer, C.; Springel, V. Connecting turbulent velocities and magnetic fields in galaxy cluster simulations with active galactic nuclei jets. *Mon. Not. R. Astron. Soc.* **2021**, *503*, 1327–1344. [[CrossRef](#)]
277. Hitomi Collaboration.; Aharonian, F.; Akamatsu, H.; Akimoto, F.; Allen, S.W.; Anabuki, N.; Angelini, L.; Arnaud, K.; Audard, M.; Awaki, H.; et al. The quiescent intracluster medium in the core of the Perseus cluster. *Nature* **2016**, *535*, 117–121. [[CrossRef](#)]
278. Hitomi Collaboration.; Aharonian, F.; Akamatsu, H.; Akimoto, F.; Allen, S.W.; Angelini, L.; Audard, M.; Awaki, H.; Axelsson, M.; Bamba, A.; et al. Atmospheric gas dynamics in the Perseus cluster observed with Hitomi. *Pub. Astron. Soc. Jap.* **2018**, *70*, 9. [[CrossRef](#)]
279. Roediger, E.; Brüggem, M.; Rebusco, P.; Böhringer, H.; Churazov, E. Metal mixing by buoyant bubbles in galaxy clusters. *Mon. Not. R. Astron. Soc.* **2007**, *375*, 15–28. [[CrossRef](#)]
280. Duan, X.; Guo, F. Metal-rich Trailing Outflows Uplifted by AGN Bubbles in Galaxy Clusters. *Astrophys. J.* **2018**, *861*, 106. [[CrossRef](#)]
281. McCourt, M.; Sharma, P.; Quataert, E.; Parrish, I.J. Thermal instability in gravitationally stratified plasmas: implications for multiphase structure in clusters and galaxy haloes. *Mon. Not. R. Astron. Soc.* **2012**, *419*, 3319–3337. [[CrossRef](#)]
282. Gaspari, M.; Temi, P.; Brighenti, F. Raining on black holes and massive galaxies: The top-down multiphase condensation model. *Mon. Not. R. Astron. Soc.* **2017**, *466*, 677–704. [[CrossRef](#)]
283. Yates, P.M.; Shabala, S.S.; Krause, M.G.H. Observability of intermittent radio sources in galaxy groups and clusters. *Mon. Not. R. Astron. Soc.* **2018**, *480*, 5286–5306. [[CrossRef](#)]
284. Wagner, A.Y.; Bicknell, G.V. Relativistic Jet Feedback in Evolving Galaxies. *Astrophys. J.* **2011**, *728*, 29. [[CrossRef](#)]
285. Wagner, A.Y.; Bicknell, G.V.; Umemura, M. Driving Outflows with Relativistic Jets and the Dependence of Active Galactic Nucleus Feedback Efficiency on Interstellar Medium Inhomogeneity. *Astrophys. J.* **2012**, *757*, 136. [[CrossRef](#)]
286. Mukherjee, D.; Bicknell, G.V.; Wagner, A.Y. Resolved simulations of jet–ISM interaction: Implications for gas dynamics and star formation. *Astron. Nachrichten* **2021**, *342*, 1140–1145. [[CrossRef](#)]
287. Schuecker, P.; Finoguenov, A.; Miniati, F.; Böhringer, H.; Briel, U.G. Probing turbulence in the Coma galaxy cluster. *Astron. Astrophys.* **2004**, *426*, 387–397. [[CrossRef](#)]
288. Sanders, J.S.; Fabian, A.C.; Smith, R.K. Constraints on turbulent velocity broadening for a sample of clusters, groups and elliptical galaxies using XMM-Newton. *Mon. Not. R. Astron. Soc.* **2011**, *410*, 1797–1812. [[CrossRef](#)]

289. Zhuravleva, I.; Churazov, E.; Kravtsov, A.; Sunyaev, R. Constraints on the ICM velocity power spectrum from the X-ray lines width and shift. *Mon. Not. R. Astron. Soc.* **2012**, *422*, 2712–2724. [[CrossRef](#)]
290. Pinto, C.; Sanders, J.S.; Werner, N.; de Plaa, J.; Fabian, A.C.; Zhang, Y.Y.; Kaastra, J.S.; Finoguenov, A.; Ahoranta, J. Chemical Enrichment RGS cluster Sample (CHEERS): Constraints on turbulence. *Astron. Astrophys.* **2015**, *575*, A38. [[CrossRef](#)]
291. Walker, S.A.; Sanders, J.S.; Fabian, A.C. Constraining gas motions in the Centaurus cluster using X-ray surface brightness fluctuations and metal diffusion. *Mon. Not. R. Astron. Soc.* **2015**, *453*, 3699–3705. [[CrossRef](#)]
292. Hofmann, F.; Sanders, J.S.; Nandra, K.; Clerc, N.; Gaspari, M. Thermodynamic perturbations in the X-ray halo of 33 clusters of galaxies observed with Chandra ACIS. *Astron. Astrophys.* **2016**, *585*, A130. [[CrossRef](#)]
293. Ruszkowski, M.; Oh, S.P. Galaxy motions, turbulence and conduction in clusters of galaxies. *Mon. Not. R. Astron. Soc.* **2011**, *414*, 1493–1507. [[CrossRef](#)]
294. Vazza, F.; Roediger, E.; Brügggen, M. Turbulence in the ICM from mergers, cool-core sloshing, and jets: results from a new multi-scale filtering approach. *Astron. Astrophys.* **2012**, *544*, A103. [[CrossRef](#)]
295. Vazza, F.; Jones, T.W.; Brügggen, M.; Brunetti, G.; Gheller, C.; Porter, D.; Ryu, D. Turbulence and vorticity in Galaxy clusters generated by structure formation. *Mon. Not. R. Astron. Soc.* **2017**, *464*, 210–230. [[CrossRef](#)]
296. ZuHone, J.A.; Markevitch, M.; Brunetti, G.; Giacintucci, S. Turbulence and Radio Mini-halos in the Sloshing Cores of Galaxy Clusters. *Astrophys. J.* **2013**, *762*, 78. [[CrossRef](#)]
297. Valdarnini, R. A Multifiltering Study of Turbulence in a Large Sample of Simulated Galaxy Clusters. *Astrophys. J.* **2019**, *874*, 42. [[CrossRef](#)]
298. Bennett, J.S.; Sijacki, D. A disturbing FABLE of mergers, feedback, turbulence, and mass biases in simulated galaxy clusters. *Mon. Not. R. Astron. Soc.* **2022**, *514*, 313–328. [[CrossRef](#)]
299. Ehlert, K.; Pfrommer, C.; Weinberger, R.; Pakmor, R.; Springel, V. The Sunyaev-Zel’dovich Effect of Simulated Jet-inflated Bubbles in Clusters. *Astrophys. J. Let.* **2019**, *872*, L8. [[CrossRef](#)]
300. Chon, G.; Böhringer, H.; Krause, M.; Trümper, J. Discovery of an X-ray cavity near the radio lobes of Cygnus A indicating previous AGN activity. *Astron. Astrophys.* **2012**, *545*, L3. [[CrossRef](#)]
301. Ubertosi, F.; Gitti, M.; Brighenti, F.; Brunetti, G.; McDonald, M.; Nulsen, P.; McNamara, B.; Randall, S.; Forman, W.; Donahue, M.; et al. The Deepest Chandra View of RBS 797: Evidence for Two Pairs of Equidistant X-ray Cavities. *Astrophys. J. Let.* **2021**, *923*, L25. [[CrossRef](#)]
302. Heinz, S.; Brügggen, M.; Young, A.; Levesque, E. The answer is blowing in the wind: Simulating the interaction of jets with dynamic cluster atmospheres. *Mon. Not. R. Astron. Soc.* **2006**, *373*, L65–L69. [[CrossRef](#)]
303. Morsony, B.J.; Heinz, S.; Brügggen, M.; Ruszkowski, M. Swimming against the current: Simulations of central AGN evolution in dynamic galaxy clusters. *Mon. Not. R. Astron. Soc.* **2010**, *407*, 1277–1289. [[CrossRef](#)]
304. Patnaik, A.R.; Malkan, M.A.; Salter, C.J. Multifrequency observations of the wide-angle tail radio source 1313+073. *Mon. Not. R. Astron. Soc.* **1986**, *220*, 351–362. [[CrossRef](#)]
305. Morsony, B.J.; Miller, J.J.; Heinz, S.; Freeland, E.; Wilcots, E.; Brügggen, M.; Ruszkowski, M. Simulations of bent-double radio sources in galaxy groups. *Mon. Not. R. Astron. Soc.* **2013**, *431*, 781–792. [[CrossRef](#)]
306. Gan, Z.; Li, H.; Li, S.; Yuan, F. Three-dimensional Magnetohydrodynamical Simulations of the Morphology of Head-Tail Radio Galaxies Based on the Magnetic Tower Jet Model. *Astrophys. J.* **2017**, *839*, 14. [[CrossRef](#)]
307. Jones, T.W.; Nolting, C.; O’Neill, B.J.; Mendygral, P.J. Using collisions of AGN outflows with ICM shocks as dynamical probes. *Physics of Plasmas* **2017**, *24*, 041402. [[CrossRef](#)]
308. O’Neill, B.J.; Jones, T.W.; Nolting, C.; Mendygral, P.J. A Fresh Look at Narrow-angle Tail Radio Galaxy Dynamics, Evolution, and Emissions. *Astrophys. J.* **2019**, *884*, 12. [[CrossRef](#)]
309. O’Dea, C.P.; Baum, S.A. Wide-Angle-Tail (WAT) Radio Sources. *Galaxies* **2023**, *11*, 67. [[CrossRef](#)]
310. O’Neill, B.J.; Jones, T.W.; Nolting, C.; Mendygral, P.J. Shocked Narrow-angle Tail Radio Galaxies: Simulations and Emissions. *Astrophys. J.* **2019**, *887*, 26. [[CrossRef](#)]
311. Nolting, C.; Jones, T.W.; O’Neill, B.J.; Mendygral, P.J. Interactions between Radio Galaxies and Cluster Shocks. I. Jet Axes Aligned with Shock Normals. *Astrophys. J.* **2019**, *876*, 154. [[CrossRef](#)]
312. Nolting, C.; Jones, T.W.; O’Neill, B.J.; Mendygral, P.J. Simulated Interactions between Radio Galaxies and Cluster Shocks. II. Jet Axes Orthogonal to Shock Normals. *Astrophys. J.* **2019**, *885*, 80. [[CrossRef](#)]
313. Springel, V.; Pakmor, R.; Pillepich, A.; Weinberger, R.; Nelson, D.; Hernquist, L.; Vogelsberger, M.; Genel, S.; Torrey, P.; Marinacci, F.; et al. First results from the IllustrisTNG simulations: Matter and galaxy clustering. *Mon. Not. R. Astron. Soc.* **2018**, *475*, 676–698. [[CrossRef](#)]
314. Sijacki, D.; Springel, V. Hydrodynamical simulations of cluster formation with central AGN heating. *Mon. Not. R. Astron. Soc.* **2006**, *366*, 397–416. [[CrossRef](#)]
315. Sijacki, D.; Pfrommer, C.; Springel, V.; Enßlin, T.A. Simulations of cosmic-ray feedback by active galactic nuclei in galaxy clusters. *Mon. Not. R. Astron. Soc.* **2008**, *387*, 1403–1415. [[CrossRef](#)]
316. Vazza, F.; Wittor, D.; Brunetti, G.; Brügggen, M. Simulating the transport of relativistic electrons and magnetic fields injected by radio galaxies in the intracluster medium. *Astron. Astrophys.* **2021**, *653*, A23. [[CrossRef](#)]
317. Vazza, F.; Wittor, D.; Di Federico, L.; Brügggen, M.; Brienza, M.; Brunetti, G.; Brighenti, F.; Pasini, T. Life cycle of cosmic-ray electrons in the intracluster medium. *Astron. Astrophys.* **2023**, *669*, A50. [[CrossRef](#)]

318. Vazza, F.; Wittor, D.; Brügggen, M.; Brunetti, G. Simulating the Enrichment of Fossil Radio Electrons by Multiple Radio Galaxies. *Galaxies* **2023**, *11*, 45. [[CrossRef](#)]
319. Brügggen, M.; Ruszkowski, M.; Hallman, E. Active Galactic Nuclei Heating and Dissipative Processes in Galaxy Clusters. *Astrophys. J.* **2005**, *630*, 740–749. [[CrossRef](#)]
320. Springel, V.; White, M.; Hernquist, L. Hydrodynamic Simulations of the Sunyaev-Zeldovich Effect(s). *Astrophys. J.* **2001**, *549*, 681–687. [[CrossRef](#)]
321. Cui, W.; Knebe, A.; Yepes, G.; Pearce, F.; Power, C.; Dave, R.; Arth, A.; Borgani, S.; Dolag, K.; Elahi, P.; et al. The Three Hundred project: A large catalogue of theoretically modelled galaxy clusters for cosmological and astrophysical applications. *Mon. Not. R. Astron. Soc.* **2018**, *480*, 2898–2915. [[CrossRef](#)]
322. Vernaleo, J.C.; Reynolds, C.S. AGN Feedback and Cooling Flows: Problems with Simple Hydrodynamic Models. *Astrophys. J.* **2006**, *645*, 83–94. [[CrossRef](#)]
323. Nixon, C.; King, A. Do Jets Precess... or Even Move at All? *Astrophys. J. Let.* **2013**, *765*, L7. [[CrossRef](#)]
324. Fabian, A.C.; ZuHone, J.A.; Walker, S.A. The interaction between rising bubbles and cold fronts in cool-core clusters. *Mon. Not. R. Astron. Soc.* **2022**, *510*, 4000–4018. [[CrossRef](#)]
325. Carilli, C.L.; Taylor, G.B. Cluster Magnetic Fields. *Annu. Rev. Astron. Astrophys.* **2002**, *40*, 319–348. [[CrossRef](#)]
326. Feretti, L.; Giovannini, G.; Govoni, F.; Murgia, M. Clusters of galaxies: Observational properties of the diffuse radio emission. *A&A Rev.* **2012**, *20*, 54. [[CrossRef](#)]
327. Pfrommer, C.; Jonathan Dursi, L. Detecting the orientation of magnetic fields in galaxy clusters. *Nat. Phys.* **2010**, *6*, 520–526. [[CrossRef](#)]
328. Shin, J.; Woo, J.H.; Mulchaey, J.S. A Systematic Search for X-Ray Cavities in Galaxy Clusters, Groups, and Elliptical Galaxies. *Astrophys. J. Suppl.* **2016**, *227*, 31. [[CrossRef](#)]
329. Mushotzky, R.; Aird, J.; Barger, A.J.; Cappelluti, N.; Chartas, G.; Corrales, L.; Eufrazio, R.; Fabian, A.C.; Falcone, A.D.; Gallo, E.; et al. The Advanced X-ray Imaging Satellite. *Bull. Am. Astron. Soc.* **2019**, *51*, 107. [[CrossRef](#)]
330. Burns, J.O.; Hallman, E.J.; Gantner, B.; Motl, P.M.; Norman, M.L. Why Do Only Some Galaxy Clusters Have Cool Cores? *Astrophys. J.* **2008**, *675*, 1125–1140. [[CrossRef](#)]
331. Chadayammuri, U.; Tremmel, M.; Nagai, D.; Babul, A.; Quinn, T. Fountains and storms: The effects of AGN feedback and mergers on the evolution of the intracluster medium in the ROMULUSC simulation. *Mon. Not. R. Astron. Soc.* **2021**, *504*, 3922–3937. [[CrossRef](#)]
332. Dunn, R.J.H.; Fabian, A.C. Investigating AGN heating in a sample of nearby clusters. *Mon. Not. R. Astron. Soc.* **2006**, *373*, 959–971. [[CrossRef](#)]
333. Panagoulia, E.K.; Fabian, A.C.; Sanders, J.S.; Hlavacek-Larrondo, J. A volume-limited sample of X-ray galaxy groups and clusters-II. X-ray cavity dynamics. *Mon. Not. R. Astron. Soc.* **2014**, *444*, 1236–1259. [[CrossRef](#)]
334. XRISM Science Team. Science with the X-ray Imaging and Spectroscopy Mission (XRISM). *arXiv* **2020**, arXiv:2003.04962. [[CrossRef](#)]
335. Croston, J.H.; Sanders, J.S.; Heinz, S.; Hardcastle, M.J.; Zhuravleva, I.; Birzan, L.; Bower, R.G.; Brügggen, M.; Churazov, E.; Edge, A.C.; et al. The Hot and Energetic Universe: AGN feedback in galaxy clusters and groups. *arXiv* **2013**, arXiv:1306.2323. [[CrossRef](#)]
336. Qiu, Y.; Bogdanović, T.; Li, Y.; Park, K.; Wise, J.H. The Interplay of Kinetic and Radiative Feedback in Galaxy Clusters. *Astrophys. J.* **2019**, *877*, 47. [[CrossRef](#)]
337. Hine, R.G.; Longair, M.S. Optical spectra of 3CR radio galaxies. *Mon. Not. R. Astron. Soc.* **1979**, *188*, 111–130. [[CrossRef](#)]
338. Laing, R.A.; Jenkins, C.R.; Wall, J.V.; Unger, S.W. Spectrophotometry of a Complete Sample of 3CR Radio Sources: Implications for Unified Models. In *The Physics of Active Galaxies*; Astronomical Society of the Pacific Conference Series; Bicknell, G.V., Dopita, M.A., Quinn, P.J., Eds.; ASP: San Francisco, CA, USA, 1994; Volume 54, p. 201.
339. Comerford, J.M.; Negus, J.; Müller-Sánchez, F.; Eracleous, M.; Wylezalek, D.; Storchi-Bergmann, T.; Greene, J.E.; Barrows, R.S.; Nevin, R.; Roy, N.; et al. A Catalog of 406 AGNs in MaNGA: A Connection between Radio-mode AGNs and Star Formation Quenching. *Astrophys. J.* **2020**, *901*, 159. [[CrossRef](#)]
340. Macconi, D.; Torresi, E.; Grandi, P.; Boccardi, B.; Vignali, C. Radio morphology-accretion mode link in Fanaroff-Riley type II low-excitation radio galaxies. *Mon. Not. R. Astron. Soc.* **2020**, *493*, 4355–4366. [[CrossRef](#)]
341. Antonuccio-Delogu, V.; Silk, J. Active galactic nuclei activity: Self-regulation from backflow. *Mon. Not. R. Astron. Soc.* **2010**, *405*, 1303–1314. [[CrossRef](#)]
342. The Dark Energy Survey Collaboration. The Dark Energy Survey. *arXiv* **2005**, arXiv:astro-ph/0510346. [[CrossRef](#)]
343. Benson, B.A.; Ade, P.A.R.; Ahmed, Z.; Allen, S.W.; Arnold, K.; Austermann, J.E.; Bender, A.N.; Bleem, L.E.; Carlstrom, J.E.; Chang, C.L.; et al. SPT-3G: A next-generation cosmic microwave background polarization experiment on the South Pole telescope. In *Society of Photo-Optical Instrumentation Engineers (SPIE) Conference Series, Proceedings of the Millimeter, Submillimeter, and Far-Infrared Detectors and Instrumentation for Astronomy VII, Montréal, QC, Canada, 22–27 June 2014*; Holland, W.S., Zmuidzinas, J., Eds.; SPIE: Bellingham, WA, USA, 2014; Volume 9153, p. 91531P. [[CrossRef](#)]
344. Merloni, A.; Predehl, P.; Becker, W.; Böhringer, H.; Boller, T.; Brunner, H.; Brusa, M.; Dennerl, K.; Freyberg, M.; Friedrich, P.; et al. eROSITA Science Book: Mapping the Structure of the Energetic Universe. *arXiv* **2012**, arXiv:1209.3114. [[CrossRef](#)]
345. Henderson, S.W.; Allison, R.; Austermann, J.; Baildon, T.; Battaglia, N.; Beall, J.A.; Becker, D.; De Bernardis, F.; Bond, J.R.; Calabrese, E.; et al. Advanced ACTPol Cryogenic Detector Arrays and Readout. *J. Low Temp. Phys.* **2016**, *184*, 772–779. [[CrossRef](#)]

346. Laureijs, R.; Amiaux, J.; Arduini, S.; Auguères, J.L.; Brinchmann, J.; Cole, R.; Cropper, M.; Dabin, C.; Duvet, L.; Ealet, A.; et al. Euclid Definition Study Report. *arXiv* **2011**, arXiv:1110.3193. [[CrossRef](#)]
347. LSST Dark Energy Science Collaboration. Large Synoptic Survey Telescope: Dark Energy Science Collaboration. *arXiv* **2012**, arXiv:1211.0310. [[CrossRef](#)]
348. Braun, R.; Bourke, T.; Green, J.A.; Keane, E.; Wagg, J. Advancing Astrophysics with the Square Kilometre Array. In Proceedings of the Advancing Astrophysics with the Square Kilometre Array (AASKA14), Sicily, Italy, 8–13 June 2014; p. 174. [[CrossRef](#)]
349. Ade, P.; Aguirre, J.; Ahmed, Z.; Aiola, S.; Ali, A.; Alonso, D.; Alvarez, M.A.; Arnold, K.; Ashton, P.; Austermann, J.; et al. The Simons Observatory: Science goals and forecasts. *J. Cosmol. Astropart. Phys.* **2019**, *2019*, 056. [[CrossRef](#)]
350. Abazajian, K.N.; Adshead, P.; Ahmed, Z.; Allen, S.W.; Alonso, D.; Arnold, K.S.; Baccigalupi, C.; Bartlett, J.G.; Battaglia, N.; Benson, B.A.; et al. CMB-S4 Science Book, First Edition. *arXiv* **2016**, arXiv:1610.02743. [[CrossRef](#)]
351. Sehgal, N.; Aiola, S.; Akrami, Y.; Basu, K.; Boylan-Kolchin, M.; Bryan, S.; Clesse, S.; Cyr-Racine, F.Y.; Di Mascolo, L.; Dicker, S.; et al. CMB-HD: An Ultra-Deep, High-Resolution Millimeter-Wave Survey Over Half the Sky. *arXiv* **2019**, arXiv:1906.10134. [[CrossRef](#)]
352. McKinnon, M.; Beasley, A.; Murphy, E.; Selina, R.; Farnsworth, R.; Walter, A. ngVLA: The Next Generation Very Large Array. *Bull. Am. Astron. Soc.* **2019**, *51*, 81.
353. Sunyaev, R.A.; Zeldovich, Y.B. The Observations of Relic Radiation as a Test of the Nature of X-Ray Radiation from the Clusters of Galaxies. *Comments Astrophys. Space Phys.* **1972**, *4*, 173.
354. Henden, N.A.; Puchwein, E.; Sijacki, D. The redshift evolution of X-ray and Sunyaev-Zel'dovich scaling relations in the FABLE simulations. *Mon. Not. R. Astron. Soc.* **2019**, *489*, 2439–2470. [[CrossRef](#)]
355. Chisari, N.E.; Mead, A.J.; Joudaki, S.; Ferreira, P.G.; Schneider, A.; Mohr, J.; Tröster, T.; Alonso, D.; McCarthy, I.G.; Martin-Alvarez, S.; et al. Modelling baryonic feedback for survey cosmology. *Open J. Astrophys.* **2019**, *2*, 4. [[CrossRef](#)]
356. van Daalen, M.P.; McCarthy, I.G.; Schaye, J. Exploring the effects of galaxy formation on matter clustering through a library of simulation power spectra. *Mon. Not. R. Astron. Soc.* **2020**, *491*, 2424–2446. [[CrossRef](#)]
357. Amon, A.; Efstathiou, G. A non-linear solution to the S_8 tension? *Mon. Not. R. Astron. Soc.* **2022**, *516*, 5355–5366. [[CrossRef](#)]
358. van Daalen, M.P.; Schaye, J.; Booth, C.M.; Dalla Vecchia, C. The effects of galaxy formation on the matter power spectrum: A challenge for precision cosmology. *Mon. Not. R. Astron. Soc.* **2011**, *415*, 3649–3665. [[CrossRef](#)]
359. Chisari, N.E.; Richardson, M.L.A.; Devriendt, J.; Dubois, Y.; Schneider, A.; Le Brun, A.M.C.; Beckmann, R.S.; Peirani, S.; Slyz, A.; Pichon, C. The impact of baryons on the matter power spectrum from the Horizon-AGN cosmological hydrodynamical simulation. *Mon. Not. R. Astron. Soc.* **2018**, *480*, 3962–3977. [[CrossRef](#)]
360. Dubois, Y.; Teyssier, R. Magnetised winds in dwarf galaxies. *Astron. Astrophys.* **2010**, *523*, A72. [[CrossRef](#)]
361. Stinson, G.S.; Bovy, J.; Rix, H.W.; Brook, C.; Roškar, R.; Dalcanton, J.J.; Macciò, A.V.; Wadsley, J.; Couchman, H.M.P.; Quinn, T.R. MaGICC thick disc - I. Comparing a simulated disc formed with stellar feedback to the Milky Way. *Mon. Not. R. Astron. Soc.* **2013**, *436*, 625–634. [[CrossRef](#)]
362. Martin-Alvarez, S.; Sijacki, D.; Haehnelt, M.G.; Farcy, M.; Dubois, Y.; Belokurov, V.; Rosdahl, J.; Lopez-Rodriguez, E. The Pandora project. I: The impact of radiation and cosmic rays on baryonic and dark matter properties of dwarf galaxies. *arXiv* **2022**, arXiv:2211.09139. [[CrossRef](#)]
363. Booth, C.M.; Agertz, O.; Kravtsov, A.V.; Gnedin, N.Y. Simulations of Disk Galaxies with Cosmic Ray Driven Galactic Winds. *Astrophys. J. Let.* **2013**, *777*, L16. [[CrossRef](#)]
364. Salem, M.; Bryan, G.L. Cosmic ray driven outflows in global galaxy disc models. *Mon. Not. R. Astron. Soc.* **2014**, *437*, 3312–3330. [[CrossRef](#)]
365. Ruzzkowski, M.; Yang, H.Y.K.; Zweibel, E. Global Simulations of Galactic Winds Including Cosmic-ray Streaming. *Astrophys. J.* **2017**, *834*, 208. [[CrossRef](#)]
366. Butsky, I.S.; Quinn, T.R. The Role of Cosmic-ray Transport in Shaping the Simulated Circumgalactic Medium. *Astrophys. J.* **2018**, *868*, 108. [[CrossRef](#)]
367. Ji, S.; Chan, T.K.; Hummels, C.B.; Hopkins, P.F.; Stern, J.; Kereš, D.; Quataert, E.; Faucher-Giguère, C.A.; Murray, N. Properties of the circumgalactic medium in cosmic ray-dominated galaxy haloes. *Mon. Not. R. Astron. Soc.* **2020**, *496*, 4221–4238. [[CrossRef](#)]
368. Buck, T.; Pfrommer, C.; Pakmor, R.; Grand, R.J.J.; Springel, V. The effects of cosmic rays on the formation of Milky Way-mass galaxies in a cosmological context. *Mon. Not. R. Astron. Soc.* **2020**, *497*, 1712–1737. [[CrossRef](#)]
369. Jubelgas, M.; Springel, V.; Enßlin, T.; Pfrommer, C. Cosmic ray feedback in hydrodynamical simulations of galaxy formation. *Astron. Astrophys.* **2008**, *481*, 33–63. [[CrossRef](#)]
370. Ackermann, M.; Ajello, M.; Allafort, A.; Baldini, L.; Ballet, J.; Barbiellini, G.; Bastieri, D.; Bechtol, K.; Bellazzini, R.; Blandford, R.D.; et al. GeV Gamma-ray Flux Upper Limits from Clusters of Galaxies. *Astrophys. J. Let.* **2010**, *717*, L71–L78. [[CrossRef](#)]
371. Ahnen, M.L.; Ansoldi, S.; Antonelli, L.A.; Antoranz, P.; Babic, A.; Banerjee, B.; Bangale, P.; Barres de Almeida, U.; Barrio, J.A.; Becerra González, J.; et al. Deep observation of the NGC 1275 region with MAGIC: Search of diffuse γ -ray emission from cosmic rays in the Perseus cluster. *Astron. Astrophys.* **2016**, *589*, A33. [[CrossRef](#)]
372. Brunetti, G.; Zimmer, S.; Zandanel, F. Relativistic protons in the Coma galaxy cluster: First gamma-ray constraints ever on turbulent reacceleration. *Mon. Not. R. Astron. Soc.* **2017**, *472*, 1506–1525. [[CrossRef](#)]
373. Morganti, R.; Fanti, R.; Gioia, I.M.; Harris, D.E.; Parma, P.; de Ruiter, H. Low luminosity radio galaxies: Effects of gaseous environment. *Astron. Astrophys.* **1988**, *189*, 11–26.

374. Hardcastle, M.J.; Worrall, D.M.; Birkinshaw, M. Dynamics of the radio galaxy 3C449. *Mon. Not. R. Astron. Soc.* **1998**, *296*, 1098–1104. [[CrossRef](#)]
375. Dunn, R.J.H.; Fabian, A.C. Particle energies and filling fractions of radio bubbles in cluster cores. *Mon. Not. R. Astron. Soc.* **2004**, *355*, 862–873. [[CrossRef](#)]
376. Birzan, L.; McNamara, B.R.; Nulsen, P.E.J.; Carilli, C.L.; Wise, M.W. Radiative Efficiency and Content of Extragalactic Radio Sources: Toward a Universal Scaling Relation between Jet Power and Radio Power. *Astrophys. J.* **2008**, *686*, 859–880. [[CrossRef](#)]
377. Nulsen, P.E.J.; David, L.P.; McNamara, B.R.; Jones, C.; Forman, W.R.; Wise, M. Interaction of Radio Lobes with the Hot Intracluster Medium: Driving Convective Outflow in Hydra A. *Astrophys. J.* **2002**, *568*, 163–173. [[CrossRef](#)]
378. Enßlin, T.A.; Pfrommer, C.; Springel, V.; Jubelgas, M. Cosmic ray physics in calculations of cosmological structure formation. *Astron. Astrophys.* **2007**, *473*, 41–57. [[CrossRef](#)]
379. Zweibel, E.G. The microphysics and macrophysics of cosmic rays. *Phys. Plasmas* **2013**, *20*, 055501. [[CrossRef](#)]
380. Zweibel, E.G. The basis for cosmic ray feedback: Written on the wind. *Phys. Plasmas* **2017**, *24*, 055402. [[CrossRef](#)] [[PubMed](#)]
381. Kulsrud, R.; Pearce, W.P. The Effect of Wave-Particle Interactions on the Propagation of Cosmic Rays. *Astrophys. J.* **1969**, *156*, 445. [[CrossRef](#)]
382. Wentzel, D.G. Cosmic-ray propagation in the Galaxy—Collective effects. *Annu. Rev. Astron. Astrophys.* **1974**, *12*, 71–96. [[CrossRef](#)]
383. Sharma, P.; Colella, P.; Martin, D.F. Numerical Implementation of Streaming Down the Gradient: Application to Fluid Modeling of Cosmic Rays and Saturated Conduction. *SIAM J. Sci. Comput.* **2010**, *32*, 3564–3583. [[CrossRef](#)]
384. Jiang, Y.F.; Oh, S.P. A New Numerical Scheme for Cosmic-Ray Transport. *Astrophys. J.* **2018**, *854*, 5. [[CrossRef](#)]
385. Thomas, T.; Pfrommer, C. Cosmic-ray hydrodynamics: Alfvén-wave regulated transport of cosmic rays. *Mon. Not. R. Astron. Soc.* **2019**, *485*, 2977–3008. [[CrossRef](#)]
386. Boehringer, H.; Morfill, G.E. On the Dynamical Role of Cosmic Rays in Cooling Flows in Clusters of Galaxies. *Astrophys. J.* **1988**, *330*, 609. [[CrossRef](#)]
387. Loewenstein, M.; Zweibel, E.G.; Begelman, M.C. Cosmic-Ray Heating of Cooling Flows: A Critical Analysis. *Astrophys. J.* **1991**, *377*, 392. [[CrossRef](#)]
388. Rephaeli, Y.; Silk, J. Energetic Proton Heating of Gas in the Core of the Perseus Cluster. *Astrophys. J.* **1995**, *442*, 91. [[CrossRef](#)]
389. Colafrancesco, S.; Dar, A.; De Rújula, A. Cooling flows or warming rays? *Astron. Astrophys.* **2004**, *413*, 441–452. [[CrossRef](#)]
390. Pfrommer, C.; Enßlin, T.A.; Springel, V.; Jubelgas, M.; Dolag, K. Simulating cosmic rays in clusters of galaxies - I. Effects on the Sunyaev-Zel'dovich effect and the X-ray emission. *Mon. Not. R. Astron. Soc.* **2007**, *378*, 385–408. [[CrossRef](#)]
391. Enßlin, T.; Pfrommer, C.; Miniati, F.; Subramanian, K. Cosmic ray transport in galaxy clusters: Implications for radio halos, gamma-ray signatures, and cool core heating. *Astron. Astrophys.* **2011**, *527*, A99. [[CrossRef](#)]
392. Fujita, Y.; Ohira, Y. Stable Heating of Cluster Cooling Flows by Cosmic-Ray Streaming. *Astrophys. J.* **2011**, *738*, 182. [[CrossRef](#)]
393. Fujita, Y.; Ohira, Y. Radio mini-halo emission from cosmic rays in galaxy clusters and heating of the cool cores. *Mon. Not. R. Astron. Soc.* **2013**, *428*, 599–608. [[CrossRef](#)]
394. Guo, F.; Mathews, W.G. Cosmic-ray-dominated AGN Jets and the Formation of X-ray Cavities in Galaxy Clusters. *Astrophys. J.* **2011**, *728*, 121. [[CrossRef](#)]
395. Croston, J.H.; Ineson, J.; Hardcastle, M.J. Particle content, radio-galaxy morphology, and jet power: All radio-loud AGN are not equal. *Mon. Not. R. Astron. Soc.* **2018**, *476*, 1614–1623. [[CrossRef](#)]
396. Su, K.Y.; Hopkins, P.F.; Hayward, C.C.; Faucher-Giguère, C.A.; Kereš, D.; Ma, X.; Orr, M.E.; Chan, T.K.; Robles, V.H. Cosmic rays or turbulence can suppress cooling flows (where thermal heating or momentum injection fail). *Mon. Not. R. Astron. Soc.* **2020**, *491*, 1190–1212. [[CrossRef](#)]
397. Butsky, I.S.; Fielding, D.B.; Hayward, C.C.; Hummels, C.B.; Quinn, T.R.; Werk, J.K. The Impact of Cosmic Rays on Thermal Instability in the Circumgalactic Medium. *Astrophys. J.* **2020**, *903*, 77. [[CrossRef](#)]
398. Gitti, M.; Ferrari, C.; Domainko, W.; Feretti, L.; Schindler, S. Discovery of diffuse radio emission at the center of the most X-ray-luminous cluster RX J1347.5-1145. *Astron. Astrophys.* **2007**, *470*, L25–L28. [[CrossRef](#)]
399. Giacintucci, S.; Markevitch, M.; Venturi, T.; Clarke, T.E.; Cassano, R.; Mazzotta, P. New Detections of Radio Minihalos in Cool Cores of Galaxy Clusters. *Astrophys. J.* **2014**, *781*, 9. [[CrossRef](#)]
400. Richard-Laferrrière, A.; Hlavacek-Larrondo, J.; Nemmen, R.S.; Rhea, C.L.; Taylor, G.B.; Prasow-Émond, M.; Gendron-Marsolais, M.; Latulippe, M.; Edge, A.C.; Fabian, A.C.; et al. On the relation between mini-halos and AGN feedback in clusters of galaxies. *Mon. Not. R. Astron. Soc.* **2020**, *499*, 2934–2958. [[CrossRef](#)]
401. Pfrommer, C.; Enßlin, T.A. Constraining the population of cosmic ray protons in cooling flow clusters with γ -ray and radio observations: Are radio mini-halos of hadronic origin? *Astron. Astrophys.* **2004**, *413*, 17–36. [[CrossRef](#)]
402. Fujita, Y.; Kohri, K.; Yamazaki, R.; Kino, M. Nonthermal Emission Associated with Strong AGN Outbursts at the Centers of Galaxy Clusters. *Astrophys. J. Lett.* **2007**, *663*, L61–L64. [[CrossRef](#)]
403. Zandanel, F.; Pfrommer, C.; Prada, F. On the physics of radio haloes in galaxy clusters: Scaling relations and luminosity functions. *Mon. Not. R. Astron. Soc.* **2014**, *438*, 124–144. [[CrossRef](#)]
404. Giacintucci, S.; Markevitch, M.; Brunetti, G.; Cassano, R.; Venturi, T. A radio minihalo in the extreme cool-core galaxy cluster RXC J1504.1-0248. *Astron. Astrophys.* **2011**, *525*, L10. [[CrossRef](#)]
405. Bravi, L.; Gitti, M.; Brunetti, G. Do radio mini-halos and gas heating in cool-core clusters have a common origin? *Mon. Not. R. Astron. Soc.* **2016**, *455*, L41–L45. [[CrossRef](#)]

406. ZuHone, J.A.; Markevitch, M.; Weinberger, R.; Nulsen, P.; Ehlert, K. How Merger-driven Gas Motions in Galaxy Clusters Can Turn AGN Bubbles into Radio Relics. *Astrophys. J.* **2021**, *914*, 73. [[CrossRef](#)]
407. ZuHone, J.; Ehlert, K.; Weinberger, R.; Pfrommer, C. Turning AGN Bubbles into Radio Relics with Sloshing: Modeling CR Transport with Realistic Physics. *Galaxies* **2021**, *9*, 91. [[CrossRef](#)]
408. Brienza, M.; Shimwell, T.W.; de Gasperin, F.; Bikmaev, I.; Bonafede, A.; Botteon, A.; Brügger, M.; Brunetti, G.; Burenin, R.; Capetti, A.; et al. A snapshot of the oldest active galactic nuclei feedback phases. *Nat. Astron.* **2021**, *5*, 1261–1267. [[CrossRef](#)]
409. Vazza, F.; Brügger, M.; Gheller, C. Thermal and non-thermal traces of AGN feedback: Results from cosmological AMR simulations. *Mon. Not. R. Astron. Soc.* **2013**, *428*, 2366–2388. [[CrossRef](#)]
410. Beckmann, R.S.; Dubois, Y.; Pellissier, A.; Olivares, V.; Polles, F.L.; Hahn, O.; Guillard, P.; Lehnert, M.D. Cosmic rays and thermal instability in self-regulating cooling flows of massive galaxy clusters. *Astron. Astrophys.* **2022**, *665*, A129. [[CrossRef](#)]
411. Spitzer, L. *Physics of Fully Ionized Gases*, 2nd ed.; Wiley: New York, NY, USA, 1962.
412. Kunz, M.W.; Jones, T.W.; Zhuravleva, I. Plasma Physics of the Intracluster Medium. In *Handbook of X-ray and Gamma-ray Astrophysics*; Bambi, C., Santangelo, A., Eds.; Springer: Singapore, 2022; p. 56. [[CrossRef](#)]
413. Bregman, J.N.; David, L.P. Heat conduction in cooling flows. *Astrophys. J.* **1988**, *326*, 639–644. [[CrossRef](#)]
414. Guo, F.; Oh, S.P. Could AGN outbursts transform cool core clusters? *Mon. Not. R. Astron. Soc.* **2009**, *400*, 1992–1999. [[CrossRef](#)]
415. Quataert, E. Buoyancy Instabilities in Weakly Magnetized Low-Collisionality Plasmas. *Astrophys. J.* **2008**, *673*, 758–762. [[CrossRef](#)]
416. Ruszkowski, M.; Oh, S.P. Shaken and Stirred: Conduction and Turbulence in Clusters of Galaxies. *Astrophys. J.* **2010**, *713*, 1332–1342. [[CrossRef](#)]
417. Roberg-Clark, G.T.; Drake, J.F.; Reynolds, C.S.; Swisdak, M. Suppression of Electron Thermal Conduction in the High β Intracluster Medium of Galaxy Clusters. *Astrophys. J. Lett.* **2016**, *830*, L9. [[CrossRef](#)]
418. Roberg-Clark, G.T.; Drake, J.F.; Reynolds, C.S.; Swisdak, M. Suppression of Electron Thermal Conduction by Whistler Turbulence in a Sustained Thermal Gradient. *Phys. Rev. Lett.* **2018**, *120*, 035101. [[CrossRef](#)]
419. Komarov, S.; Schekochihin, A.A.; Churazov, E.; Spitkovsky, A. Self-inhibiting thermal conduction in a high- β whistler-unstable plasma. *J. Plasma Phys.* **2018**, *84*, 905840305. [[CrossRef](#)]
420. Fabian, A.C.; Reynolds, C.S.; Taylor, G.B.; Dunn, R.J.H. On viscosity, conduction and sound waves in the intracluster medium. *Mon. Not. R. Astron. Soc.* **2005**, *363*, 891–896. [[CrossRef](#)]
421. Fabian, A.C.; Sanders, J.S.; Allen, S.W.; Crawford, C.S.; Iwasawa, K.; Johnstone, R.M.; Schmidt, R.W.; Taylor, G.B. A deep Chandra observation of the Perseus cluster: Shocks and ripples. *Mon. Not. R. Astron. Soc.* **2003**, *344*, L43–L47. [[CrossRef](#)]
422. Chew, G.F.; Goldberger, M.L.; Low, F.E. The Boltzmann Equation and the One-Fluid Hydromagnetic Equations in the Absence of Particle Collisions. *Proc. R. Soc. Lond. Ser. A* **1956**, *236*, 112–118. [[CrossRef](#)]
423. Schekochihin, A.A.; Cowley, S.C.; Kulsrud, R.M.; Hammett, G.W.; Sharma, P. Plasma Instabilities and Magnetic Field Growth in Clusters of Galaxies. *Astrophys. J.* **2005**, *629*, 139–142. [[CrossRef](#)]
424. Braginskii, S.I. Transport Processes in a Plasma. *Rev. Plasma Phys.* **1965**, *1*, 205.
425. Kunz, M.W.; Schekochihin, A.A.; Cowley, S.C.; Binney, J.J.; Sanders, J.S. A thermally stable heating mechanism for the intracluster medium: turbulence, magnetic fields and plasma instabilities. *Mon. Not. R. Astron. Soc.* **2011**, *410*, 2446–2457. [[CrossRef](#)]
426. Ley, F.; Zweibel, E.G.; Riquelme, M.; Sironi, L.; Miller, D.; Tran, A. A Heating Mechanism via Magnetic Pumping in the Intracluster Medium. *Astrophys. J.* **2023**, *947*, 89. [[CrossRef](#)]
427. Sanders, J.S.; Fabian, A.C. A deeper X-ray study of the core of the Perseus galaxy cluster: The power of sound waves and the distribution of metals and cosmic rays. *Mon. Not. R. Astron. Soc.* **2007**, *381*, 1381–1399. [[CrossRef](#)]
428. Wang, S.C.; Yang, H.Y.K. Production efficiencies of sound waves in the intracluster medium driven by AGN jets. *Mon. Not. R. Astron. Soc.* **2022**, *512*, 5100–5109. [[CrossRef](#)]
429. Choudhury, P.P.; Reynolds, C.S. Acoustic waves and g-mode turbulence as energy carriers in a viscous intracluster medium. *Mon. Not. R. Astron. Soc.* **2022**, *514*, 3765–3788. [[CrossRef](#)]
430. Kempster, P.; Quataert, E.; Squire, J. Sound-wave instabilities in dilute plasmas with cosmic rays: implications for cosmic ray confinement and the Perseus X-ray ripples. *Mon. Not. R. Astron. Soc.* **2020**, *493*, 5323–5335. [[CrossRef](#)]
431. Kunz, M.W.; Schekochihin, A.A.; Stone, J.M. Firehose and Mirror Instabilities in a Collisionless Shearing Plasma. *Phys. Rev. Lett.* **2014**, *112*, 205003. [[CrossRef](#)]
432. Pfrommer, C.; Enßlin, T.A.; Sarazin, C.L. Unveiling the composition of radio plasma bubbles in galaxy clusters with the Sunyaev-Zel’dovich effect. *Astron. Astrophys.* **2005**, *430*, 799–810. [[CrossRef](#)]
433. Abdulla, Z.; Carlstrom, J.E.; Mantz, A.B.; Marrone, D.P.; Greer, C.H.; Lamb, J.W.; Leitch, E.M.; Muchovej, S.; O’Donnell, C.; Plagge, T.J.; et al. Constraints on the Thermal Contents of the X-ray Cavities of Cluster MS 0735.6+7421 with Sunyaev-Zel’dovich Effect Observations. *Astrophys. J.* **2019**, *871*, 195. [[CrossRef](#)]
434. Orłowski-Scherer, J.; Haridas, S.K.; Di Mascolo, L.; Sarmiento, K.P.; Romero, C.E.; Dicker, S.; Mroczkowski, T.; Bhandarkar, T.; Churazov, E.; Clarke, T.E.; et al. GBT/MUSTANG-2 9” resolution imaging of the SZ effect in MS0735.6+7421. Confirmation of the SZ cavities through direct imaging. *Astron. Astrophys.* **2022**, *667*, L6. [[CrossRef](#)]
435. Wootten, A.; Thompson, A.R. The Atacama Large Millimeter/Submillimeter Array. *IEEE Proc.* **2009**, *97*, 1463–1471. [[CrossRef](#)]
436. Dicker, S.R.; Ade, P.A.R.; Aguirre, J.; Brevik, J.A.; Cho, H.M.; Datta, R.; Devlin, M.J.; Dober, B.; Egan, D.; Ford, J.; et al. MUSTANG 2: A Large Focal Plane Array for the 100 m Green Bank Telescope. *J. Low Temp. Phys.* **2014**, *176*, 808–814. [[CrossRef](#)]

437. Adam, R.; Adane, A.; Ade, P.A.R.; André, P.; Andrianasolo, A.; Aussel, H.; Beelen, A.; Benoît, A.; Bideaud, A.; Billot, N.; et al. The NIKA2 large-field-of-view millimetre continuum camera for the 30 m IRAM telescope. *Astron. Astrophys.* **2018**, *609*, A115. [[CrossRef](#)]
438. ZuHone, J.A.; Markevitch, M.; Ruszkowski, M.; Lee, D. Cold Fronts and Gas Sloshing in Galaxy Clusters with Anisotropic Thermal Conduction. *Astrophys. J.* **2013**, *762*, 69. [[CrossRef](#)]
439. ZuHone, J.A.; Kunz, M.W.; Markevitch, M.; Stone, J.M.; Biffi, V. The Effect of Anisotropic Viscosity on Cold Fronts in Galaxy Clusters. *Astrophys. J.* **2015**, *798*, 90. [[CrossRef](#)]
440. Su, Y.; Kraft, R.P.; Roediger, E.; Nulsen, P.; Forman, W.R.; Churazov, E.; Randall, S.W.; Jones, C.; Machacek, M.E. Deep Chandra Observations of NGC 1404: Cluster Plasma Physics Revealed by an Infalling Early-type Galaxy. *Astrophys. J.* **2017**, *834*, 74. [[CrossRef](#)]
441. Wang, Q.H.S.; Markevitch, M. A Deep X-ray Look at Abell 2142—Viscosity Constraints From Kelvin-Helmholtz Eddies, a Displaced Cool Peak That Makes a Warm Core, and A Possible Plasma Depletion Layer. *Astrophys. J.* **2018**, *868*, 45. [[CrossRef](#)]
442. Zhuravleva, I.; Churazov, E.; Schekochihin, A.A.; Allen, S.W.; Vikhlinin, A.; Werner, N. Suppressed effective viscosity in the bulk intergalactic plasma. *Nat. Astron.* **2019**, *3*, 832–837. [[CrossRef](#)]
443. Kraft, R.; Markevitch, M.; Kilbourne, C.; Adams, J.S.; Akamatsu, H.; Ayromlou, M.; Bandler, S.R.; Barbera, M.; Bennett, D.A.; Bhardwaj, A.; et al. Line Emission Mapper (LEM): Probing the physics of cosmic ecosystems. *arXiv* **2022**, arXiv:2211.09827. [[CrossRef](#)]
444. Gaskin, J.A.; Swartz, D.A.; Vikhlinin, A.; Özel, F.; Gelmis, K.E.; Arenberg, J.W.; Bandler, S.R.; Bautz, M.W.; Civitani, M.M.; Dominguez, A.; et al. Lynx X-Ray Observatory: An overview. *J. Astron. Telesc. Instruments Syst.* **2019**, *5*, 021001. [[CrossRef](#)]

Disclaimer/Publisher’s Note: The statements, opinions and data contained in all publications are solely those of the individual author(s) and contributor(s) and not of MDPI and/or the editor(s). MDPI and/or the editor(s) disclaim responsibility for any injury to people or property resulting from any ideas, methods, instructions or products referred to in the content.